UNIVERSITI SAINS MALAYSIA

Laporan Akhir Projek Penyelidikan Jangka Pendek

Investigation of Dynamic Characteristics of Ground Motion Using Microtremor Observation

by
Dr. Lau Tze Liang
Assoc. Prof. Dr. Taksiah A. Majid
Mr. Teoh Chun Li
Mr. Tan Teik Ning

2012

ASEAN University Network /
Southeast Asia Engineering Education Development Network
AUN/SEED-Net

Technical Report
Special Research Program for Alumni Members (SRA)

(Project Reference No. USM SRA-1101)

Project Title:
Investigation of Dynamic Characteristics of Ground Motion Using Microtremor Observations

Principal Investigator:
Dr. Lau Tze Liang, Universiti Sains Malaysia

Japanese Co-Investigator:
Prof. Dr. Hitoshi Morikawa,
Tokyo Institute of Technology

Co-Researcher:
Assoc. Prof. Dr. Taksiah A. Majid, Universiti Sains Malaysia

Research Assistant:
Mr. Teoh Chun Li, Universiti Sains Malaysia
Mr. Tan Teik Ning (Replace Mr. Tan Chee Ghuan),
Universiti Sains Malaysia

CONTENTS

CHAPTER 1
INTRODUCTION

1.1 General

Mircrotremor also known as ambient vibration or ambient noise is the ground vibration / movement caused by artificial disturbance such as traffic, industrial machines and so on. The microtremor survey method has applied to the study of near-field geology of the Earth for over 50 years ago (Okada, 2003). It has amplitude in the range of 0.1 to 1 micron and the period in the range of 0.05 s to 2 s. Mirotremor has been used in the study relating not only to the natural earthquakes but also the explosion seismic waves (Kanai and Tanaka, 1961).

Microtremor measurement has been applied to study the dynamic characteristics of the ground and structure in Japan, US and other parts of the world which are earthquake prone countries. However, this technique is still new in the low to moderate seismicity country such as Malaysia. The ground vibration in Malaysia due to earthquake originated in Sumatra has drawn the attention of the scientists and engineers after the 2004 Banda Aceh Earthquake. Several small magnitude earthquakes have been recorded in Bukit Tinggi areas. The details of these incidents are not made known due to insufficient measurement data and there is a possibility that the Bukit Tinggi fault is reactivated by the great Sumatra earthquake happened recently. Even though the level of seismicity is not low, the seismic risk could be significant. Therefore, the government has insisted to impose seismic design for important structures in Malaysia by introducing seismic design code for Malaysia. To do this, extensive studies on dynamic characteristics of the ground and structures should be carried out to investigate the effect of the local soil formation to the behaviour of the structures.

There are various approaches can be used to assess the potential earthquake site response. These include the determination of physical properties of the local setting by conducting borehole and/or seismic profile studies. Measured parameters can then be used in theoretical models to predict the site response. The main disadvantages of this method are the high cost and time consumed in conducting the geotechnical or geophysical surveys. As

compared to this approach, microtremor offers better solution. First introduced by Kanai (1957), the earthquake site response is estimated using the ambient seismic noise. The potential for using microtremors to characterize earthquake site response is attractive because of the relative ease and economy of the method. Were a reliable procedure to be developed, large regions could be surveyed in a relatively short period of time.

Various methods are available to analyze the mircotremor data such as Kanai method, Aki method (Aki, 1956), *f-k* method and Nakamura method (Nakamura, 1989). The application of microtremor in seismic hazard analysis especially with regard to seismic microzonation and first order evaluations of site response, in particularly using Nakamura (1989) technique, has shown great importance (Field et al., 1990; Lermo and Chavez-Garcia, 1994; Field et al., 1995).

1.2 Research Background

Malaysia is located in seismically stable Sunda plate and has not experienced any disastrous earthquake occurrences. Because of this reason, there is no seismic code in Malaysia and most of our buildings and structures are designed without considering earthquake loading. However, due to the location close to two of the most seismically active plate boundaries, i.e. Indo-Australian and Eurasian plates, Malaysia has experienced numerous strong tremors occurrence and they becomes more frequent in the last decade with the increasing seismic activity since the major earthquake in Banda Aceh and the unprecedented Indian Ocean Tsunami in 2004. Even though Malaysia is located far from seismic sources, it has a substantial seismic risk from distant earthquakes due to the local geology such as the underlying soft soil to amplify ground motions. Therefore, it is imperative to conduct a detailed site-specific seismic hazard assessment and produce seismic microzonation map for specific sites.

Penang is a state situated in northwest coast of Peninsular Malaysia (Figure 1.2). It consists of an island 293 square kilometres located in the Straits of Malacca and a narrow hinterland 753 square kilometres on the peninsula. The study area of this research is the Penang Island. Georgetown is the capital of the state of Penang Island and is the second largest

metropolitan in Malaysia by population. It is a highly urbanized and economically important state in Malaysia. The Northeast Penang Island District (Figure 1.3) that covers 121 square kilometres has almost fully developed with high-rise buildings and important structures. Due to it close vicinity to Sumatra, numerous tremors have been experienced by the people especially the residents staying in high-rise buildings and some cracking on non-structural member of buildings are reported. Whenever moderate and strong earthquakes occur in Sumatra, tremors are felt and high-rise building dwellers flee their houses and scurry for safety. Among the buildings rocked by the earthquake are the 65-storey complex, the highest building in Penang consists of offices and the Penang state government's office, commercial areas along Sultan Ahmad Shah Street, high-rise buildings in the southern part of Penang such as Teluk Kumbar and Gertak Sanggul, Weld Quay, Macallum Street, Tanjung Bungah, Tanjung Tokong, Gurney Drive, Lintang P. Ramlee, Sungai Nibong and Bandar Baru Air Itam.

The occurrence of this incident has attracted the attention of public and professionals such as scientists, engineers and government authorities. The safety of non-seismically designed buildings under repeated ground motions is unknown. Due to the lack of research and information available for the dynamic characteristics of the site, the detailed investigation on the estimation of ground motion characteristics using microtremor is one of the feasible techniques. This method involves the measurement of low amplitude of ambient vibration caused by human-made or atmospheric disturbance. It can be used for seismic microzonation. Microtremor measurement has been proved to produce accurate results and require less manpower, cost and time consumption.

Micortremor measurement is a new technique in Malaysia and very few researchers has the experience in this application. Therefore, technology transfer and guidance from Japan counterpart is needed. In this research, basic knowledge and training were provided by Tokyo Institute of Technology and field measurements were then carried out in various observation sites in Penang Island by Universiti Sains Malaysia. To ensure the goal of this research is achieved, visit by Japanese professor and postgraduate students to Universiti Sains Malaysia was planned. This has given better platform for researchers and students from both institutions to discuss important issues in this research area.

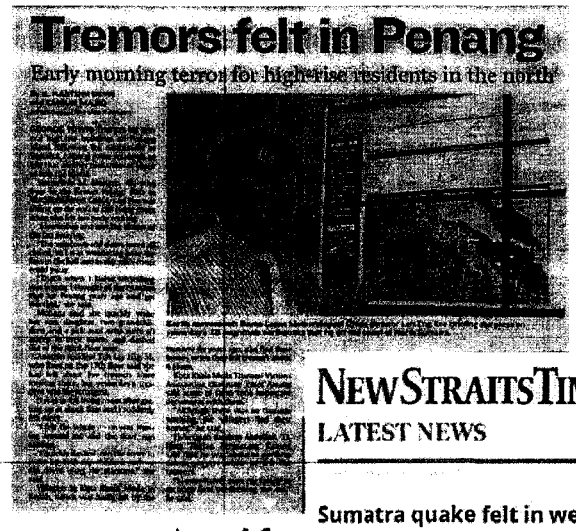

Tremors felt in Penang

Early morning terror for higher-rise residents in the north

thestar online

Tremors felt in Penang

NEW STRAITS TIMES

LATEST NEWS

Sumatra quake felt in west coast Malaysia

Kuala Lumpur: Several states in the west coast of Peninsular Malaysia experienced tremors following a magnitude 8.0 earthquake which hit Indonesia's Aceh region today.

Kuala Lumpur Fire and Rescue Department assistant operations directo Azizan Ismail when contacted by Bernama confirmed the matter and said the tremors were felt in Kuala Lumpur, Penang and Perak.

The tremors were felt around 4.50pm. -- Bernama

Quake tremors rock Penang

Posted on May 10, 2010

GEORGE TOWN: Tremors from an earthquake that struck off Aceh province in Suma several parts of the island as Penangites were enjoying a leisurely Sunday.

The shocks lasting several seconds rattled already jittery citizens to despite The Star with enquiries

One caller, who only wanted to be known as Doi, said he was watching a movie at a cine shopping complex at around 2pm yesterday when a group of foreign tourists suddenly rushed o

"I thought they were fooling around, so I just ignored them."

MYsinchew.com

Massive jolts Aceh, tremors felt in Malaysia

Natural disasters News 2012-04-11 10:15

KUALA LUMPUR, April 11 (Bernama) -- Several states in the west coast of Peninsular Malaysia experienced tremors following a magnitude 8.7 earthquake which hit Indonesia's Aceh region today.

The Malaysian Meteorological Department warned the public to stay away from the coast in Kedah, Perlis, Langkawi, Penang and Perak as there was a possible tsunami risk.

Kuala Lumpur Fire and Rescue Department assistant operations director Azizan Ismail when contacted by Bernama confirmed the matter and said the tremors were felt in Kuala Lumpur, Penang and Perak.

The tremors were felt around 4.50pm.

Azizan said fire and rescue personnel were despatched to areas where the members of the public sent distress calls.

He said the department received calls at around 4.47 about tremors felt in places like Ampang and Jalan Tun Razak.

Staff at the Malaysian National News Agency (Bernama's) headquarters located off Jalan Tun Razak also reported feeling tremors which lasted about 10 minutes.

In **KANGAR**, residents at the Seri Sena flats in Kampung Bakau rushed out of their homes and gathered in the parking lot after experiencing the tremors.

The residents said they became afraid when the 12-storey flats shook during the tremors.

The tremors were also reported to have been felt at the EPF building in the city and also at Kampung Bukit Lagi near here as well as in Kuala Perlis.

thestar online

Published: Sunday August 16, 2009 MYT 5:37:00 PM
Updated: Sunday August 16, 2009 MYT 6:58:06 PM

Quake rocks Sumatra; tremors felt in KL, Penang, Johor

KUALA LUMPUR: Residents staying in high-rise buildings in some areas here felt tremors as a strong underwater earthquake reportedly struck western Indonesia.

Residents in Bandar Tun Razak here reportedly felt tremors Sunday afternoon.

Tremors were also felt in the southern part of Penang such as Telok Kumbar and Gertak Sanggul.

The Meteorological Department noted that a moderate earthquake measuring 6.3 on the Richter scale was felt in southern Sumatra.

"We have received a few calls from the police and people in Penang about the tremors, but there is no danger," a spokesperson said.

thestar online

Wednesday September 7, 2011

Tremors jolt Penangites Sumatra quake felt in tall buildings

GEORGE TOWN: Hundreds of residents from high-rise buildings ran out of their homes following tremors after a 6.6-magnitude earthquake jolted the western Indonesian island of Sumatra.

Among the affected people here were those living in Weld Quay, Macalister Street, Tanjung Bungah, Tanjung Tokong, Gurney Drive, Lintang P Ramlee, Sungai Nibong and Bandar Baru Air Itam.

Penang Fire and Rescue Department assistant director (operations) Mohd Razam Taja Rahim said the department received 16 reports about the tremors.

He said most of the reports came from residents staying at high-rise buildings and hotels along the Batu Ferringhi tourist bel.

Penang Island Voluntary Patrol Unit and Community Policing members also kept a close watch by calling each other on walkie-talkies after the tremors.

State Health, Welfare, Environment and Caring Society Committee chairman Phee Boon Poh urged the residents associations and joint management boards of high-rise residential buildings to prepare a contingency plan.

He said Penangites can check for any tsunami alert after a tremor at *http://pmc.weather.gov*.

In PUTRAJAYA, Higher Education Department director-general Prof Datuk Dr Rujhan Mustafa said all Malaysian students in Indonesia were safe.

Thursday September 15, 2007

Tremors felt in Penang, too

thestar online

By BERNARD SEE

PENANG: Tremors caused by the 7.8-magnitude earthquake off Sumatera Thursday morning caused more than 4,000 workers from three government buildings here to flee their offices.

The tremors were felt at the EPF building in Jalan Sultan Ahmad Shah, Komtar and Bangunan Tunku Syed Putra in Downing Street between 7.50am and 8.15am Thursday.

State Finance, Trade and Consumer Affairs Ministry enforcement chief M. Gunasekan said he had just reached his 8th floor office on Downing Street when he suddenly felt dizzy.

"I thought nothing of it until one of my staff told me that there was a tremor. I then walked to the ground floor with the rest of my staff," he said.

Penang Water Supply Corporation Sdn Bhd clerk Lim Saw Ean, 52, whose office was on the 28th floor of Komtar, said she and her colleagues felt their chairs sway at about 8am.

"I have experienced quite a few tremors over the years, but this was one of the worst. I went back to the office after the Fire and Rescue department gave the green light at 9.25am."

Figure1.1: Newspaper reports on the tremor felt in Penang

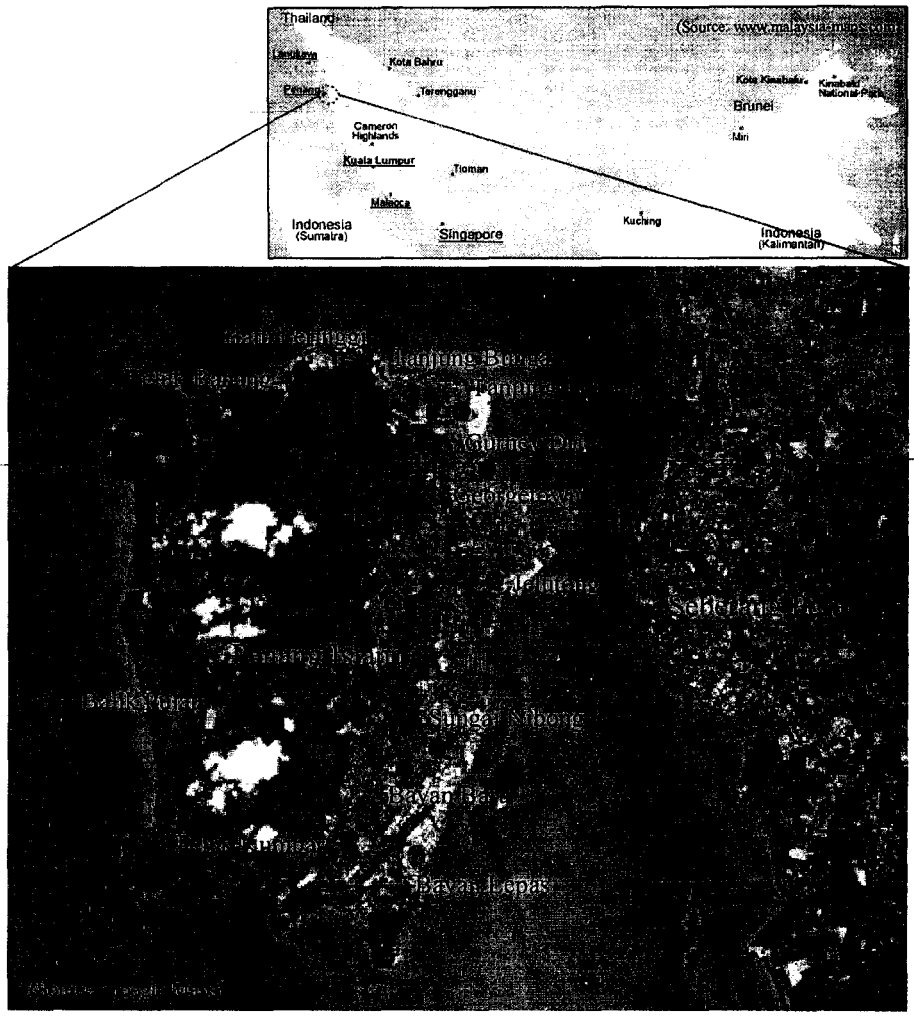

Figure 1.2: Map of Penang Island

Figure 1.3: Aerial view of the northeastern part of Penang Island (Wikipedia, 2012)

CHAPTER 2
LITERATURE REVIEW

2.1 General

The surface of the Earth is always in motion at seismic frequencies, even without earthquake. This ubiquitous, weak, low amplitude vibration may be recorded on the surface of the Earth using a very sensitive acceleration or velocity sensors are called microtremors. They are natural signals or phenomena. Various research projects in the past have documented the relationship between microtremor and subsurface structure. These findings have demonstrated that the microtremor can be applied to the estimation of subsurface structure. Apart from that, microtremor observation is also applied to the estimation of the dynamic characteristic of building.

2.2 Characteristics of Microtremors

Microtremors have extremely small amplitudes. Displacements are in the order of 10^{-4} to 10^{-2} mm and therefore, below human sensing. Microtremors are caused by daily human activities such as movement of machinery in factories, motorcars and people walking and natural phenomena such as flow of water in rivers, rain, wind, variation of atmosphere pressure and ocean waves. Both human activity and natural phenomena vary with time. The variation is very complex, irregular and not repeatable. Microtremors are an assemblage of waves traveling in various directions.

The microtremors originating from human activities are dominated by the components with periods shorter than one second, or higher than 1 Hz in frequency while the microtremors due to natural phenomena have dominant periods greater than one second, or lower than 1 Hz in frequency. Microtremors vary depending upon location. Figure 2.1 shows an example of three-component microtremor records. The observation of microtremor is plotted in a power spectrum. A typical microtremor record in power spectrum is shown in Figure 2.2. The spectra of microtremors are largely similar worldwide as shown in Figure

2.3. The records vary both spatially and temporally. The recorded microtremors show complex variations, but the degree of complexity does not vary during the recording period. However, the amplitude envelop varies vastly between the recorded mircrotremors.

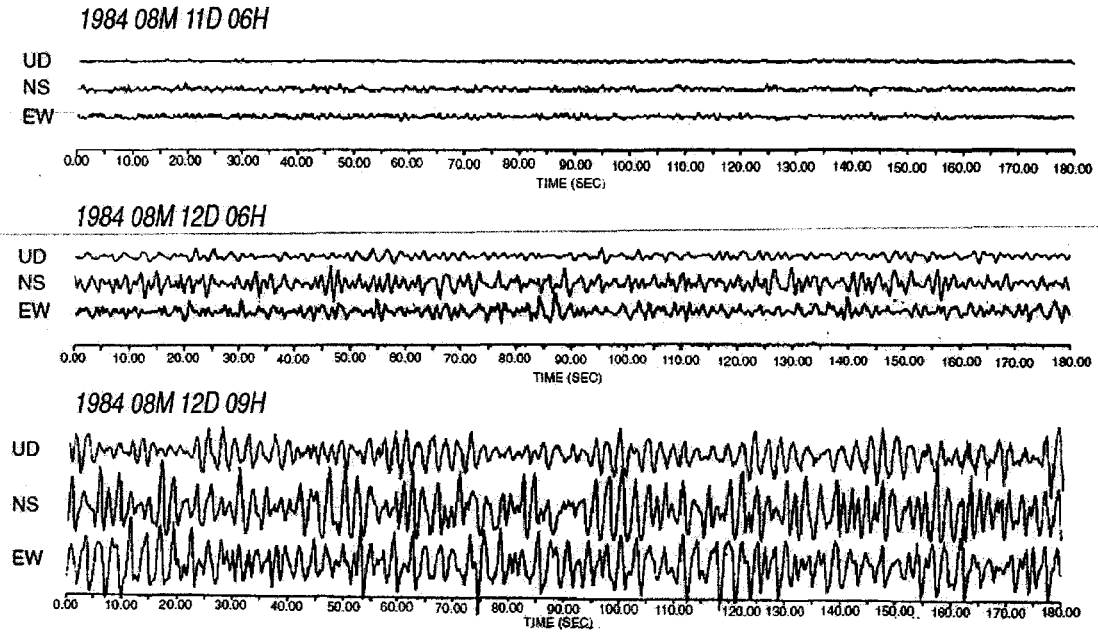

Figure 2.1: An example of microtremor records in suburban Sapporo (Okada, 2003)

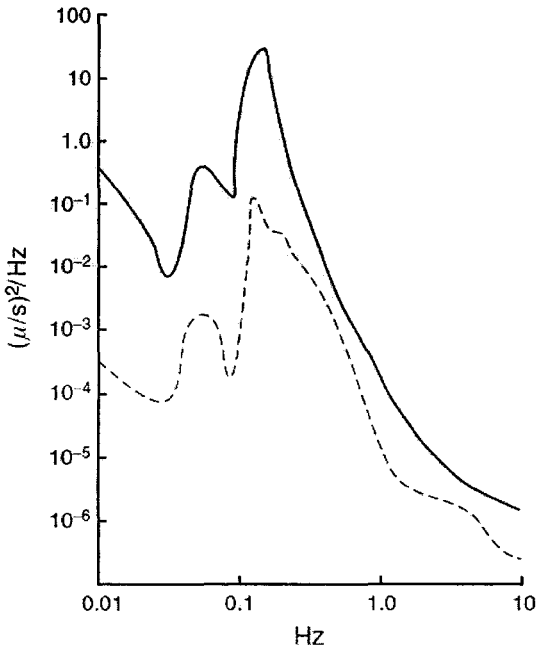

Figure 2.2: Power spectra of microtremors (Okada, 2003)

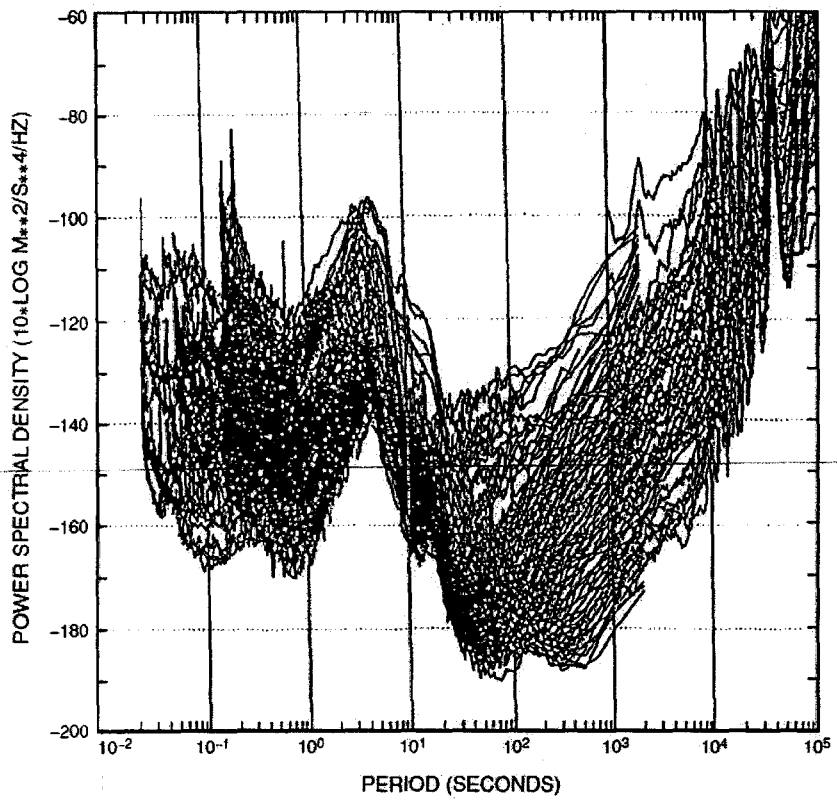

Figure 2.3: Acceleration power spectra of microtremors recorded at the 75 permanent seismic observatories (Okada, 2003)

2.3 H/V Method Fundamental Theories

H/V spectral ratio technique was found by Nakamura (1989) where horizontal motion and vertical motion of both soft and hard soil was taken via microtremor equipments and then the horizontal to vertical ratio was derived from the recorded data. The results of these findings show good resemblance of ground characteristic of both soft and hard soils which the hard soil has higher natural frequency while softer soil has lower natural frequency. The fundamental theory about H/V ratio on amplification factor stated that the vertical motion is not amplified when the wave propagate from below the ground to surface of the ground.

However, horizontal motion will be amplified depending on the type of soil. This is due to the fact that P wave velocity is about three to four times faster than S wave velocity (Nakamura, 2008). And assuming that Rayleigh wave does not have significant effect, vertical motion from bedrock will be same as vertical motion on surface. In such, the

vertical component is considered to be the same when travelled from bedrock while horizontal motion will be amplified. Hence, by measuring the vertical and horizontal component of ground motion, the amplification factor can be found by dividing the horizontal component with vertical component. The simple graphical explanation is shown in Figure 2.4. Even though there are not much supporting theories behind this method, it have been used in many countries across the world and the prediction by H/V method have shown good accuracy. Moreover, the simplicity and cost effectiveness of microtremor analysis have gain good popularity among researchers.

Numerical simulation was done by Bonnefoy-Claudet et al. (2006) using numerical ground model of two layer with basement and surface grounds with 6.5 of impedance ratio. The first dominant frequency is set to be at 2 Hz, and various shape, depth and location are adopted for analysis. It is assumed that effect of S wave dominates the peak at 2 Hz except Rayleigh wave is near the source of data acquisition. The peak value at 2 Hz shown impedance ratio difference between five to eight, which is around impedance ratio of 6.5 set before analysis. This finding concludes that amplification factor estimated through H/V method can be used to predict the ground motion characteristic.

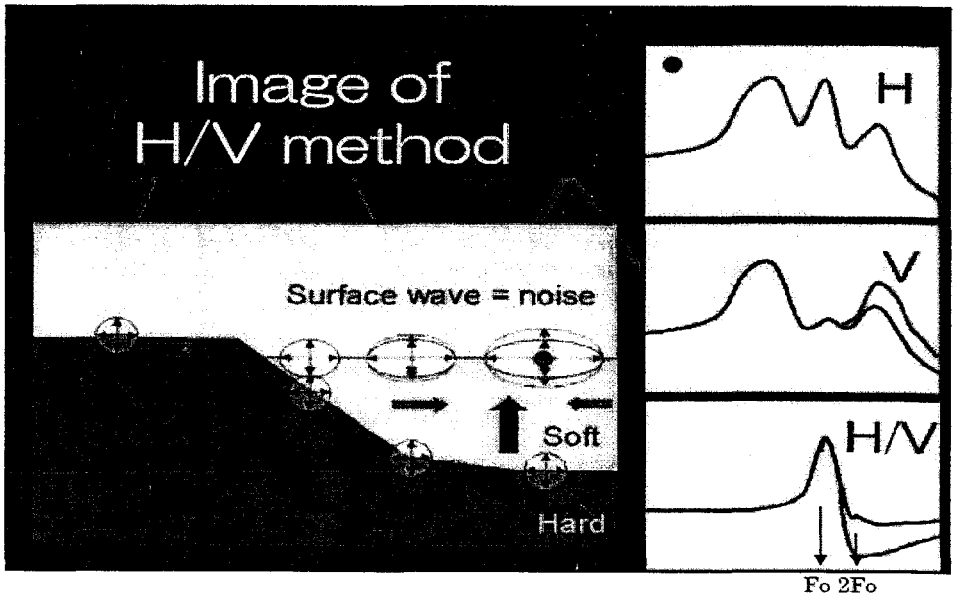

Figure 2.4: Graphical Explanation of H/V Method (Nakamura, 2008).

Figure 2.5 shows the normal shape of H/V spectral ratio graph where the first peak of H/V is mainly consist of S wave alone. Following the first peak, the trough around $2F_0$ is caused

by Rayleigh wave. As the Rayleigh wave increases from F_0, and grow until reaches its first peak around $2F_0$. With larger effect from Rayleigh wave, the amplitude of graph will be reduced. Hence, the trend of graph after the first peak shows the influence of Rayleigh wave, the effect of Rayleigh wave is shown in the figure (Nakamura, 2008). As first predominant period are of main interest, Rayleigh wave does not have significant effects in determination of the first soil natural frequency.

Figure 2.6 shows comparison between Vertical component (Vf), Horizontal component (Hf), Theoretical Transfer Function (Ah) and also Quasi – Transfer Spectra (QTS), which is H/V technique. It is shown that the QTS is lower than the transfer function. As the effect of Rayleigh waves increases, the QTS will become lower due to the influence of Rayleigh waves in vertical component. As the amplification of bedrock (Hb) is equal to one (no amplification), this means the effect of Rayleigh wave in vertical component might cause the QTS to get amplification lower than one. However, the first order frequency is mainly consist of SH wave in the surface layer and its amplification factor can be calculated correctly (Nakamura, 2000).

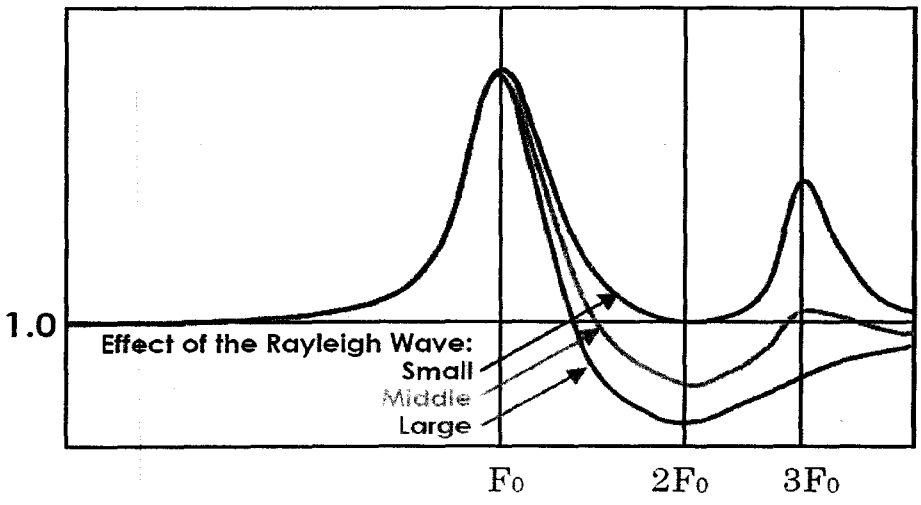

Figure 2.5: Effect of Rayleigh Wave on H/V Method (Nakamura, 2008)

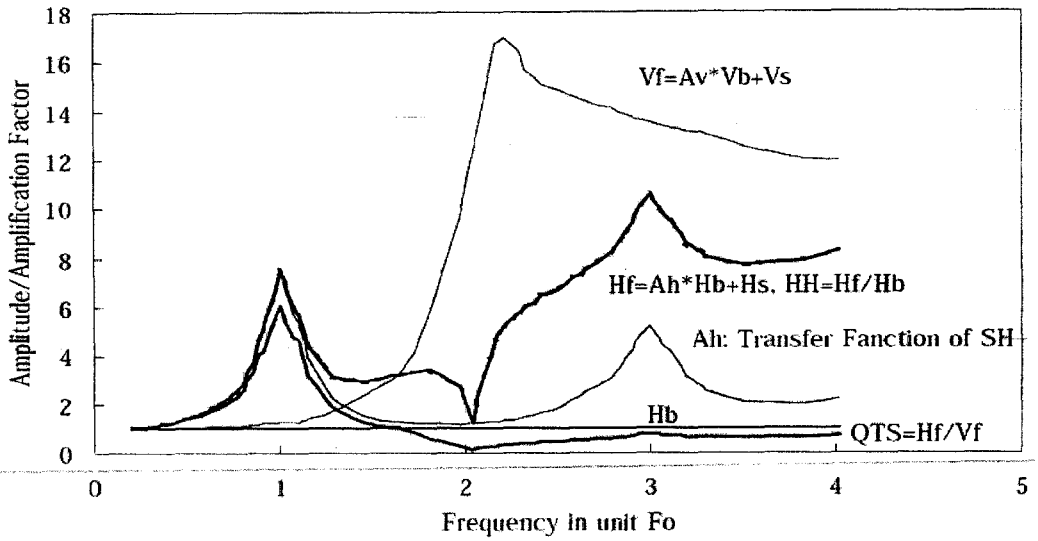

Figure 2.6: Comparison of Different Component of Microtremor Analysis (Nakamura, 2000)

2.4 Effect of Rayleigh Wave on H/V Method

The microtremor waves recorded by the equipment consist of various types of waves which include both surface and body waves. However, there is no confirmation found regarding the main contributing wave inside the microtremor. Assumption done by Nogoshi and Igarashi (1971) which proposed that there are similarities between the peak of H/V with the ellipticity of Rayleigh waves due to the resemblance of Rayleigh wave in vertical component (Figure 2.7). Besides that, the ellipticity of the Rayleigh wave also have a high enough impedance contrast between the surface and deep materials and this ellipticity is also frequency dependant (Nakamura, 2008).

However, Nakamura (2008) explains the relationship between H/V ratio and Rayleigh waves which concludes that Rayleigh wave does not have effect on H/V ratio. By modifying data from Nogoshi and Igarashi (1971), the relationship between H/V method and Rayleigh wave is clearly shown. From Figure 2.7, it is clear that during the peak of H, Rayleigh wave does not have high peak. However, the vertical component graph shown some similarities with Rayleigh wave which it shows peak about the frequency of about 13 Hz. While during the peak of H/V at 5 Hz, amplitude of Rayleigh wave is almost at minimal and Rayleigh wave only reach its maximum peak after H/V ratio graph lower than

its trough. Judging from this comparison, it is concluded that the peak of H/V is not caused by Rayleigh waves.

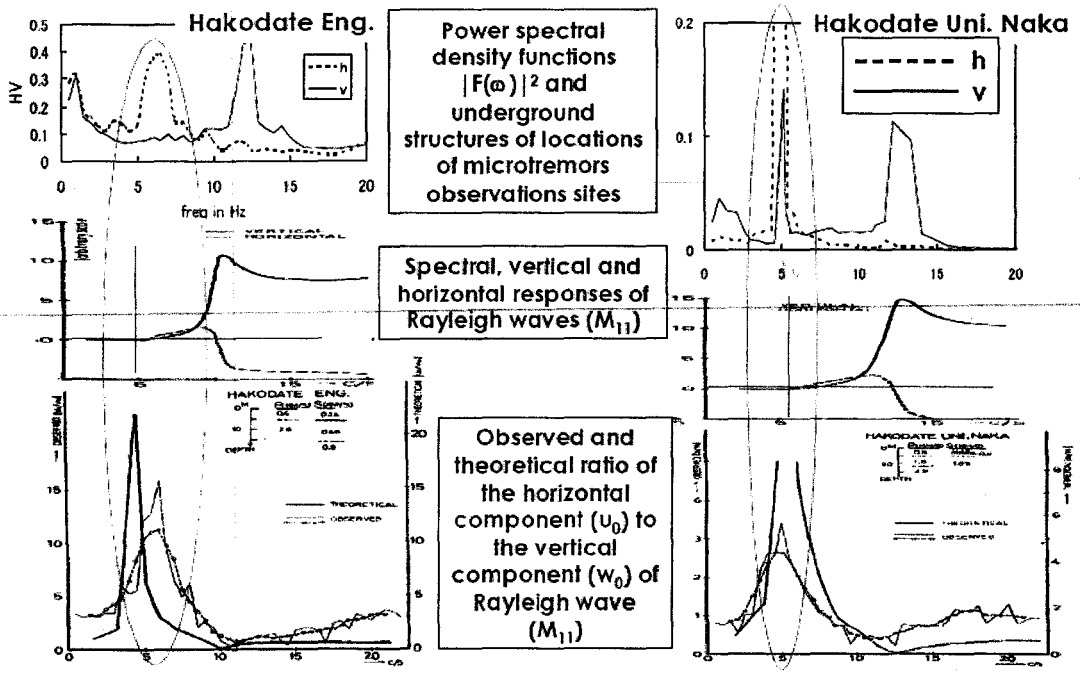

Figure 2.7: Explanation of Rayleigh Wave effects on H/V Method (Nakamura, 2008)

2.5 Accuracy of H/V Method on Strong and Weak Motions

Figure 2.8 illustrates the method of H/V used for various ground motions. The left figure (H/V of strong motion acceleration) shows two differences earthquake recorded at same station. Although both waveforms look different, the H/V ratios after process are similar. Hence, the results from both readings show consistency and proven that QTS can be used on ground on different time and result achieved will still be of use (Nakamura, 2000).

The usages of microtremor on different soil condition yield varying result depending on the density and characteristic of the soil. Figure 2.9 presents different QTS of different type of soil condition. It can be seen that QTS of alluvium ground have predominant frequency of around 2 to 3 Hz, where harder soil condition tends to have higher frequency of around 6 to 7 Hz. The amplification of softer soil is also lower compared to harder soil condition, which is 2.5 and 3.2 in this case (Theodufidis, 1995). The predominant frequency shown by

the comparison above concluded that softer soil will amplify the waves on lower frequency where as harder soil condition will amplify the soil on higher frequency range (usually more than 5 Hz). At the same frequency, harder soil condition will have lower amplification compared to softer soil condition. This matches the assumption where soft soil will amplify at higher period.

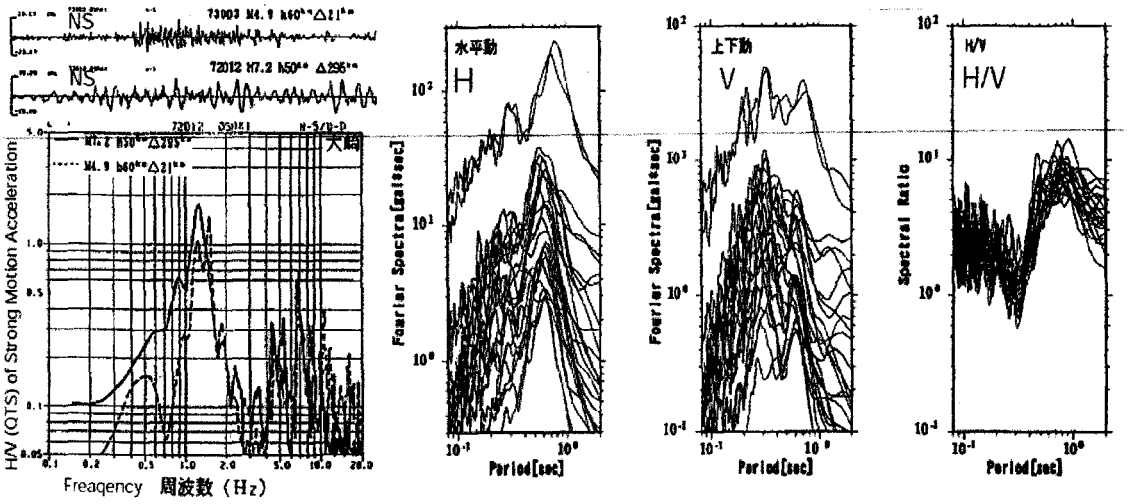

Figure 2.8: H/V Method done during different motion intensity (Nakamura, 2008)

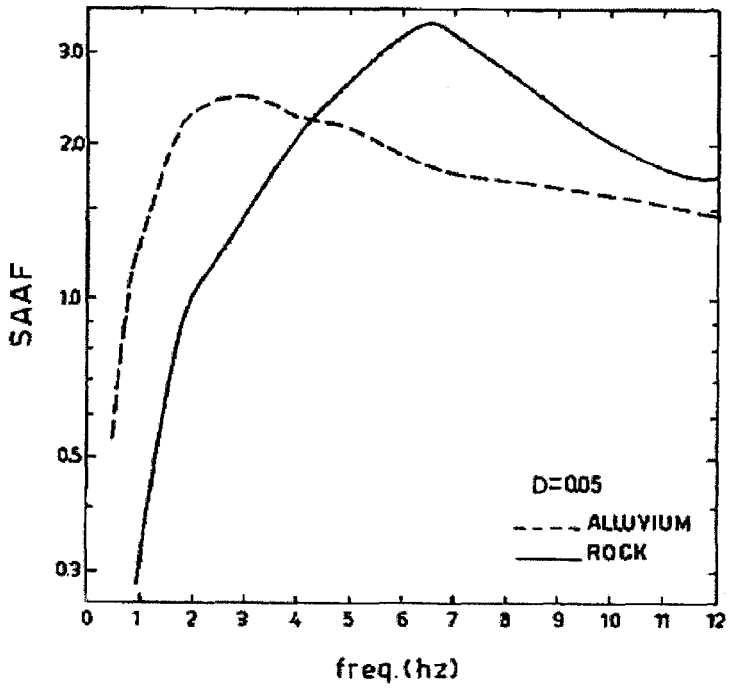

Figure 2.9: H/V Method on Different Soil Conditions (Theodufidis, 1995)

2.6 Reliability of H/V Method

Figure 2.10 shows the comparison between two data taken in different period of time. Thick lines resemble the data taken in year 1996 while thin black lines are data taken in year 1995. From the graph shown, it is found that the data from different year shows similarity. In point 39, even though the amplification factor of year 1996 is lower than 1995, the frequency of amplification is still the same as previous year. While at point 40 and 41, the lines are almost the same for both years. Hence, it is concluded that even though the data acquisition time varies, the result obtained shown consistency and will not varies excessively, especially for frequency of the soil.

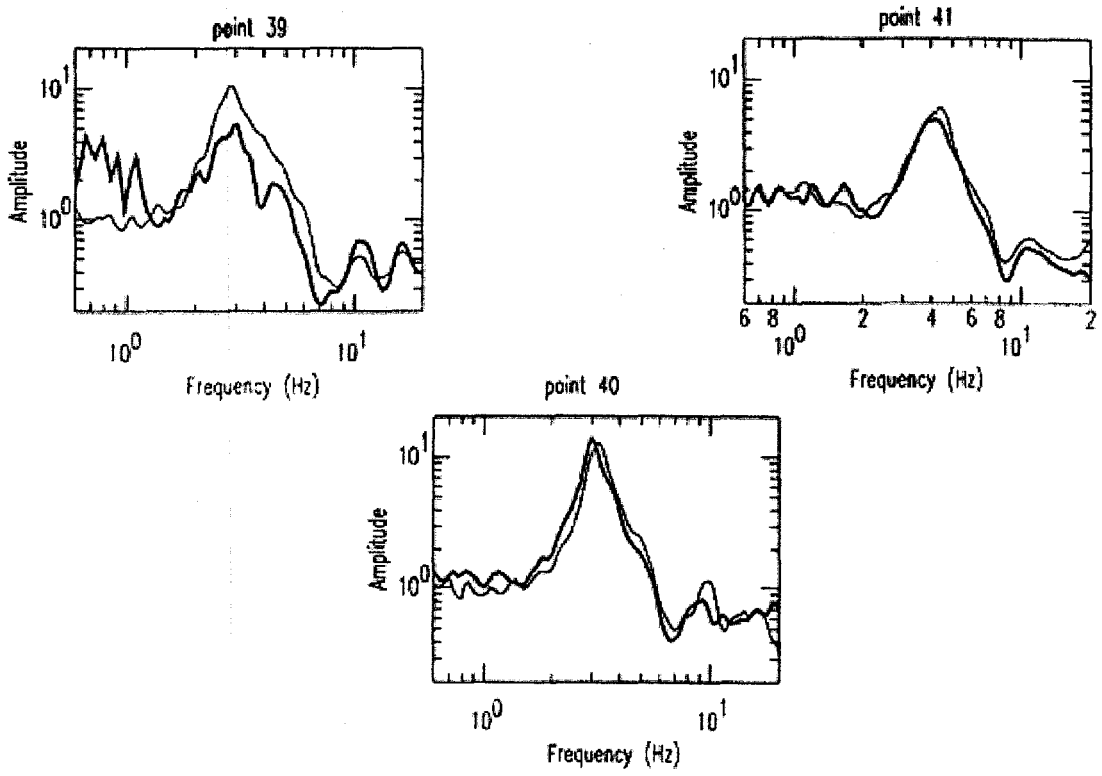

Figure 2.10: Microtremor Data taken in different time period (Bour et al., 1998)

Bour et al. (1998) has concluded that there are good resemblances between the two transfer methodology, by software SHAKE and QTS method (H/V Method). The figure above shows readings taken from France which includes both SHAKE and QTS method. In Figure 2.11, column 6 is derived from rock for both methods. Hence, the predominant frequency is higher, which is about 20 Hz via manual calculation. The SHAKE graph in the figure shown does not have a clear peak in the figure while H/V method also does not show

a clear indication of peak in the graph. Whereas in column 5, the H/V method varies by 1 Hz with SHAKE. For surficial formation of less than 10m thick, Nakamura method, also known as H/V method shows a close resemblance to SHAKE transfer while at thickness greater than 10 m; H/V method will show greater amplification of more than 50 %. Bour et al. (1998) has reported that H/V method is good for determining the fundamental frequency of soil and hence, would be able to help in producing predominant frequency map.

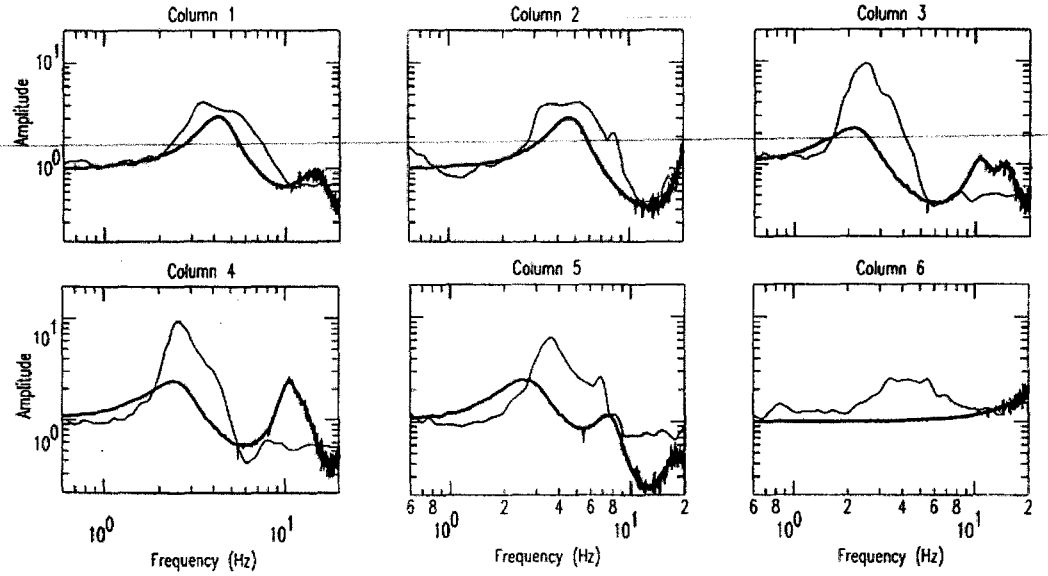

Figure 2.11: Comparison of H/V Method with SHAKE Transfer (Bour et al., 1998)

2.7 H/V Method on Alluvium Ground

Another research using microtremor analysis was done by Teves-Costa and Matias (1996) in Lisbon. Lisbon town has lies in a tectonic active area and has been receiving a lot of damages from previous earthquakes. The ground characteristic of Lisbon is mainly consisting of thin to shallow alluvium layer. The area of investigation is river shore and alluvial basin which have the alluvium depth of 5 to 40 m and 5 to 20 m, respectively.

Figure 2.12 shows borehole log of river shore locations where microtremor method will be used nearby those borehole log point. From the figure, the depth of alluvium can be roughly determined and therefore, correlation between the borehole logs and microtremor analysis result can be made. The general type of soil layer is mostly topped by alluvium, underlain by basalt and Miocene limestone follow by cretaceous limestone as bedrock.

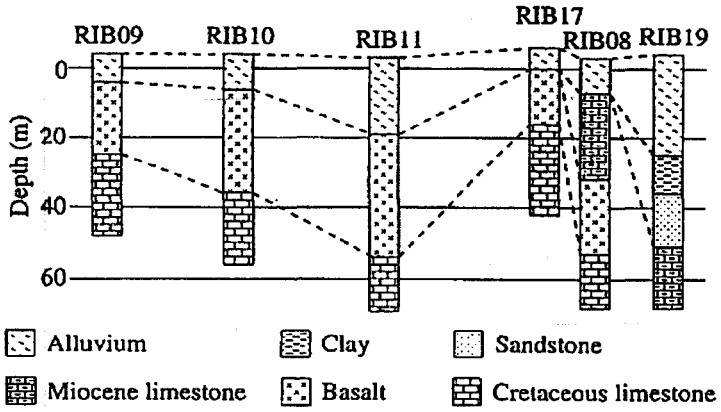

Figure 2.12: Soil Layer of Lisbon Town (Teves-Costa and Matias, 1996).

The results of microtremor analysis were shown in Figure 2.13. From the outcome of the analysis, it is shown that almost all of the predominant frequencies of the selected points show accordance with the borehole logs. Except for point RIB08 which has the dominant frequency is less than expected. As the most of the points have thicker alluvium compared to this point, it is suppose to have higher frequency. This phenomenon can be explained by the wrong estimation of soil layer as a single borehole log location might be insufficient to correctly address the layers of soil underneath the surface. Other than this location, cross checking with borehole logs shown beforehand shows that the result obtained from microtremor is consistent with the soil condition and therefore, microtremor analysis do have good potential and accuracy in determining the dominant frequency of soil.

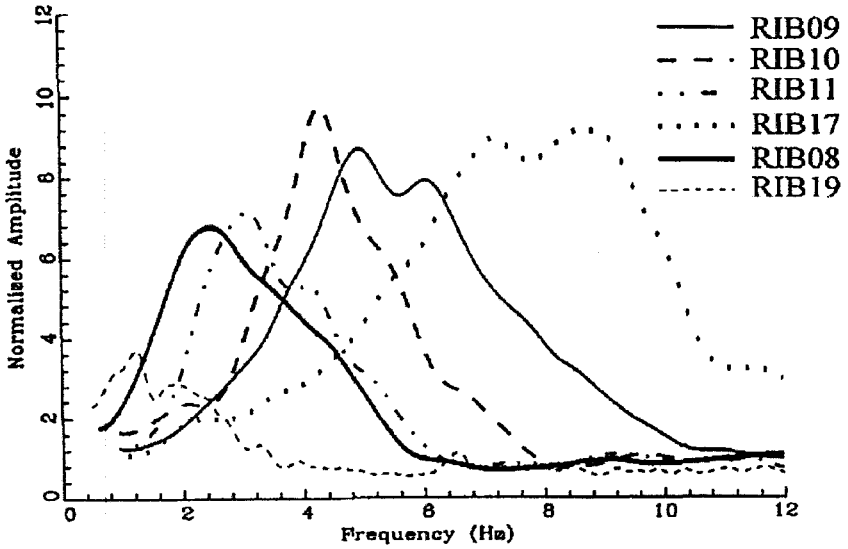

Figure 2.13: H/V Results for Lisbon Town (Teves-Costa and Matias, 1996)

2.8 Comparison of Different Types of Techniques

Ojeda and Escallon (2000) stated that microtremor is very useful in determining the frequency of soil. Two different methods, Kagami method and Nakamura Method were used to analyze soil characteristic in Pereira Colombia and the results are compared as shown in Figures 2.14 and 2.15.. From the results obtained, Kagami method was in good terms when it comes to both strong and weak motion. As for Nakamura's Method, the result shows some deficiencies when it comes to strong ground motion. However, during weak motion testing, the results are clear and accurate.

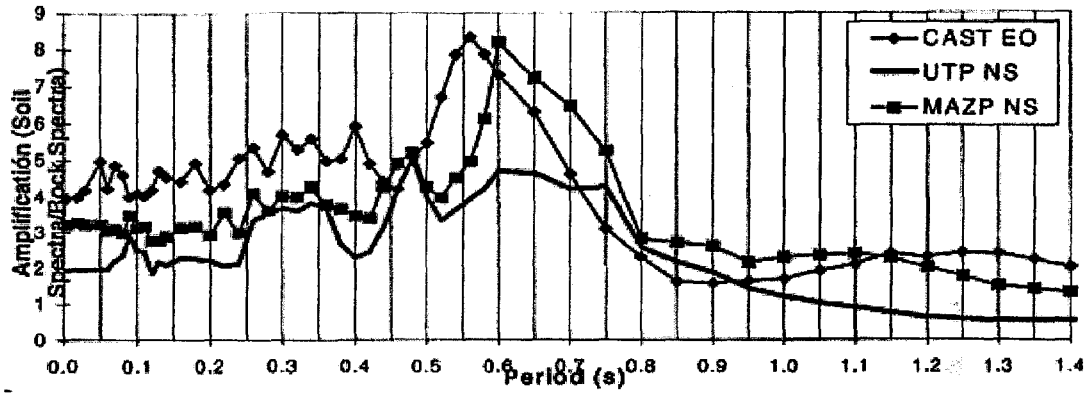

Figure 2.14: Kagami Method (Ojedaa and Escallon, 2000)

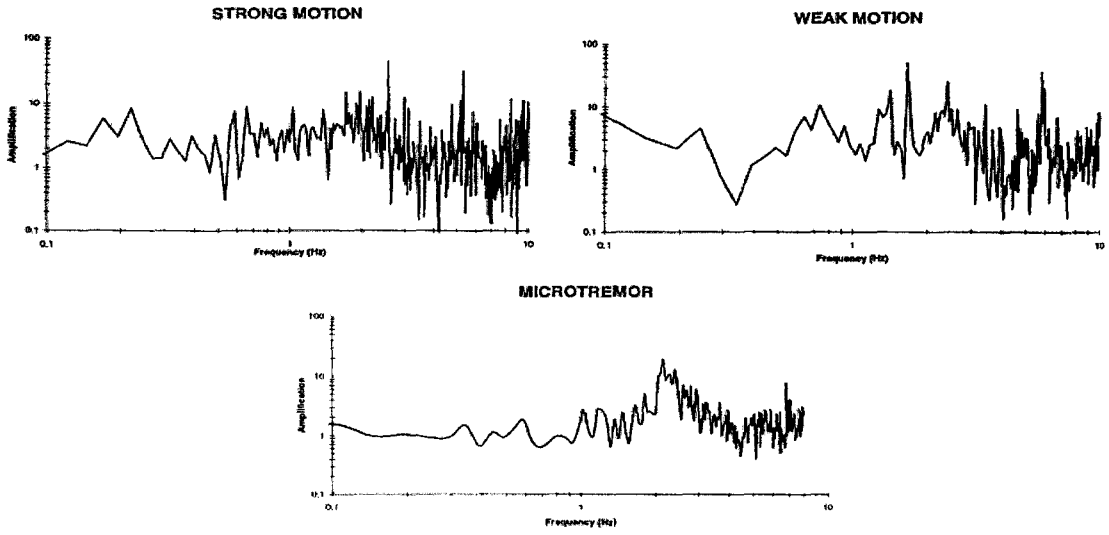

Figure 2.15: Nakamura Method (Ojedaa and Escallon, 2000)

2.9 Site Testing Using H/V Method

Mukhopadhyaya and Bormann (2004) has stated that there are three types of results obtained from the microtremor analysis for ground investigation in Delhi, India. The first type of result is graph with a lot of noise, as shown in Figure 2.16. Second type of result is graph with several peaks (Figure 2.17). Usually with the first peak having the highest magnitude and the following peaks will be considered as resonance peaks. The third type is graph with very clear peak and with least noise (Figure 2.18). The first two type of graph are usually on ground with thin layer of alluvium whereas the third graph is usually found on analysis done in ground with thick alluvium layer.

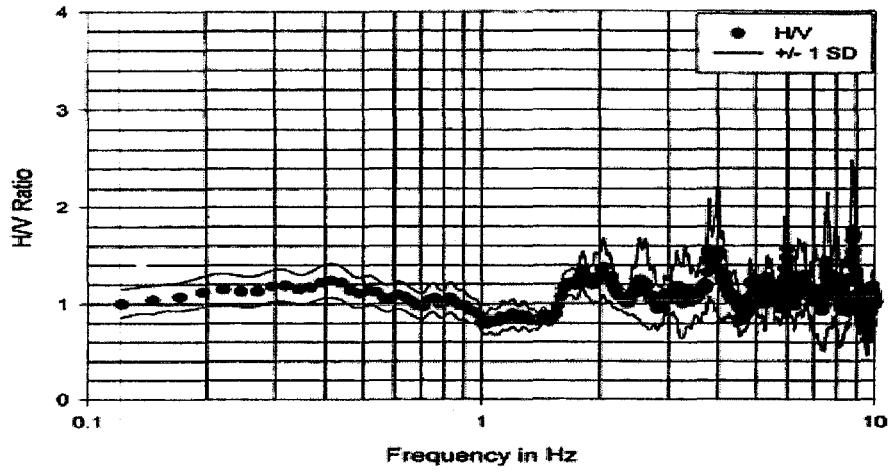

Figure 2.16: Result with noises (Mukhopadhyaya and Bormann, 2004)

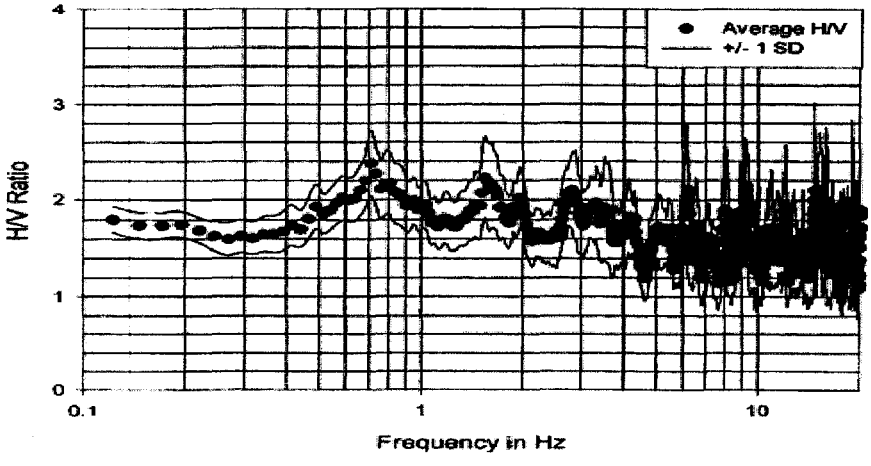

Figure 2.17: Result with several peaks (Mukhopadhyaya and Bormann, 2004)

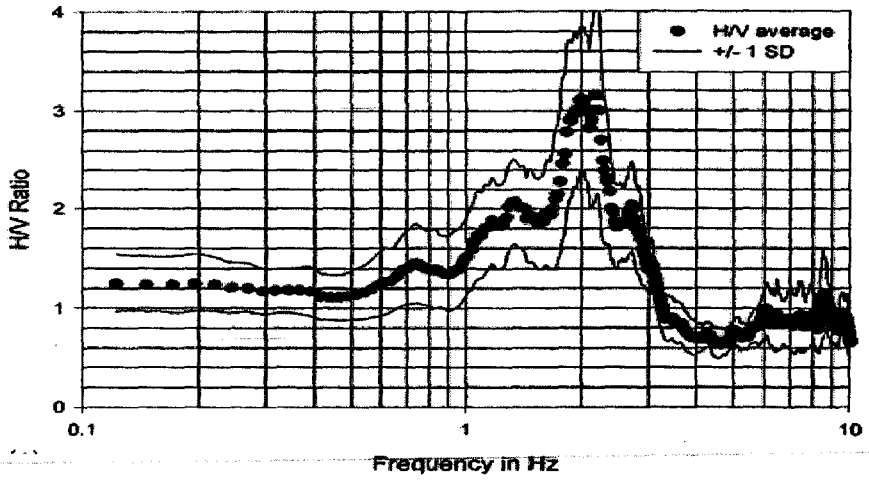

Figure 2.18: Result with clear peak (Mukhopadhyaya and Bormann, 2004)

From the application of H/V method, Mukhopadhyaya and Bormann (2004) has produced a microzonation map of natural frequency and soil amplification factor for Delhi, India (Figure 2.19). The findings shown in the frequency contour map are in correlation with the soil profile of Delhi where shallower alluvium layer have give out higher frequency while area with thick alluvium deposit such as area around Yamuna river have lower frequency recorded. The amplification factor obtained is within the range of 1.8 to 5.8. The dominant frequency acquired during normal condition was also compared with six earthquake data and the resonance frequency shows good matches with the reading taken during earthquake.

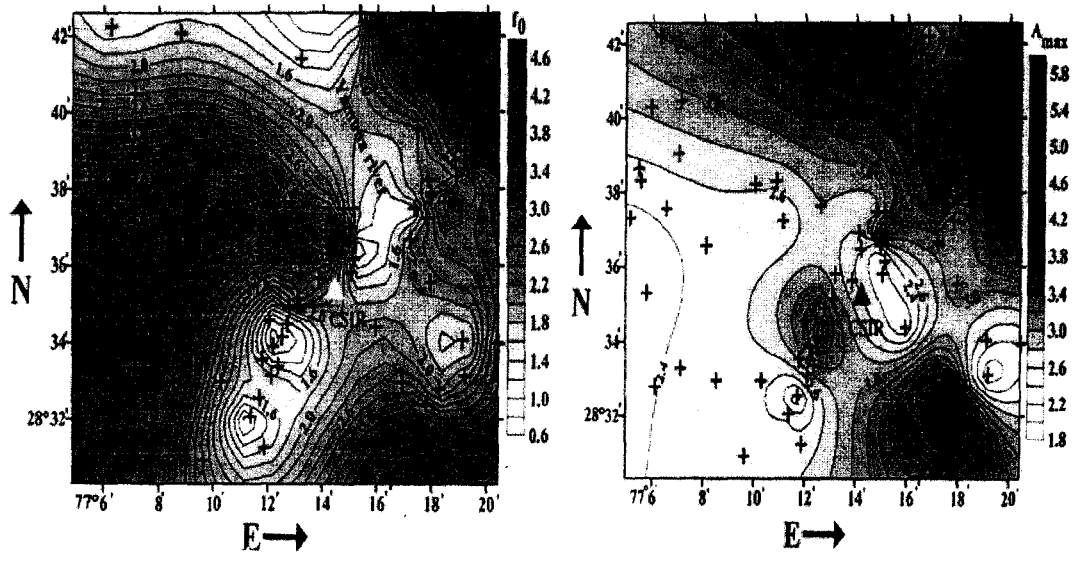

Figure 2.19: Frequency (left) and amplification (right) maps

(Mukhopadhyaya and Bormann, 2004)

The amplification factor map is done based on the level of amplification during the peak frequency of the soil. Therefore, to know the soil amplification effect on different frequency, map of amplification factor with fixed frequency can be produced.

Bovec basin in Slovenia has been struck by two major earthquakes in the past in years 1998 and 2004, causing extensive damages to the area. Bovec basin is majorly consisting of glacial and fluvial sediment. Figure 2.20 shows the geological map of Bovec basin. Microtremor analyses have been done on 124 points at Bovec basin and 20 buildings around that area and microzonation map for Bovec basin have been proposed by Gosar (2007). In the microzonation map, the frequency between 6 to 12 Hz is shaded as Microtremor analyses on most of the buildings have shown frequency of 7-11 Hz. Hence, the probability of resonance between building and soil at this frequency range. The frequencies obtained are closely related to the thickness of lithified sand-gravels and glacial moraine. The microtremor analyses for Bovec basin soil have shown frequency of 3 to 22 Hz where as the frequency of range 6 to 12 Hz occupies more than 60 % of the area. This reading has overlap with the majority of soil resonance frequency on Brdo and Mala. This findings in good terms with damage distribution during the previous earthquakes as Brdo and Mala have received most of the damages during the previous earthquakes. From the study done by Gosar (2007), it is concluded that the possibility of damages on buildings during earthquakes can be predicted by measuring the resonance frequency of both soil and building. However, more buildings need to be assessed in terms of the dynamic behavior, materials and other properties of structure in order to present a better conclusion. In this way, the soil structure resonance can be avoided by varying the dominant frequency of the building. Moreover, microtremor analysis is proven to be able to provide good estimation of soil resonance frequency in cold climate country with glacial sediments, helping to develop a microzonation for the mentioned location (Figure 2.21).

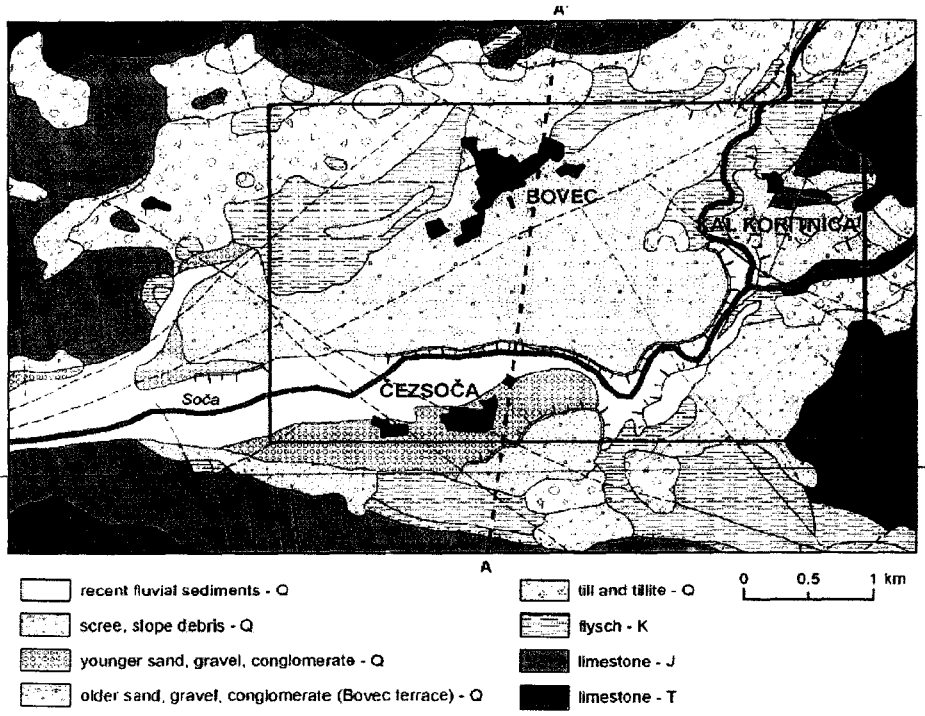

Figure 2.20: Mineralogy map of Bovec Basin (Gosar, 2007)

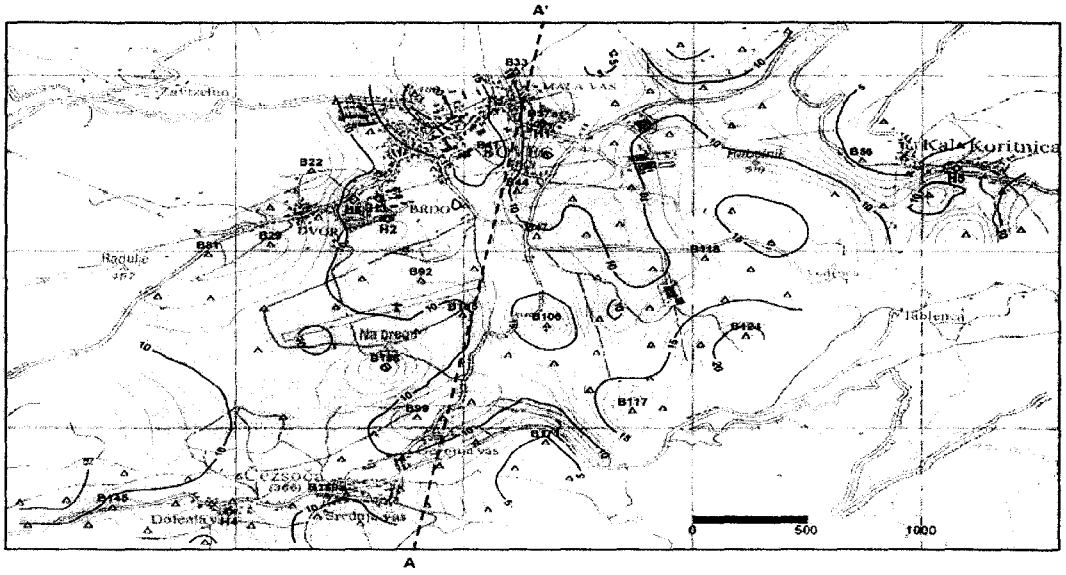

Figure 2.21: Microzonation of Bovec Basin based on frequency (Gosar, 2007)

2.10 Microzonation Mapping using H/V Method

The main purpose for microtremor study is to provide microzonation map of an earthquake prone area. Microzonation map constructed using H/V Method was done in various locations in the world with great accuracy in prediction of ground motion characteristic. In

order to construct a microzonation map, the natural soil period of the ground must be obtained. With the information of soil in hand, the microzonation map can be prepared.

Field et al. (1990) used microtremors to assess the potential earthquake site response for Flushing Meadows in New York City. Portable 5-sec period seismometers were used to record microtremor in a densely populated urban environment. The observed spectral peaks represented soil layer resonance in the site. Resonance frequencies predicted by one-dimensional modeling show good agreement with observations. Microzonation and site-response information were gathered for seismic hazard analysis. Similar study had also performed in Giumri (formerly Leninakan), Armenia (Field et al., 1995). It has been concluded that Nakamura's method may be a reliable procedure for determining the fundamental resonant frequency of sedimentary deposits.

Konno (1996) estimated the ground-motion characteristics using microtremor measurement at 546 junior high schools in 23 wards of Tokyo. Based on the spectral ratio between horizontal and vertical components of microtremor as known as Nakamura's method, the fundamental periods and amplification factors of the site had been estimated and the site periods and amplification factors in the area were mapped, as shown in Figure 2.22.

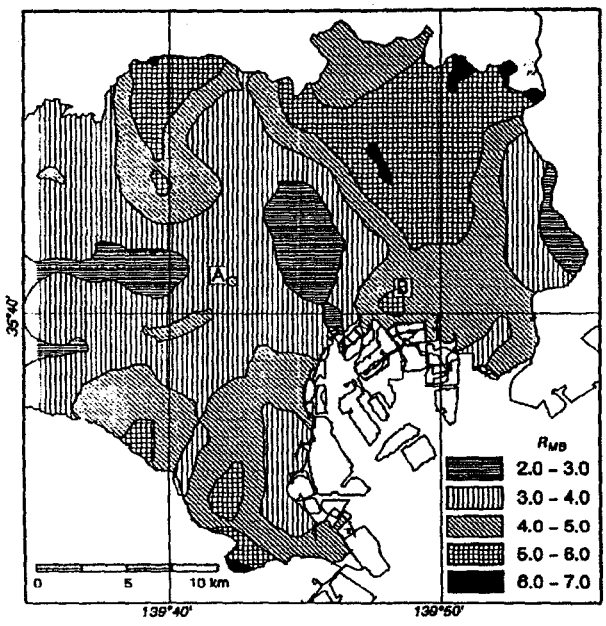

Figure 2.22: Microzonation map for Tokyo (Konno, 1996)

Microzonation study in the highly industrialized Cologne area (Germany) was conducted by Parolai et al. (2004) using microtremor and earthquake recordings from two field campaigns. Classical spectral ratio technique was applied and it is found that the spatial variation in the thickness of the sedimentary cover is reliably retrieved using the fundamental resonance frequency estimated from the peaks of the H/V ratio. The predominant periods of the ground at all the sites were determined from the H/V spectral ratios of microtremors and a microzonation map was developed on the basis of the variation of the predominant period of the ground. Panou et al. (2005) investigated the validity of the estimation of seismic site response characteristics from microtremor measurements in the downtown district of the city of Thessaloniki (Northern Greece). From the 250 observation sites, the fundamental frequency and amplification factor were estimated and mapped.

Tuladhar et al. (2004) have analyzed and predicted the predominant period of Hanoi, Vietnam using microtremor observations based on 63 sites scattered in the area. The microzonation map is plotted from the predominant obtained, as shown in Figure 2.23. The microzonation map agrees with the soft soil condition of Hanoi where the majority of map are of period of 0.4s and above as shown in Figure 2.24. This concludes the reliability of microtremor observations in helping to develop microzonation map.

Talchir Basin in India is rich in coal deposits and have a maximum sediment thickness of 1500 m. A study for ground motion characteristic was done at 35 stations in Talchir Basin. This method was chosen due to its cost effectiveness and require relatively short amount of time. The microzonation map of natural soil frequencies constructed is shown in Figure 2.25, where the dominant frequency inside the basin are shown to be in the range of 0.3 to 2.4 Hz, where as the borders of basin which the ground are mainly consist of hard rocks shows higher frequency of 7.8 Hz. The amplification factor inside the basin are within the range of 3 to 9. However, Walling (2009) has concluded that the amplification factors need further clarification for ground behaviour during strong ground motion. Generally, the microtremor analysis shows good correlation on the ground properties and will be able to contribute well in seismic hazard studies.

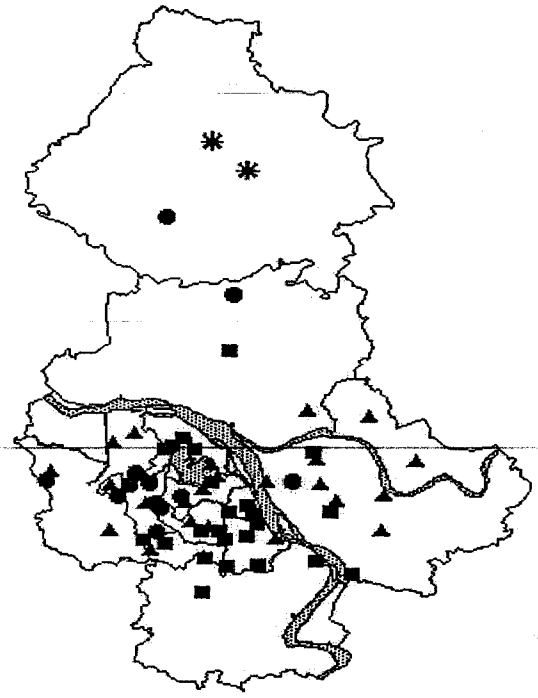

Figure 2.23: Observation points in Hanoi (Tuladhar et al., 2004)

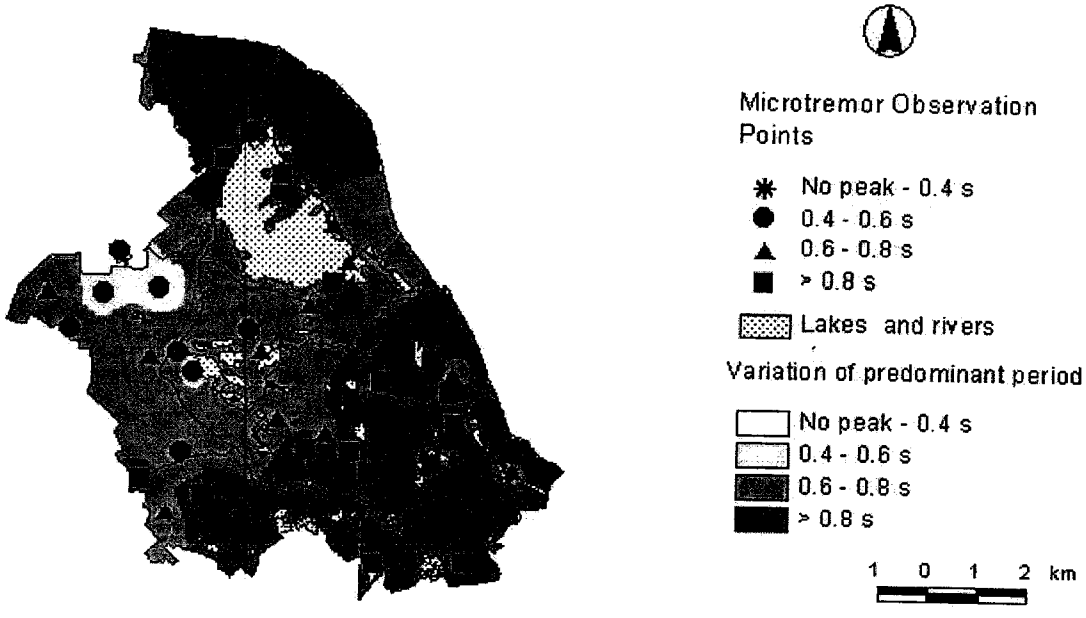

Figure 2.24: Microzonation map of Hanoi based on predominant period (Tuladhar et al. 2004)

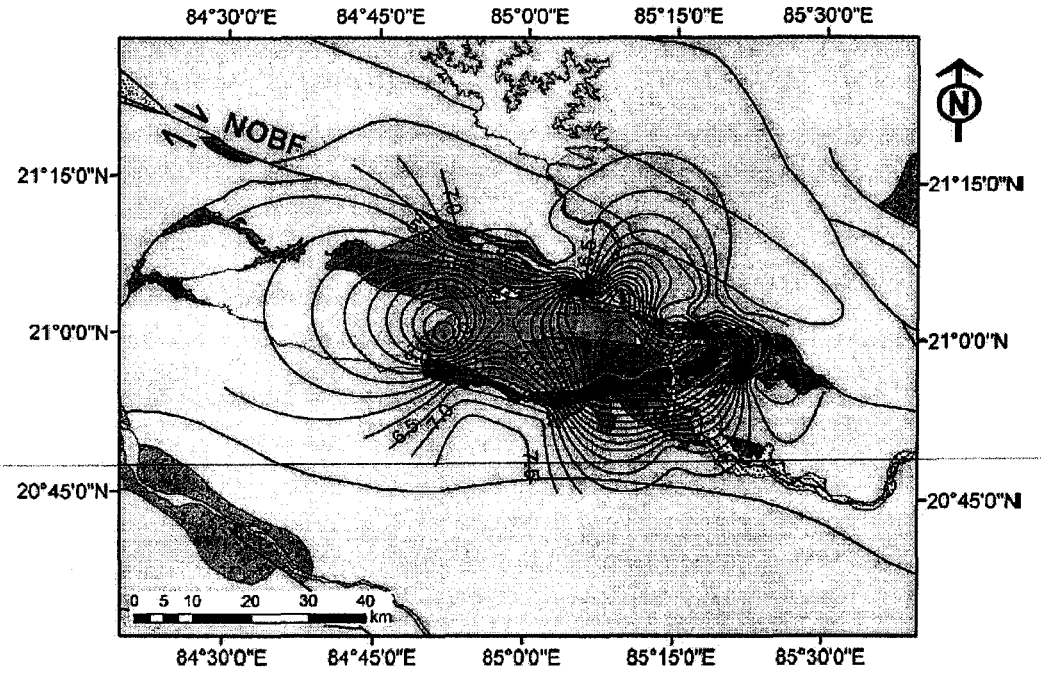

Figure 2.25: Frequency map of Talchir, India (Walling et al., 2009)

Mexico City lies in alluvium basin which amplifies greatly during earthquake strikes. This can be seen during September 1985 earthquake which have taken over thousands of live and resulted in collapse of buildings. To determine the ground motion characteristic of Mexico City, Lermo (1994) have conducted microtremor tests in Mexico City. Total of 409 testing points were scattered evenly in Mexico city and were tested. The microzonation map of Mexico City is then produced from the predominant soil period obtained from H/V Method, as shown in contour map format in Figure 2.26. The results obtained show that most of the areas are within the period of 0.5 to 4 s, with most of the area falling into 1 to 2 s. There are also comments where the destruction during 1985 Earthquake is mainly due to the resonance frequency of soil with the frequency of building as the dominant frequency of soil is fairly low and this poses high threat to high rise buildings.

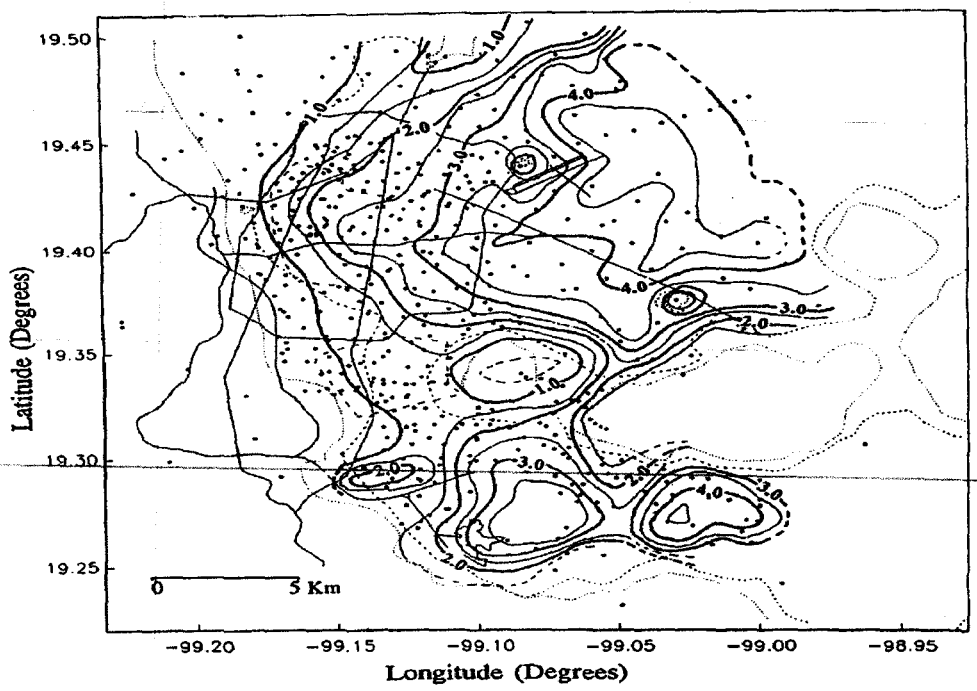

Figure 2.26: Frequency map of Mexico City (Lermo et al., 1994)

From this study, the author have also commented that on period of 0.5 to 2.5 s, there is a linear relation between Amplification and Period which suggest that S-wave velocity are more important that variation in thickness. Also, the damping of soil layer was 5 % and site response analysis should increase the damping effect of soil layer. However, for strong motion data recorded, the empirical transfer functions shows good correlation with microtremors analysis. In conclusion, microtremor was able to help to construct a more robust and detailed map of predominant period of Mexico City.

Another example of microzonation map is shown in Tuladhar (2004). More than 150 sites detail have been recorded via microtremor and the result of the microzonation map in Figure 2.27 shows that majority of the area are from 0.8s to 1.2s which are considerably high. The result from microtremor analysis is compared with SHAKE transfer and good correlations are report from the comparison process. This further strengthens the reliability of H/V Method in use of microzonation mapping.

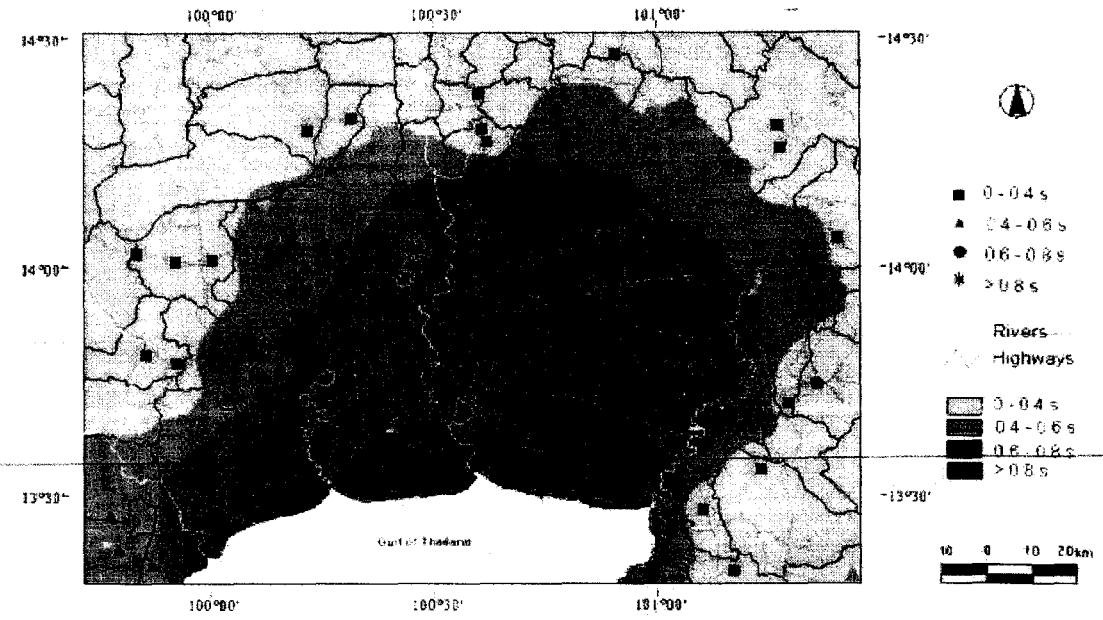

Figure 2.27: Microzonation map of Greater Bangkok on the basis of variation of predominant period (Tuladhar et al. 2004)

2.11 H/V Method Analysis Details

To acquire enough information of soil from microtremor analysis, recording time is crucial to determine the precision and accuracy of the outcome. In most of the journals review, the interval for data acquisition time is approximately 3 to 10 minutes. The window is then split into smaller interval of 15 to 50 seconds. The results of different window of 15 seconds, 20 seconds, 30 seconds and 50 seconds are shown in Figures 2.28 to 2.31, respectively. From the different interval chosen, it is observed that the choosing of different interval for analysis window does not affect the result as the graphs still show clear indication of peaks and trough. The microtremor analyses based on different recording interval are compared as shown in those figures.

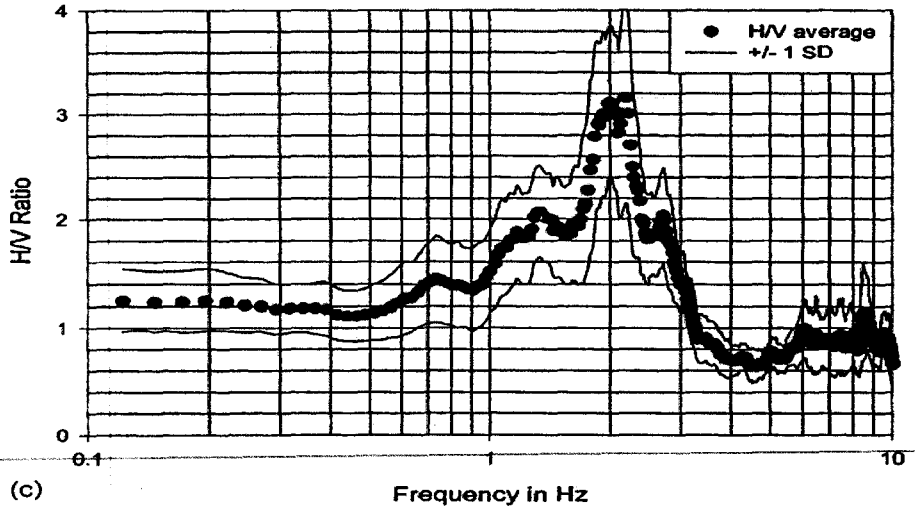

Figure 2.28: 15 seconds window (Mukhopadhyaya and Bormann, 2004)

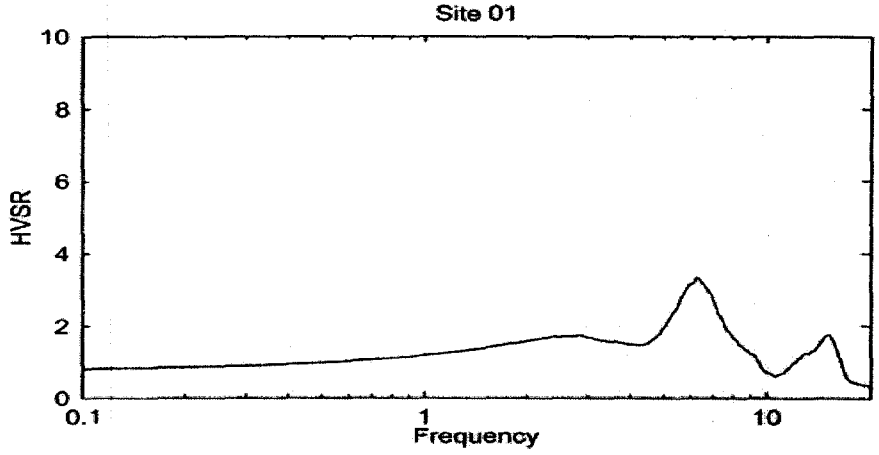

Figure 2.29: 20 seconds window (Walling et al., 2009)

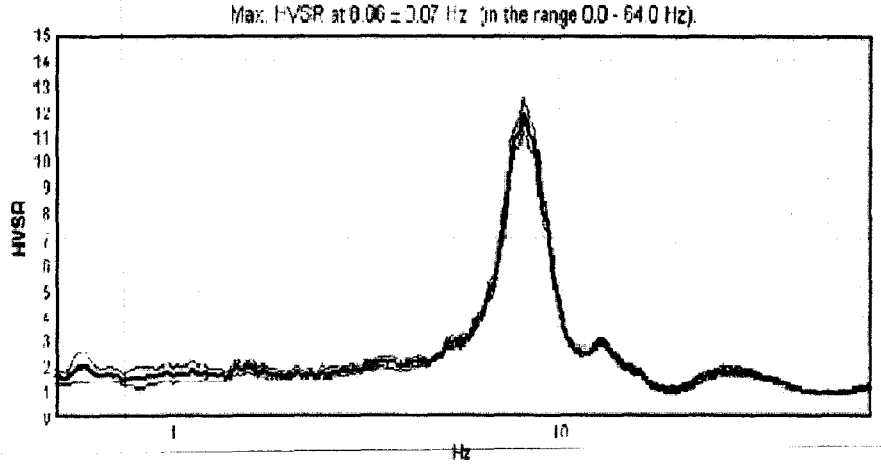

Figure 2.30: 30 seconds window (Gosar, 2007)

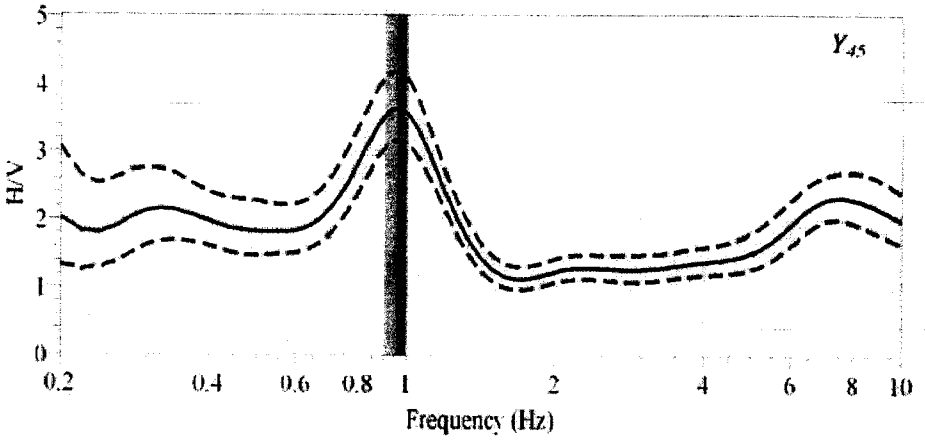

Figure 2.31: 50 seconds window (Fnais et al., 2010)

CHAPTER 3
RESEARCH METHODOLOGY

3.1 General

Microtremor measurement was carried out using high sensitivity vibration sensors at various observation points in Penang Island. Field works were conducted in six stages, covering two districts on Penang Island. The measuring instrument consists of a velocity sensor, a data logger, a GPS antenna and a data acquisition system. A sensor was placed on the ground surface of the observation point or the building to measure the ground motion in three directions (two horizontal components and one vertical component) at the same time for five minutes. After field measurement, Fourier spectrum for each component was calculated. Frequency spectrum of one component was estimated by averaging the three Fourier spectra. Then, from a spectral ratio of horizontal to vertical components, QTS (Quasi-Transfer Spectrum) was calculated. Predominant period / frequency and amplification level which represent dynamic characteristics of the observation points were then obtained and mapped for seismic microzonation purpose.

In order to enhance the physical background of QTS, microtremor array observations were commenced in August 2012 through the collaboration with Professor Hitochi Morikawa and his students from Tokyo Institute of Technology, Japan. Since this is the inaugural microtremor array observation in Penang Island, several students from Universiti Sains Malaysia had taken part in this fieldwork. The required instrumentations were brought from Japan. The recorded data were analyzed and the detailed information of shear wave velocity profile of the observation point was obtained.

Figure 3.1 illustrates the overview of the research methodology. Generally the study can be categorized into three main stages, i.e. desk study, data collection and data analysis. The results of this study are essential for design of structures subjected to earthquake ground motion. Based on the outcome of this study, the vulnerability of the site and the dynamic characteristics of the building can be evaluated.

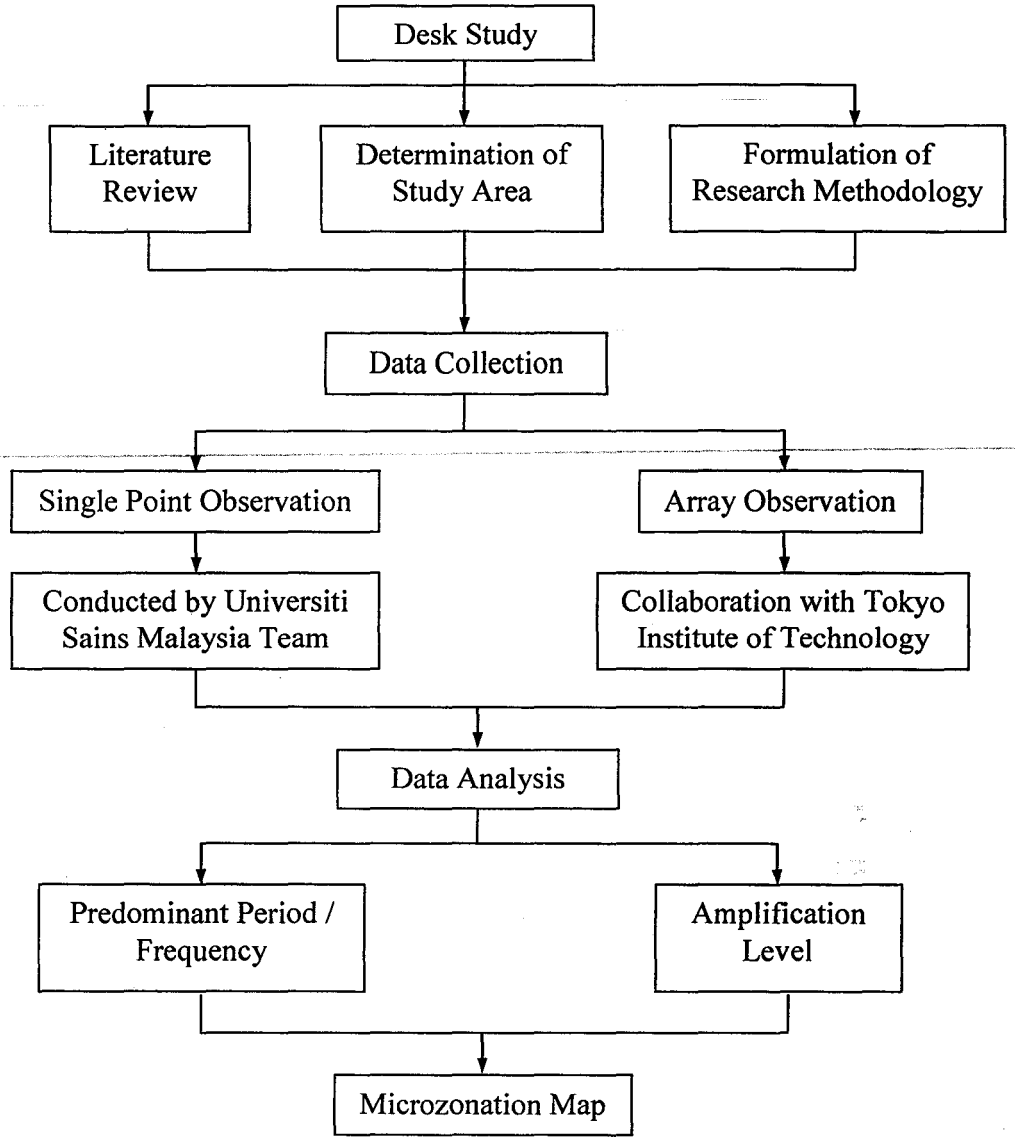

Figure 3.1: Research methodology

3.2 Desk Study

At the onset of the project, the study location, observation points, method and materials of fieldwork and analysis were determined. These had been done through literature review on past studies in other countries and also taken consideration of the requirement and constraint of the current project.

3.2.1 Determination of Study Area

Penang Island, the most developed and economically important state in Malaysia, had been selected as the study area due to the lack of understanding to its dynamic ground characteristics and its location close to Universiti Sains Malaysia Engineering Campus. The first step to choose the study location was examination the geological features of Penang Island. This was done by visiting the geological map stipulated in the local mineral resource map as shown in Figure 3.2.

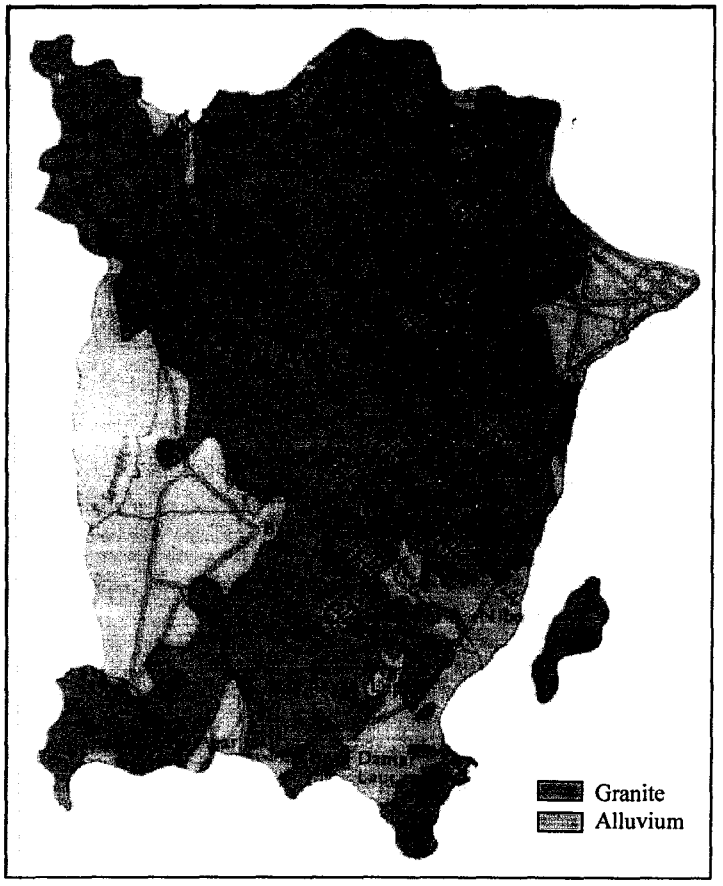

Figure 3.2: Mineral resource map of Penang Island (JUPEM, 1983)

From the map shown in Figure 3.2, it can be seen that most of the areas in Penang Island are consisted of granite except major parts of Georgetown, Bayan Baru, Bayan Lepas, Teluk Kumbar and Balik Pulau in West Penang Island areas are mainly formed by alluvium ground layer. There are a lot of high rise buildings constructed in these two areas including Komtar building, the Penang highest building with total of 65 floors. Other than that, most of the occupants in highrise buildings in these areas had reported to experience shaking and

discomfort during previous earthquakes that strikes Sumatra. These further strengthen the need to investigate the ground motion characteristic of these areas.

3.2.2 Determination of Observation Points

From previous studies, the density of observation points varies in range of 100 m to few kilometers depends on the site condition. With less contrast of soil type between two points, the points can be more scatter around while if the soil properties changes drastically in a short distance, denser data observation points are need to provide better understanding and illustration of the characteristic of site. Grids are built to allocate the observation points around the research area. The use of grids helps the site observation with good coverage of research area. In this study, the distance apart from each observation point was set to be 500 m to 1000 m. Figure 3.3 shows the grid line constructed for Georgetown area.

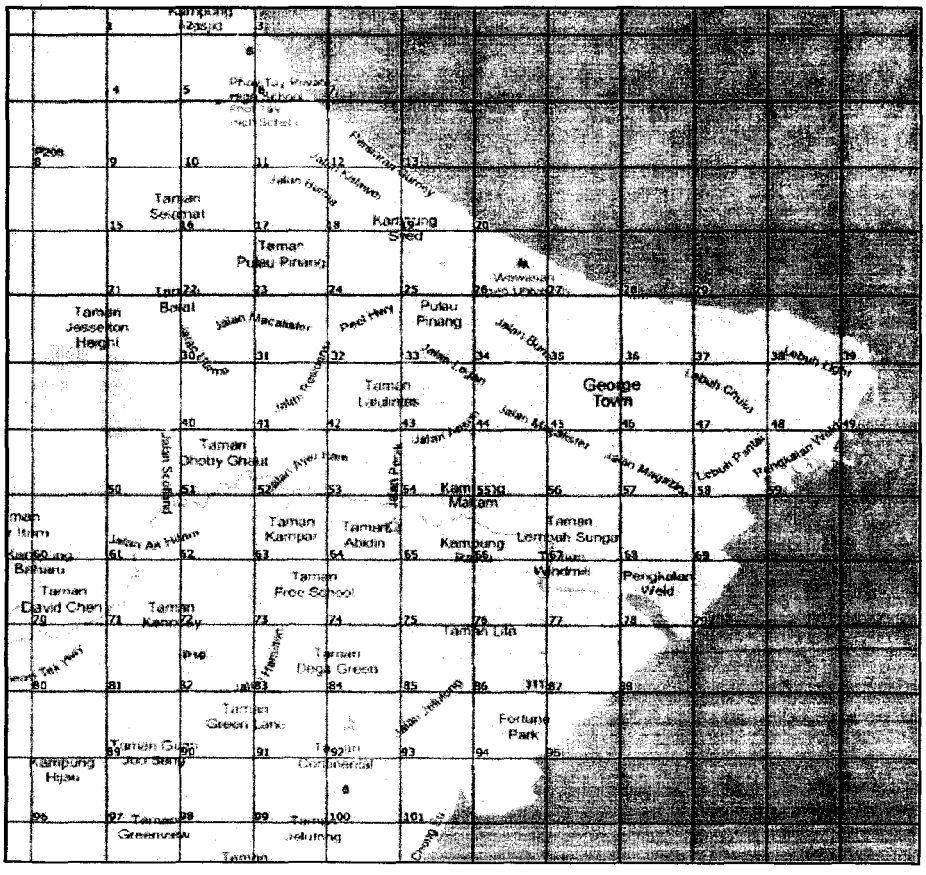

Figure 3.3: Constructed grid lines in Georgetown area

3.3 Data Collection

Data collection is the main part of this study. To determine the dynamic characteristics of ground motion in Penang Island, the primary data of ground vibration is essential to be obtained and analyzed. For this study, microtremor data is recorded by appropriate instrument due to no microtremor data available for Penang Island. A unit of microtremor measuring instrument consists of a high sensitivity of velocity sensor, GPS antenna and data logger was purchased. Therefore, USM team conducted single point observation and array observation was carried out with the technical and manpower supports from Tokyo Institute of Technology.

3.3.1 Instrumentation

Field observations are done solely using microtremor measuring instrument as shown in Figure 3.4. The equipment consists of a KINKEI type velocity sensor, ITK type data logger and a GPS antenna to provide GPS time. The technical specifications of velocity sensor are given in Table 3.1.

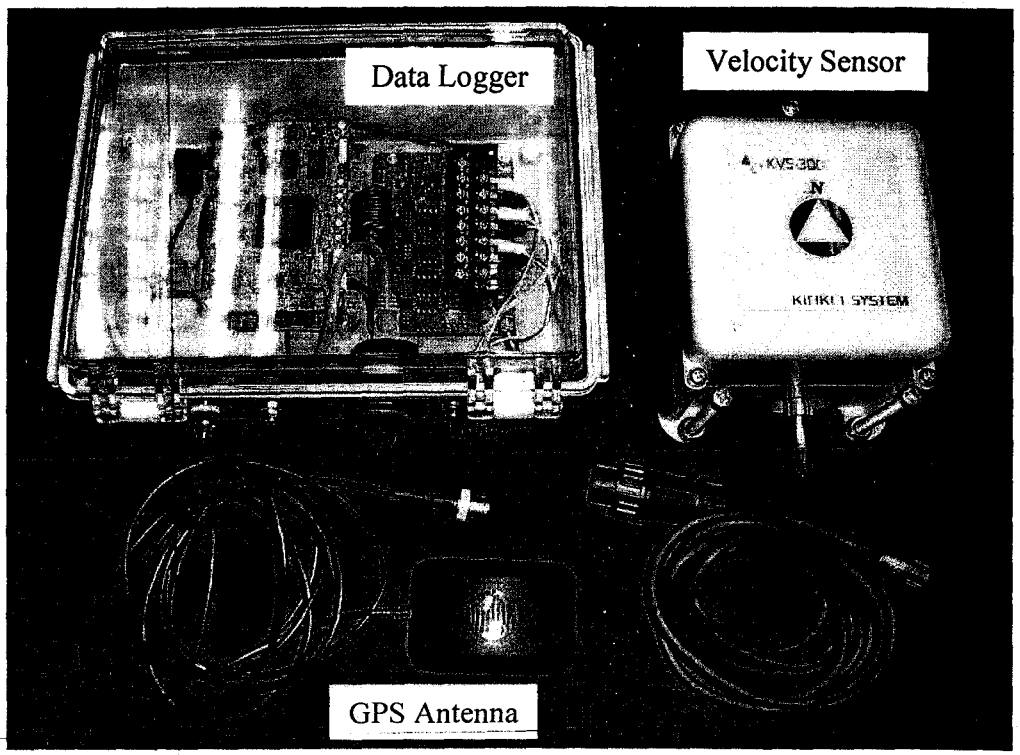

Figure 3.4: Microtremor measuring instrument

Table 3.1 Specifications for KINKEI KVS-300 velocity sensor

Dimension	104 (W) x 104 (H) x 104 (D) mm (Adjustable height)
Weight	About 1.5 kg
Sensor Type	Moveable Coil
Measuring Composition	3 components (X, Y, Z)
Predominant Frequency	1.9 Hz – 2.1 Hz
Sensitivity	Above 0.8 V/kine
Damping Ratio	0.7 (When connected to an external 100 kΩ wiring)
Shunt Impedance	Built-in
Environmental Condition	-20^0C – + 55^0C
Amplitude Measurement Range	±2 mm (Range of movement 5.4 mmpp)
Moveable Mass	29 g – 40 g
Coil Resistance	7000 Ω -7700 Ω
Waterproof Performance	IP65 Protection Level

3.3.2 Single Point Observation

Single point observation using microtremor instrument was carried out from April to August 2012. A total of 379 points were measured in Penang Island. The observation points are located within 500 m to 1000 m apart. The sensor is placed on the ground to measure the ground motion in three directions at the same time. Data logger records microtremor reading for three to five minutes. During the recording of the ground motion data, disturbance or undesired signal should be avoided. Figure 3.5 shows the setting up of the microtremor instrument during field observation.

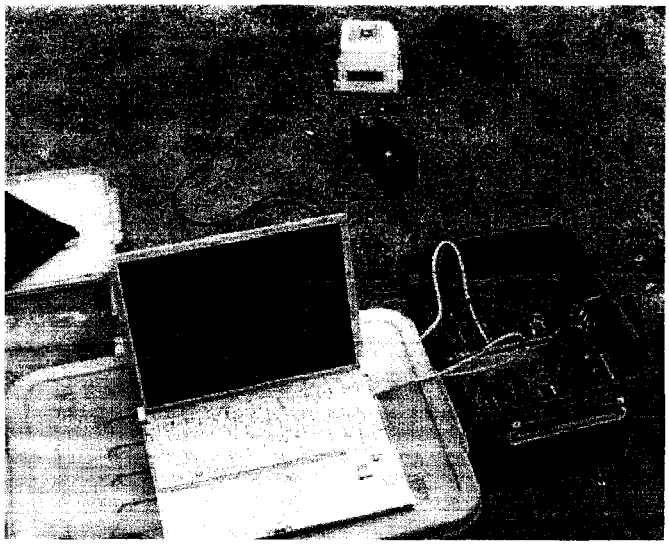

Figure 3.5: Single point observation using microtremor instrument

3.3.3 Array Observation

Microtremer array observation is carried out to measure the ambient vibration of ground surface caused by both human activity and natural phenomena. The recorded data is employed for the delineation of subsurface structure of the ground by exploiting the S-wave velocity. The basic procedures of estimating the subsurface structure are the array observation on the ground surface at the intended sites, estimation of dispersion of the recorded surface wave and estimation of subsurface structure of the site by means of inversion. This research is proposed to conduct extensive microtremor array measurement and study the analysis method of the microtremor array observation data using Spatial Autocorrelation (SPAC) method. A minimum of four sensors is needed to form an array network as shown in Figure 3.6.

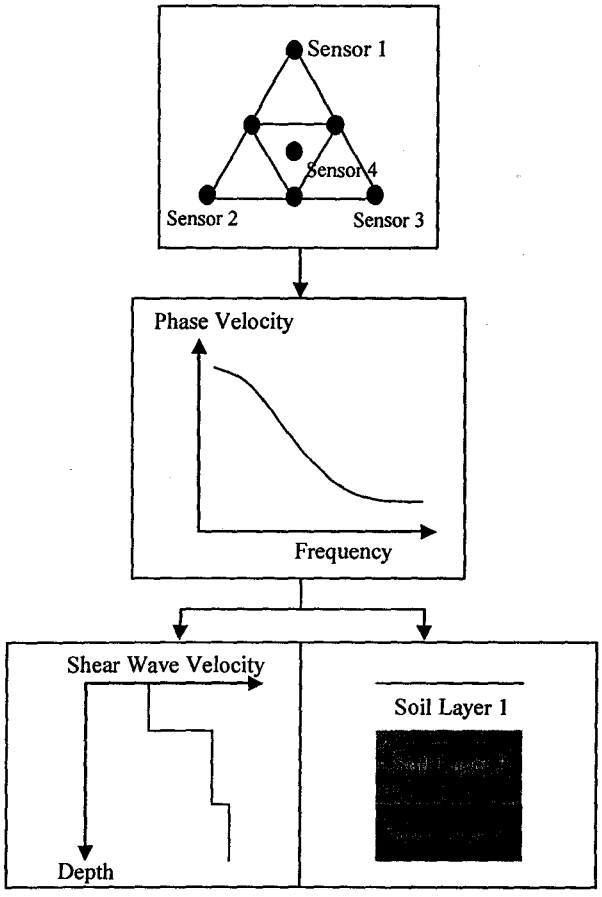

Figure 3.6: Procedure of microtremor array measurement

Microtremors are highly variable temporally and spatially due to the complex sources, path medium and site condition. Microtremors are dominated by surface waves. Since the

velocity of surface waves varies depending on the frequency or period, dispersion of surface wave, which is in the function of subsurface structure, is used to estimate the subsurface structure of the ground by exploiting the S-wave velocity. Through standard procedure and instrumentation used in the array observation network, the phase velocity frequency dispersion curve is determined as a response to the structure underneath the observation sites. The subsurface geological structure is then estimated by means of inversion.

Microtremor array observation is conducted together with the team from Tokyo Institute of Technology comprising Professor Hitoshi Morikawa, Mr. Shohei Hamasaki, Ms. Yumiko Ogura and Mr. Shohei Nakamura from 1 to 11 August 2012. The purpose of this survey is to estimate the substructure of the ground in selected sites in Penang Island. The array observation is carried out at 16 sites in the eastern part of Penang Island. Two or three types of triangular array networks with the radii varies from 1 m to 73 m are formed based on the condition of the site. Four velocity sensors are used in each array observation. The recorded data were then analyzed using the program developed in Morikawa Laboratory, Tokyo Institute of Technology.

3.4 Data Analysis

After the measurement, the recorded data by the data logger are converted into ASCII format and retrieved using the data acquisition system. A program was written in MATLAB to process the recorded data from microtremor instrument into H/V spectrum. The velocity data loaded into MATLAB program are split into two sets of data with 30 seconds record each (Figure 3.7). Only the data which does not have sudden spikes and discontinuity are used. The noise induced nearby data recording point may cause inaccuracy of the calculated H/V ratio. The data are then used to plot out a graph of recorded velocity versus time. This step is done to check the quality of data and occurrence of noises. The data is differentiated with respect to time to obtain acceleration time history of the recorded data. Then, the acceleration data are processed using Fast Fourier Transform to obtain the power spectra of the data in their respective axis (Figure 3.8). The Fourier amplitudes in X and Y horizontal components are merged together using this formula:

$$H = \sqrt{\frac{X^2 + Y^2}{2}} \tag{3.1}$$

After that, the merged horizontal component is divided by vertical Z component to obtain H/V spectral ratio versus frequency. The graph obtained is then used to determine the predominant frequency of the soil and also the soil amplification level.

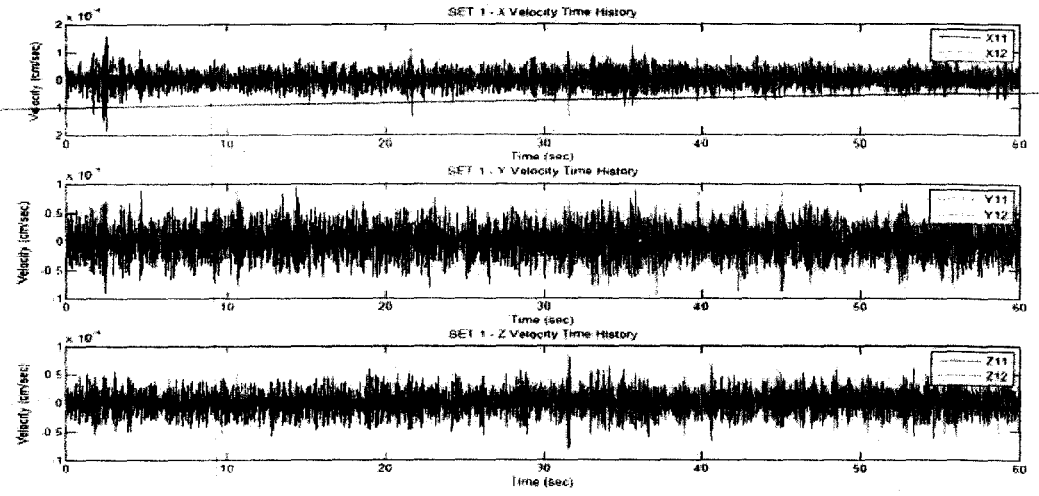

Figure 3.7: Recorded velocity time history for X-component (top), Y-component (middle) and Z-component (bottom)

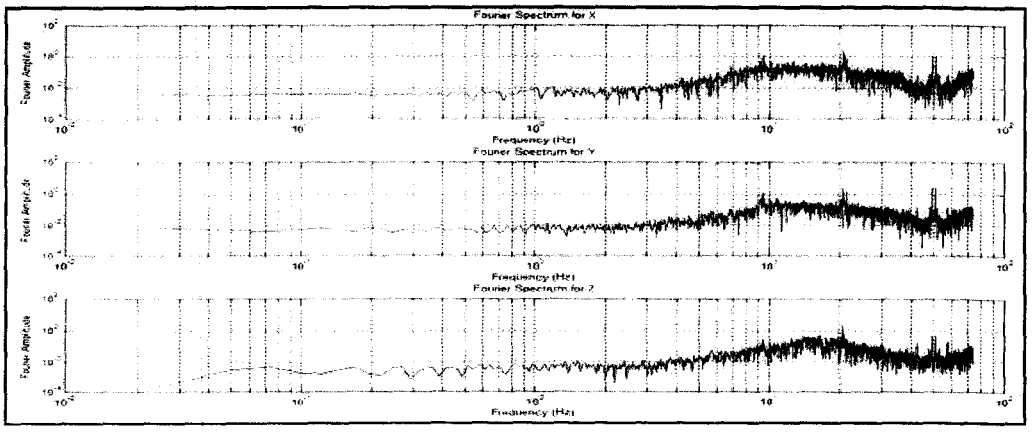

Figure 3.8: Example of Fourier spectra obtained

After dividing horizontal component with vertical component, the result obtained will be a graph with a lot of spikes (Figure 3.9). To enable better locating of peak, smoothing of graph will be required. There are various methods used by researchers around the world to smooth the H/V result. Few of the famous smoothing functions used are Parzenwin, Konno

and Ohmachi (1998) algorithm and moving average approach. The selection of smoothing kernel has slight effect on the curve. The most important factor in smoothing the graph is the bandwidth used to smooth the graph. If the bandwidth use is too high, it leads to over smoothing of graph, resulting in loss of original peak while if the bandwidth used is too low, the smoothing effect is not sufficient to give a clear view of the curve.

After some trial and error, it is decided that bandwidth of 5% of frequency will be used. Kernel density estimation, which is non-parametic method, will be used. There are several types of kernel available, such as Gaussian, Linear, Cauchy and Tricubic. The smoothing kernel that will be used is tricubic kernel which enables the peak of the H/V curve to be preserved better than other kernels. The results of smoothing are shown in Figure 3.8, where the cyan line is the unsmoothed graph and black color line is the smoothed data.

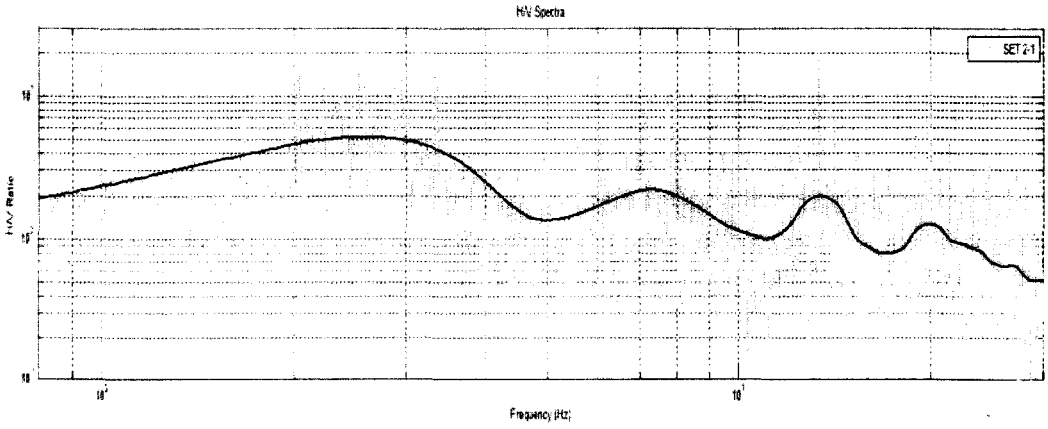

Figure 3.9: Smoothing the graph

The method to obtain amplification level and predominant frequency of the ground is fairly simple. Referring to Figure 3.10, the first step is to locate the first peak of the graph, then the H/V ratio and Frequency of that point is then located from the graph. The obtained value is the soil amplification value and also the predominant frequency of the site. There will be peaks following the first peak. However, those are also known as the secondary frequency and it is not of concern in this research. The frequency obtained from the inverse of period.

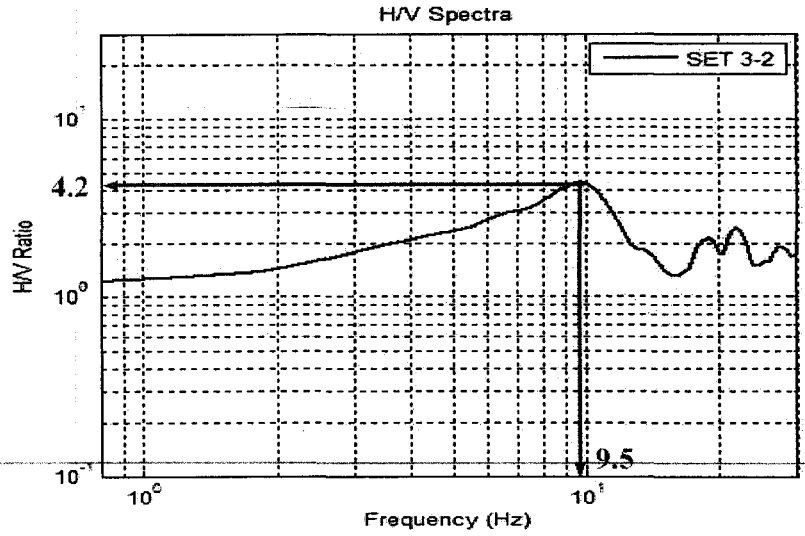

Figure 3.10: Analysis of H/V graph

After obtaining the amplification level and predominant period of the ground around the study area, the findings are then presented in an appropriate map. The microzonation map showing the soil predominant period, frequency and amplification level are plotted based on the results at all the observation points studied.

CHAPTER 4
RESULTS AND DISCUSSION

4.1 General

This chapter discusses the obtained results in term of natural frequency / period and amplification level of ground from the analysis using MATLAB. The results are summarized and mapped as presented in this chapter.

4.2 Single Point Observation

Single point observation was carried out in this study to measure the microtremor and determine the predominant period / frequency and amplification level of ground at various sites in Penang Island. A total of 339 sites were measured during the project period throughout the whole Penang Island area as shown in Figure 4.1. Table 4.1 lists the site ID and its corresponding location in terms of coordinate. Figure 4.2 summarizes the H/V sprctra for all observation sites. There are ten sets of data (30 seconds each) measured in 5 minutes. Only one of the H/V spectra that having closest values to mean values of predominant frequency/period and amplification lelvel is presented here. The details of the results for the mean values of predominant frequency, predominant period, amplification levels at 2 Hz and 4 Hz, and maximum amplification level are given in Appendix A. The mean values of predominant frequency, perdominant period and maximum amplification level are then mapped as presented in Figures 4.3 to 4.5.

Different sites show different characteristics of H/V spectra. Some of the data collection points show good shape of H/V spectra which the amplification level and natural frequency can be determined easily. These kind of results are obtained in conditions which there are minimal noises in the surrounding area during data collection process and the type of ground of the data collection point. Beside that, this type of graph usually occurs in lower frequency soil where softer soil are categorized in.

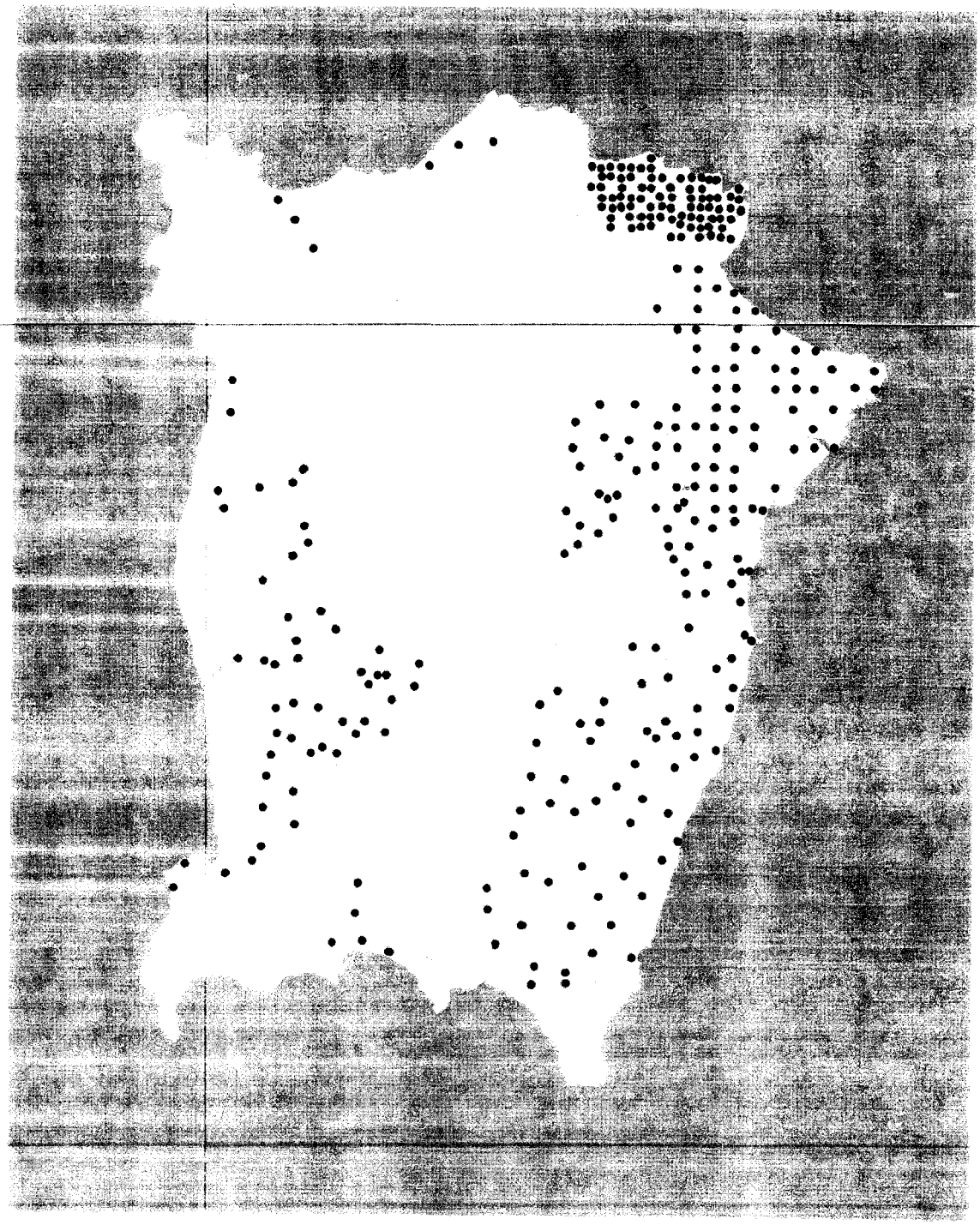

Figure 4.1: Observation points

Table 4.1: Details of observation sites

Site ID	Location	Longitude	Latitude
1	Pasir Panjang	100.1845	5.300806
2	Pasir Panjang	100.1869	5.307194
3	Jalan Pulau Betong	100.1965	5.304214
4	Jalan Sekolah Agama	100.2021	5.307056
5	Jalan Bahru	100.2045	5.319139
6	Pintasan Pondok Upeh 2	100.2179	5.333417
7	Jalan Pulau Betong	100.2215	5.331722
8	Lorong Pondok Upih 3	100.2256	5.336167
9	Lintang Pondok Upeh	100.2275	5.33925
10	Jalan Pulau Betong	100.2321	5.336694
11	Jalan Pulau Betong	100.2342	5.343861
12	Lintang Bukit Penara 4	100.2397	5.352389
13	Lorong Chong Teik	100.2389	5.347222
14	Jalan Quah Sin Keng	100.2324	5.349833
15	Jalan Paya Kongsi	100.2286	5.347861
16	-	100.2173	5.342222
17	Lebuh Seri Genting 1	100.2224	5.339167
18	Jalan Kampung Terang	100.2156	5.331917
19	Jalan Kampung Terang	100.2115	5.323111
20	Jalan Kampung Genting	100.2118	5.3155
21	Jalan Bahru	100.2044	5.3105
22	Jalan Bahru	100.2054	5.326389
23	Jalan Bahru	100.2063	5.331528
24	Jalan Sungai Nipah	100.2115	5.334972
25	Jalan Bahru	100.2073	5.336194
26	Jalan Bahru	100.2074	5.34175
27	-	100.2114	5.343167
28	P232	100.1981	5.353806
29	P232	100.2046	5.352806
30	Jalan Titi Teras	100.212	5.35325
31	Jalan Bahru	100.2116	5.357389
32	Jalan Bahru	100.2101	5.362222
33	Jalan Impian 3	100.2306	5.349583
34	Jalan Kongsi	100.2267	5.350111
35	Paya Kongsi	100.2075	5.351806
36	Solok Titi Teras 2	100.2307	5.35575
37	Jalan Titi Teras	100.221	5.359861
38	Jalan Bahru	100.2174	5.36425
39	Jalan Sungai Air Putih	100.2163	5.371861
40	Jalan Permatan Pasir	100.2042	5.371139
41	Jalan Tok Wan Don	100.2111	5.371028
42	-	100.2117	5.376861
43	-	100.2145	5.379861
44	Jln Kuala Sungai Pinang	100.2034	5.392278
45	Jln Kuala Sungai Pinang	100.1954	5.3875

Table 4.1: Details of observation sites (Cont'd.)

Site ID	Location	Longitude	Latitude
46	Jln Kuala Sungai Pinang	100.1939	5.391194
47	Jalan Pantai Acheh	100.1969	5.409194
48	Jalan Pantai Acheh	100.1971	5.416722
49	-	100.2129	5.396111
50	P236 Teluk Bahang	100.2109	5.393306
51	-	100.2136	5.383631
S1	Jalan Sg. Batu	100.2423	5.283583
S2	Lintang Teluk Kumbar 3	100.2337	5.286333
S3	Jln Kampung Masjid	100.2256	5.295083
S4	-	100.2333	5.298
S5	Jln Haji Sulaiman Jusoh	100.2267	5.301944
S6	Lengkok Kampung Masjid	100.2278	5.289
S7	Tingkat Pasir Belanda	100.2205	5.288417
S8	-	100.1991	5.284211
S9	-	100.2376	5.290367
n1	Jalan Sungai Emas	100.2562	5.471139
n2	Persiaran Sungai Emas	100.2483	5.470028
n3	Batu Ferringhi Waterfall	100.2419	5.465333
n4	Teluk Bahang Dam	100.2156	5.446611
n5	Lengkok Teluk Bahang	100.2112	5.453472
n6	Lengkok Teluk Bahang	100.207	5.457139
260	Jalan Thean Tek Lama	100.28958	5.39622
270	Jalan Angsara & Lengkok Angsara	100.28463	5.39070
E275	Nudar Angsara 3 & 4	100.28333	5.38992
E285	Jalan Sarawak Api/ Lorong Sarawak Api 1	100.28402	5.38587
290	Lorong Sarawak Api 3	100.28095	5.38238
E286	Lebuh Rambai 9	100.27662	5.38408
296	Lebuh Rambai 1	100.27620	5.37988
309	Tingkat Paya Terubong 3	100.27623	5.37085
295	Jalan Oriental 6	100.27312	5.37740
269	Jalan Ru 2	100.28122	5.39082
229	Lorong Kampung Melayu	100.28790	5.40302
E214	Jalan Padang Tembak	100.28913	5.41133
279	Solok Paya Terubong 7	100.27357	5.38700
257	Jalan Paya Terubong	100.27640	5.39695
245	Jalan Pisang Raja	100.28568	5.39927
242	Jalan Balik Pulau Air Itam	100.27498	5.40133
211	Jalan Taman Lintang	100.27567	5.40668
212	Jalan Taman Cantik 4	100.28117	5.41112
227	Jalan Matang Kucing	100.28200	5.40347
321	Persiaran Sungai Gelugor 2	100.31373	5.36685
308	Persiaran Tunku Kudin Gelugor	100.31288	5.37675
314	Jalan Akuarium Gelugor	100.31405	5.37352
313	Tingkat Sungai Gelugor 10	100.31160	5.37115
288(1)	Kintang Hajjah Rehmah Jelutong	100.30078	5.38913

Table 4.1: Details of observation sites (Cont'd.)

Site ID	Location	Longitude	Latitude
288(2)	Metro Ave	100.31858	5.38737
308B	Lebuh Tunku Kudin 1	100.31530	5.37343
344A	Under Penang Bridge	100.31632	5.35810
351	Jalan Batu Uban 4	100.31160	5.35398
358	Persiaran Bayan Indah	100.31190	5.34738
364A	Jerejak Jetty	100.31150	5.34277
395	Queensbay Carpark	100.30823	5.33283
350	Jalan Batu Uban 2	100.30818	5.35160
363	Jalan Pantai Jerejak 9	100.30373	5.34213
383	Persiaran Pantai Jerejak 10	100.30375	5.33713
393	Lebuh Bukit Kecil 5	100.30328	5.33150
382	Jalan Bukit Kecil 1	100.29892	5.33630
370	Medan Nipah	100.29645	5.33927
381	Lebuh Nipah 2	100.29465	5.33558
380	Lebuh Nipah 5	100.29238	5.33710
294	Solok Dumber	100.31188	5.38498
292	Jalan Taman Gelugor	100.30722	5.38357
297	Cangkat Delima 3	100.29732	5.37880
298	Lorong Delima 13	100.30175	5.37903
291A	Cangkat Delima 6	100.29698	5.38325
291	Lintang Delima 5	100.30303	5.38510
319	Pemancar Hilir	100.30557	5.36870
311	Pemancar Hilir	100.30110	5.37365
304	Cangkat Bukit Gambir	100.29812	5.37613
318	Tingkat Permai	100.30130	5.36828
415	Kampung Jawa Highway	100.29958	5.31228
479	Jalan Batu Maung,Restoran Ocean Bay Seafood	100.28867	5.28531
484	Taman Jeliti	100.27411	5.27994
487	Lorong Kekabu 1	100.27139	5.27428
476	Jalan Permatang Damar Laut	100.25617	5.28436
485	Jalan Damar	100.26631	5.27928
486	LintangBeringin 9	100.26681	5.28336
478	Lorong Batu Maung 4	100.28006	5.28650
483	Medan Batu Maung 4	100.27425	5.28192
470	Airport-Jalan Batu Maung	100.27533	5.29244
454	Pintasan Batu Maung 6	100.28167	5.29919
461	Lintang Bayan Lepas	100.28433	5.29267
455	Medan Bayan Lepas-near HW Factory	100.29178	5.29953
443	Jalan Sungai Keluang	100.29606	5.30728
449	Sg Keluang 5 Hilir	100.28753	5.30417
432	Gerbang Kampung Jawa	100.29733	5.31828
413	Lengkok Kampung Jawa 1	100.29139	5.32156
403	Lebuh Kampung Jawa	100.29842	5.32872
374	Cangkat Sungai Ara 10	100.26714	5.33417
391	Pintasan Mashuri	100.28989	5.32939

Table 4.1: Details of observation sites (Cont'd.)

Site ID	Location	Longitude	Latitude
396	Jalan Sungai Ara 7	100.26603	5.32661
398	Persiaran Bayan	100.27344	5.32603
400	Lintang Mayang Pasir 4	100.28539	5.32450
410	Medan Mashuri 1	100.28072	5.32122
416	Changkat Kerani	100.26358	5.31861
418	Lorong Kenari	100.27033	5.32050
430	Jalan Sungai Keluang	100.28903	5.31603
433	Kenari Ptn	100.26225	5.31297
439	Solok Sungai Pasir	100.27597	5.31844
441	Lorong Sungai Tiram	100.27783	5.30622
444	Lengkuk Kericap	100.25583	5.30083
445	Lorong Merbah 1	100.26461	5.30464
447	Lorong Sungai Tiram 1	100.27022	5.30247
458	-	100.25608	5.29642
459	Jalan Garuda	100.26422	5.29261
466	Tingkat Kampung Bukit	100.24669	5.28889
466(2)	Tingkat Kampung Bukit (1)	100.24761	5.29044
468	Jalan Permatang Damar Laut	100.25792	5.28814
365	Lebuh Relau	100.26769	5.34300
352	Lebuh Relau 4	100.27172	5.34625
366	Persiaran Paya Terubong 1	100.27703	5.33914
377	Persiaran Bukit Jambul 9	100.27967	5.33508
367	Persiaran Bukit Jambul	100.28192	5.33897
359	Lintang Bukit Jambul 1	100.28258	5.34372
338	Halaman Bukit Gambir 9	100.28894	5.35644
339	Filter Lane	100.29428	5.35608
333	Jalan Tadika	100.30206	5.36072
335	Jalan Universiti (E)	100.31442	5.35950
354	Lorong Merak 2	100.29706	5.34947
353	Jalan Bukit Gambier	100.29133	5.34772
306	Jalan Bunga Raya (Solok)	100.30606	5.37486

Point 1

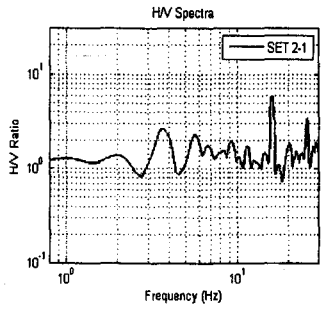

Point 2

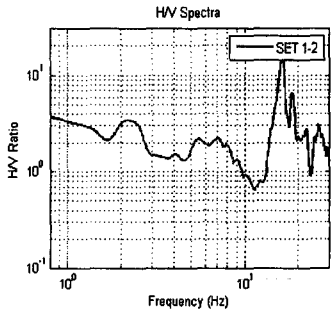

Point 3

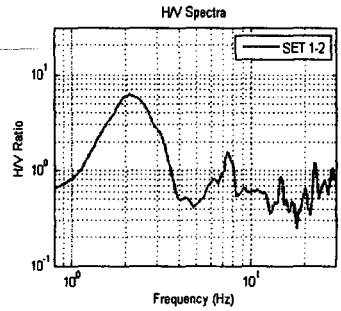

Point 4

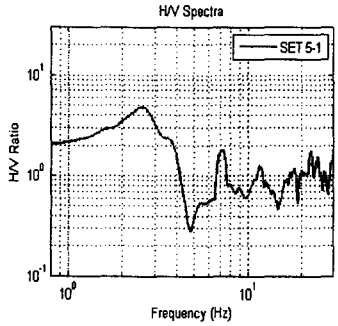

Point 5

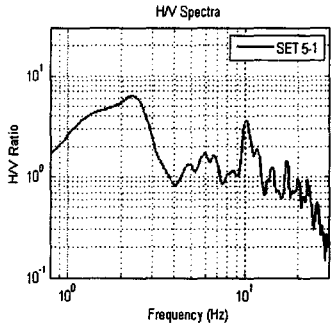

Point 6

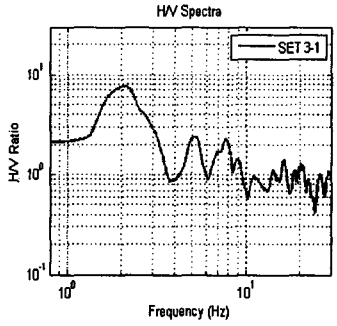

Point 7

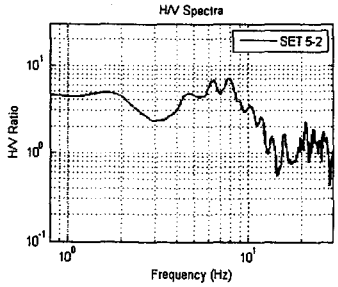

Point 8

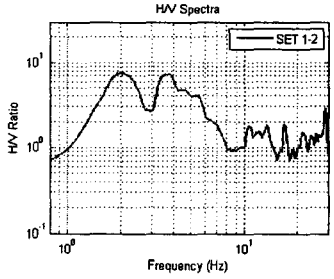

Point 9

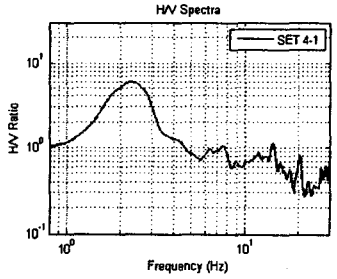

Point 10

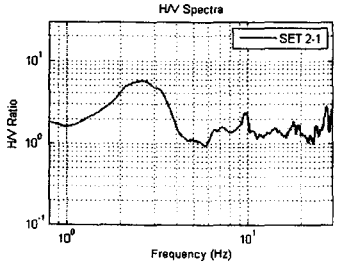

Point 11

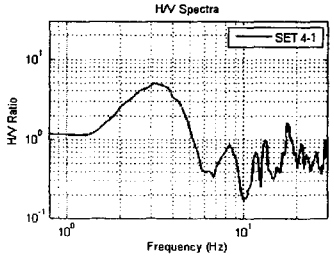

Point 12

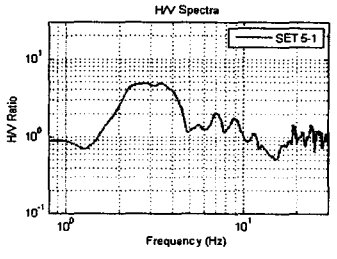

Figure 4.2: H/V spectra for each observation site

Point 13

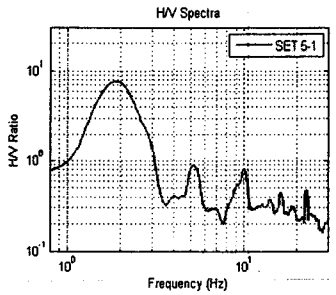

Point 14

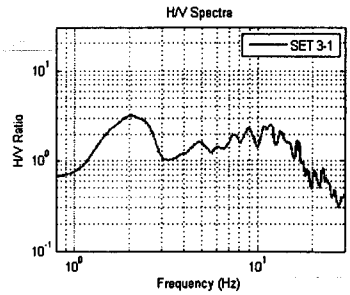

Point 15

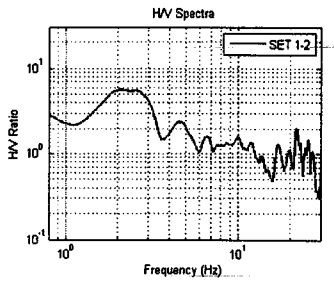

Point 16

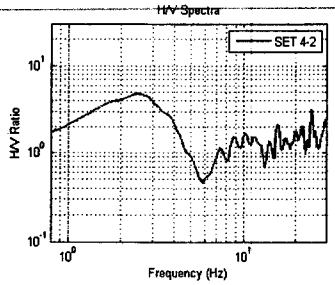

Point 17

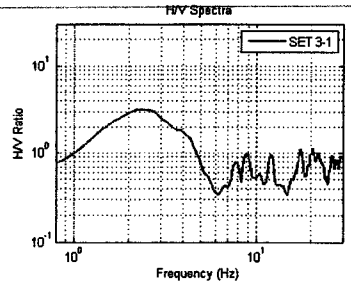

Point 18

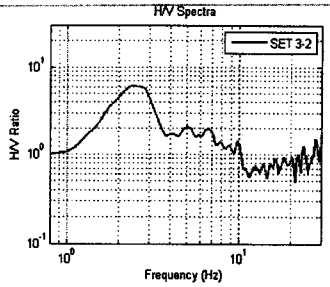

Point 19

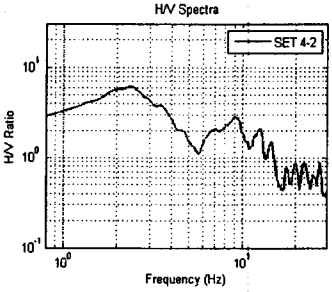

Point 20

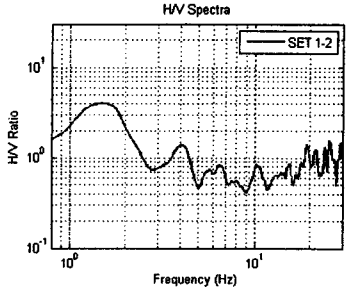

Point 21

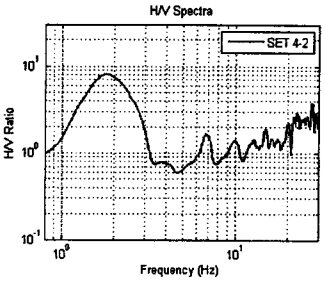

Point 22

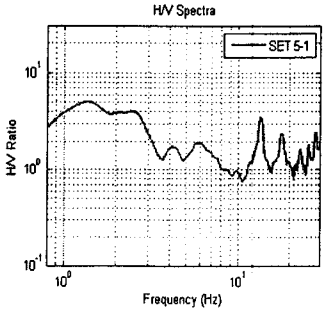

Point 23

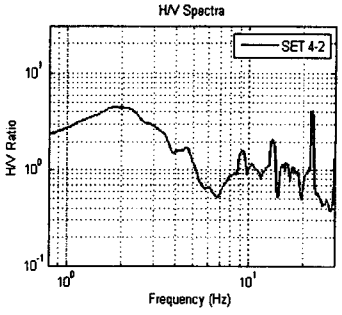

Point 24

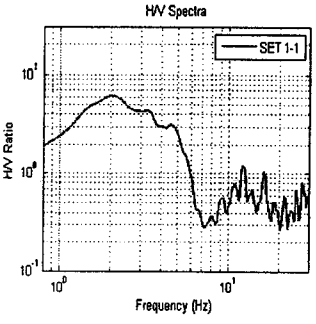

Figure 4.2: H/V spectra for each observation site (Cont'd.)

Point 25

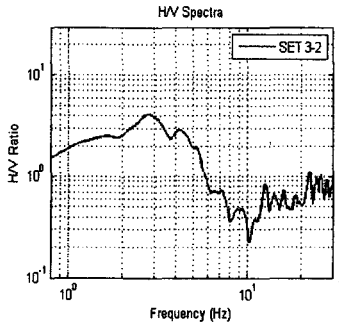

Point 26

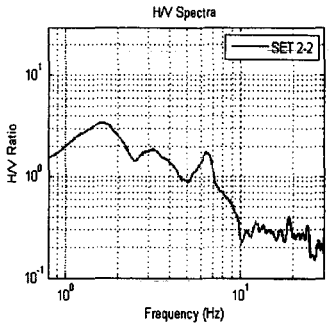

Point 27

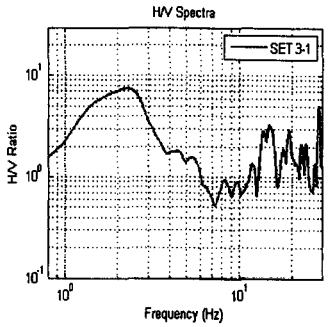

Point 28

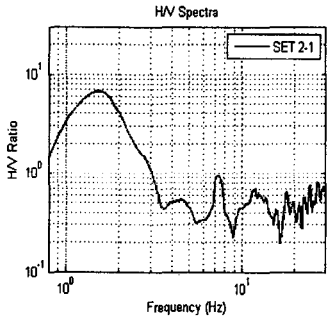

Point 29

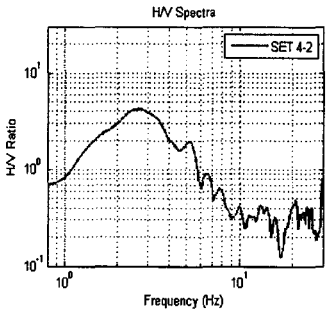

Point 30

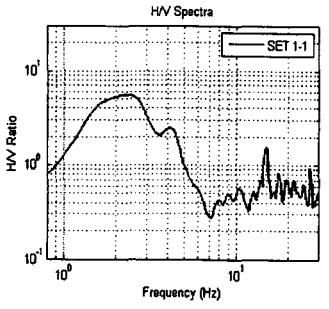

Point 31

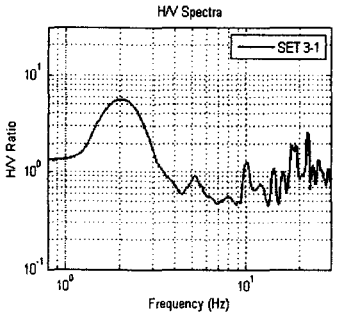

Point 32

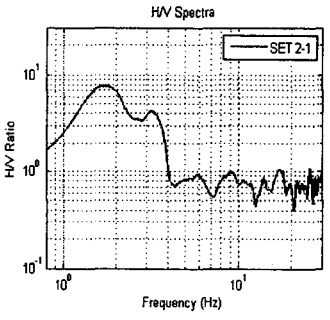

Point 33

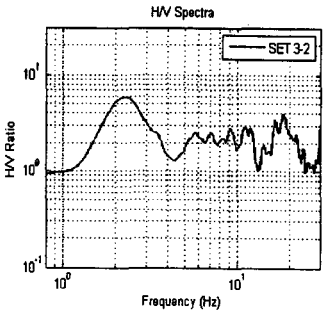

Point 34

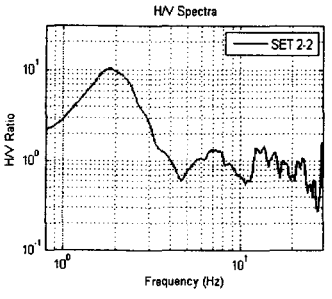

Point 35

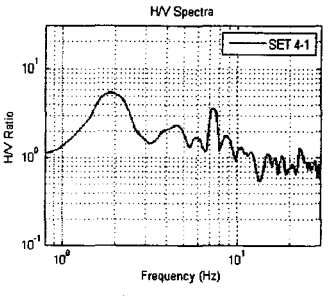

Point 36

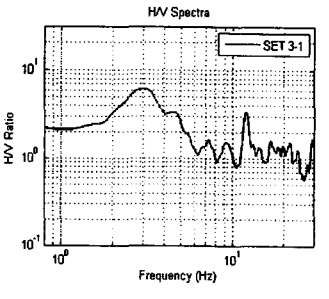

Figure 4.2: H/V spectra for each observation site (Cont'd.)

Point 37

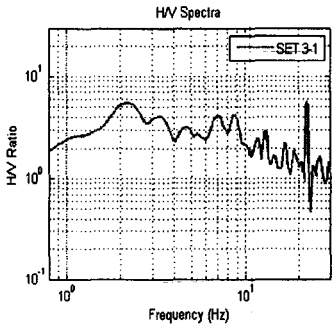

Point 38

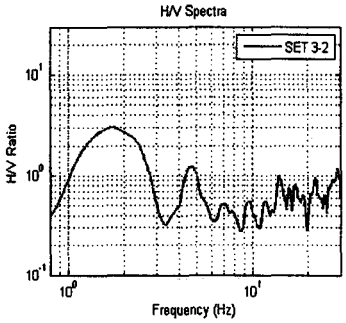

Point 39

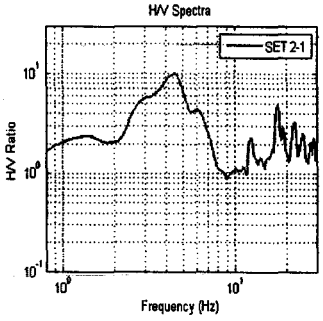

Point 40

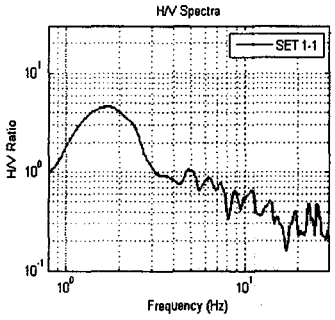

Point 41

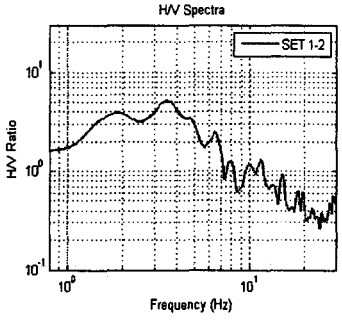

Point 42

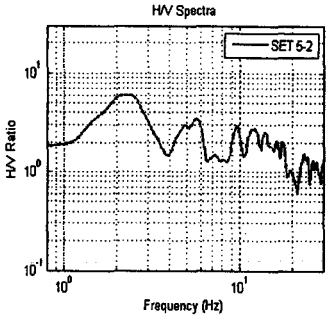

Point 43

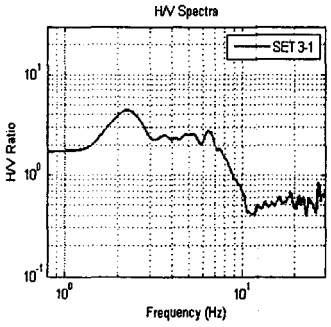

Point 44

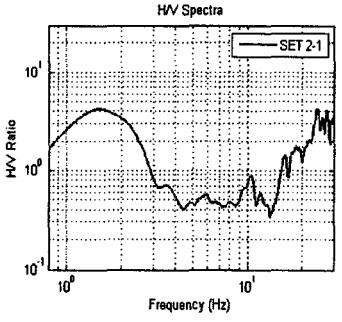

Point 45

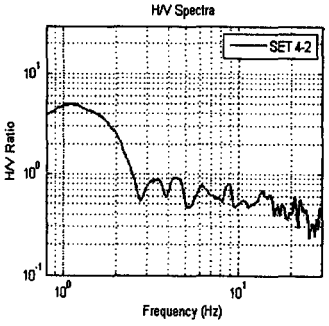

Point 46

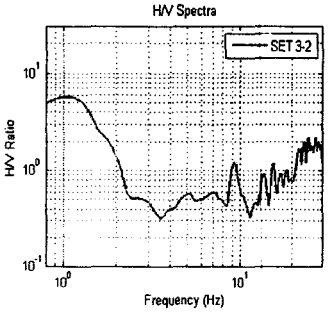

Point 47

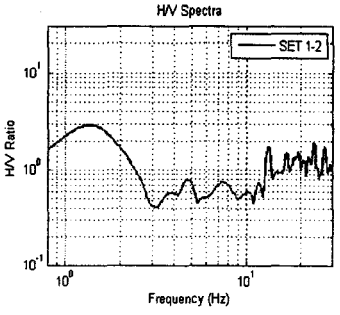

Point 48

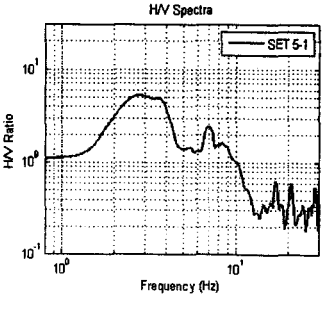

Figure 4.2: H/V spectra for each observation site (Cont'd.)

Point 49

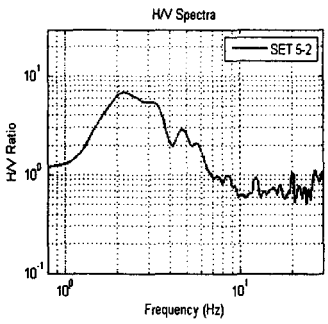

Point 50

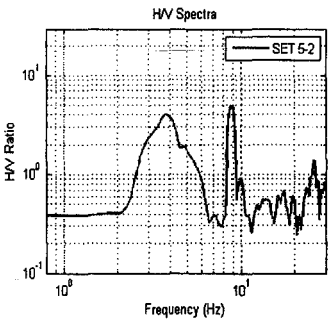

Point 51

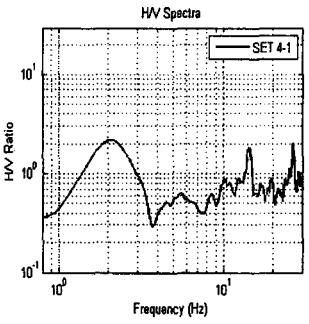

Point S1

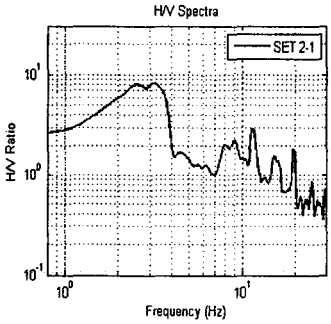

Point S2

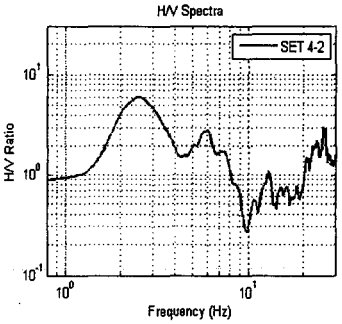

Point S3

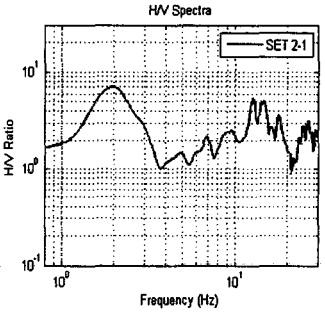

Point S4

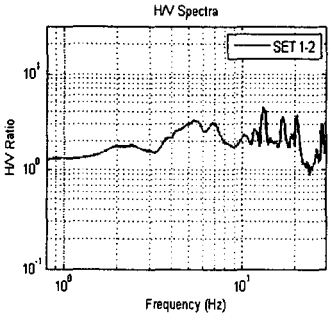

Point S5

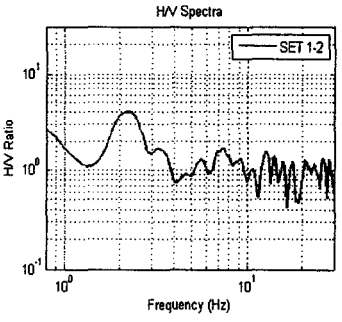

Point S6

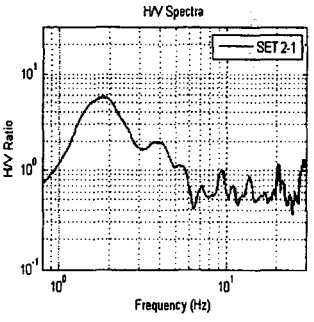

Point S7

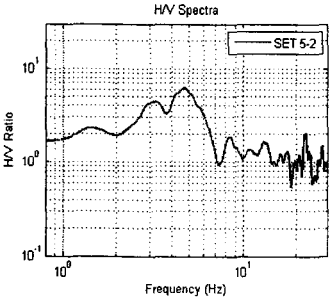

Point S8

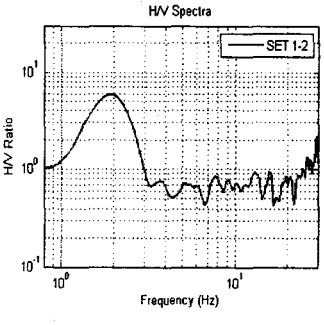

Point S9

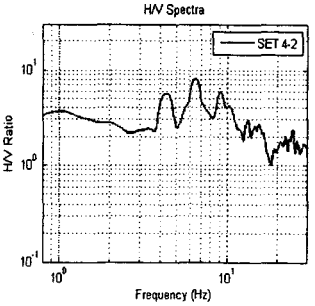

Figure 4.2: H/V spectra for each observation site (Cont'd.)

Point N1

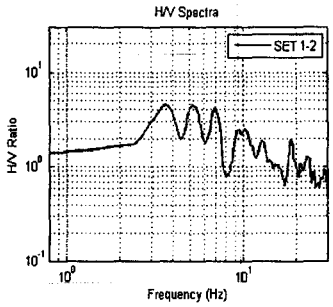

Point N2

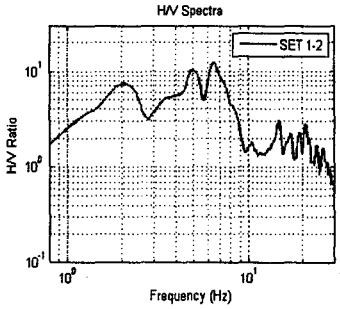

Point N3

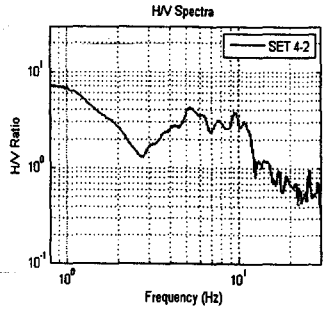

Point N4

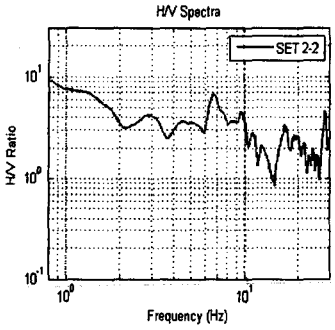

Point N5

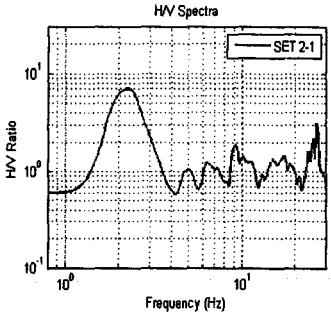

Point N6

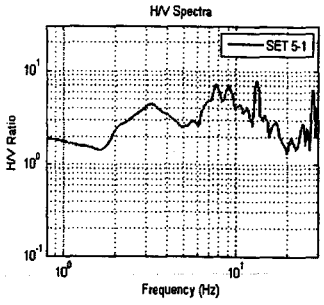

Point 260

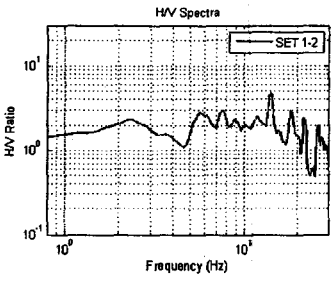

Point 270

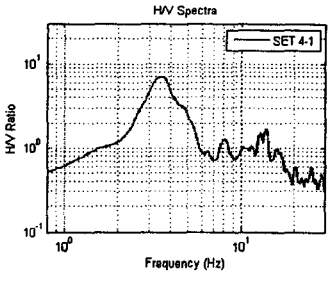

Point E275

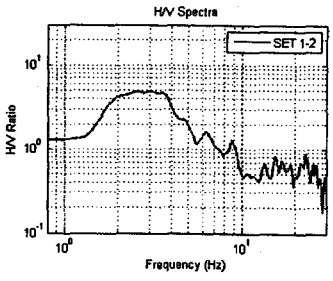

Point E285

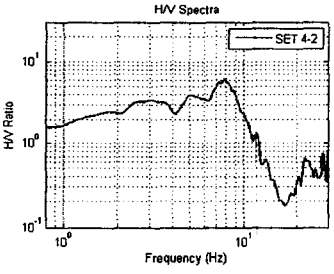

Point 290

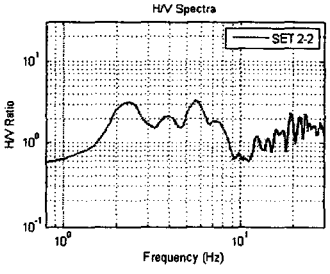

Point E286

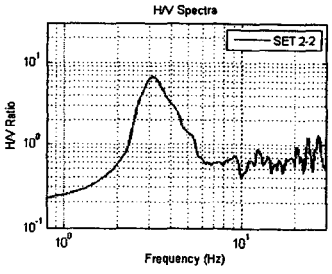

Figure 4.2: H/V spectra for each observation site (Cont'd.)

Point 296

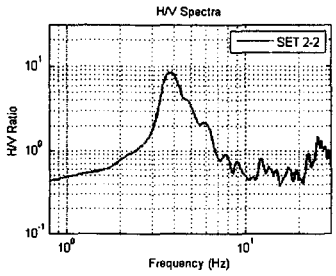

Point 295

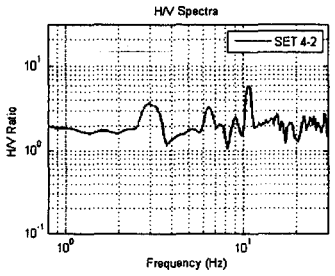

Point 269

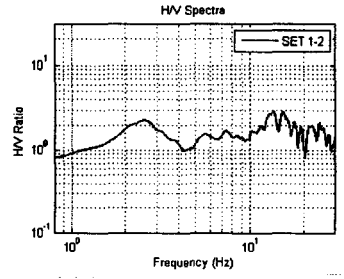

Point 229

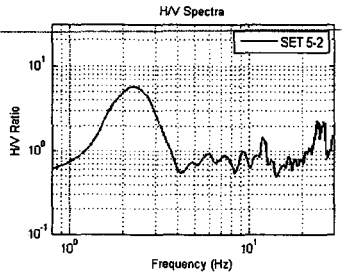

Point E214

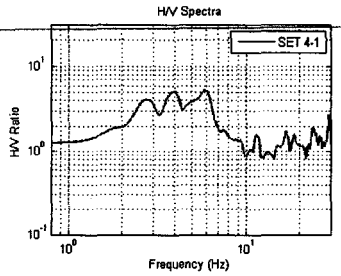

Point 279

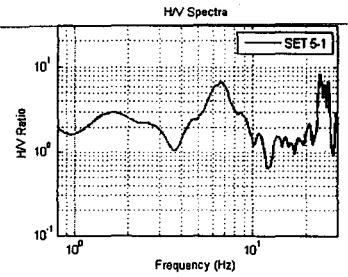

Point 257

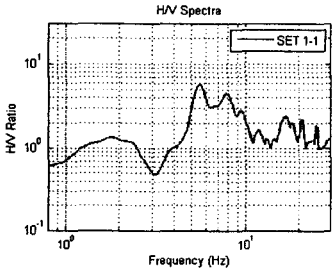

Point 245

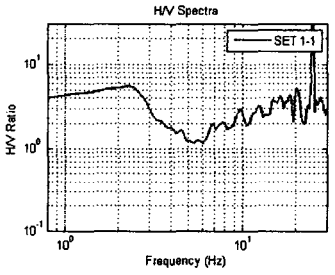

Point 242

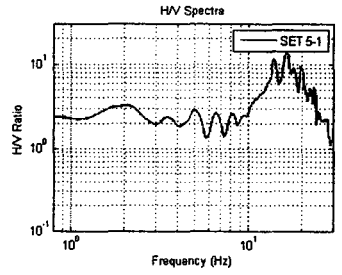

Point 211

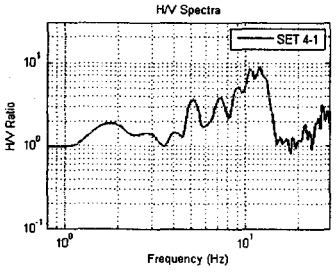

Point 212

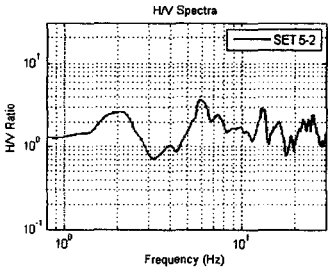

Point 227

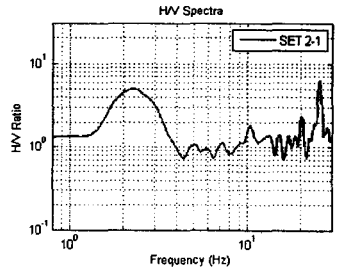

Figure 4.2: H/V spectra for each observation site (Cont'd.)

Point 321

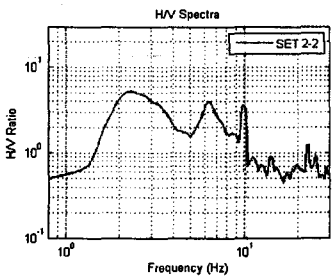

Point 308

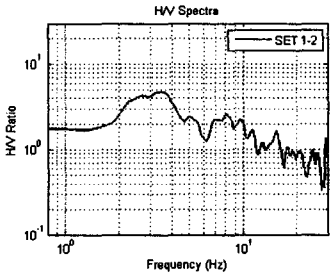

Point 314

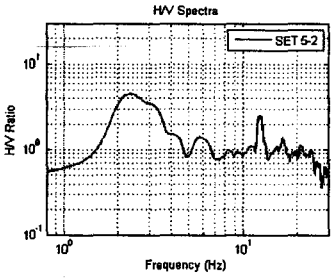

Point 313

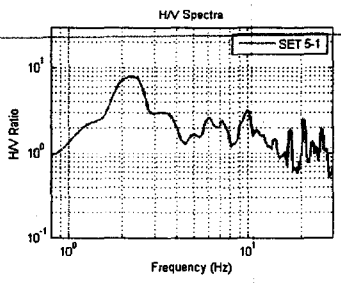

Point 288(1)

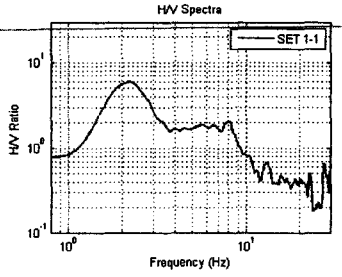

Point 288(2)

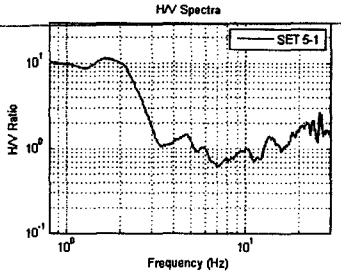

Point 308B

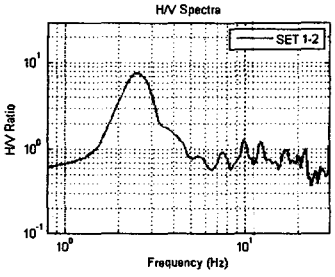

Point 344A

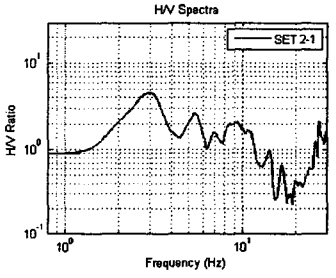

Point 351

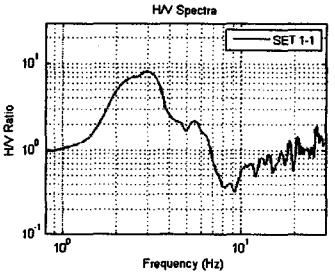

Point 358

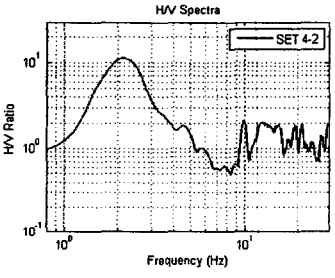

Point 364A

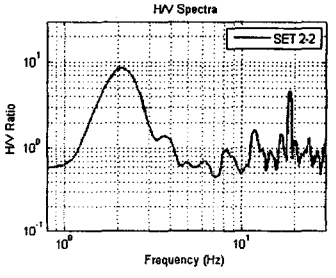

Point 395

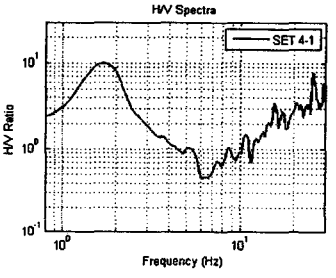

Figure 4.2: H/V spectra for each observation site (Cont'd.)

Point 350

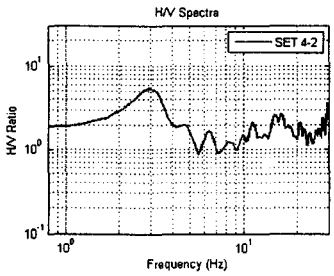

Point 306

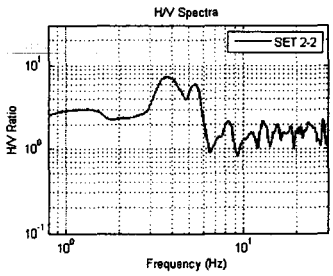

Point 363

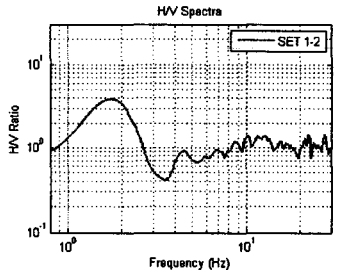

Point 383

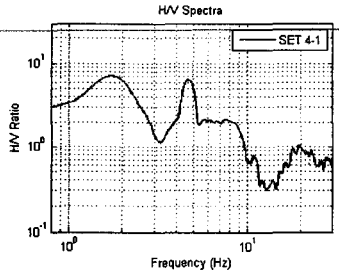

Point 393

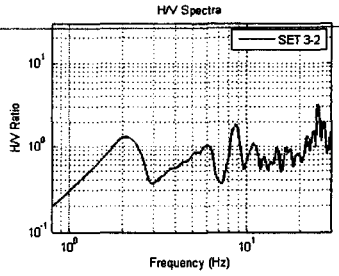

Point 382

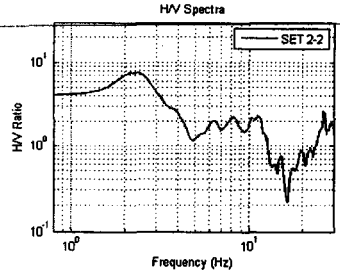

Point 370

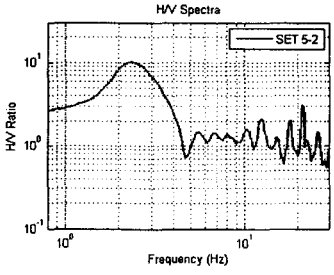

Point 381

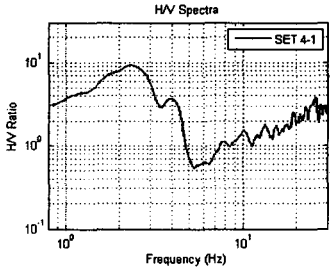

Point 380

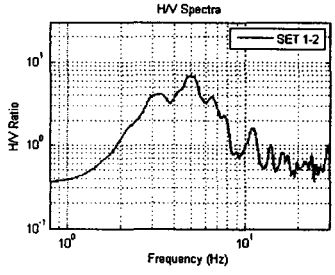

Point 294

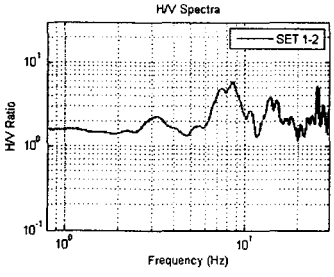

Point 292

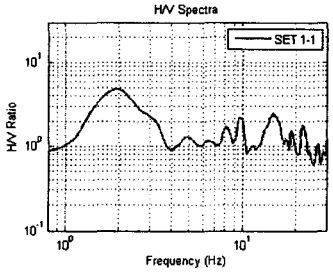

Point 297

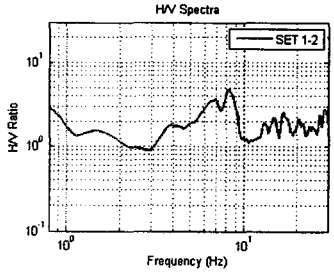

Figure 4.2: H/V spectra for each observation site (Cont'd.)

Point 298

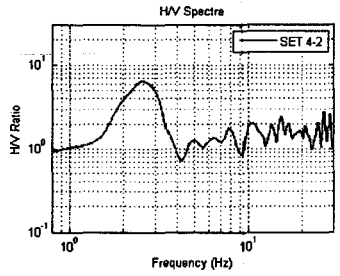

Point 291A

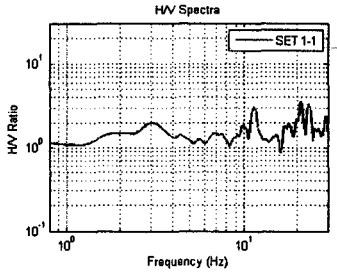

Point 291

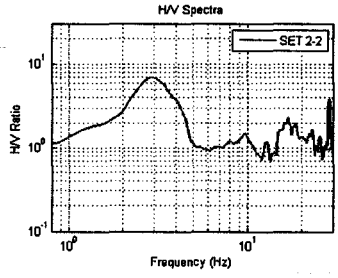

Point 319

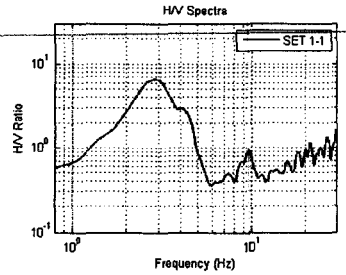

Point 311

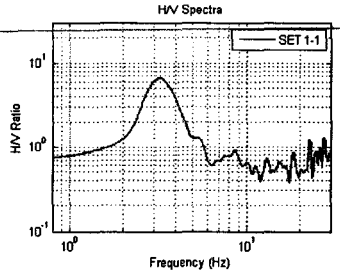

Point 304

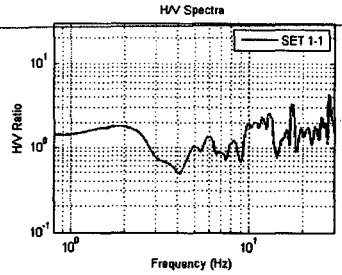

Point 308

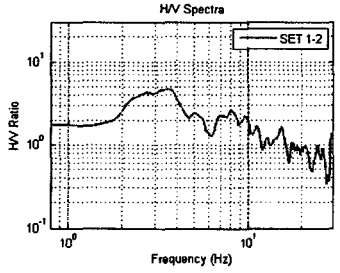

Point 415

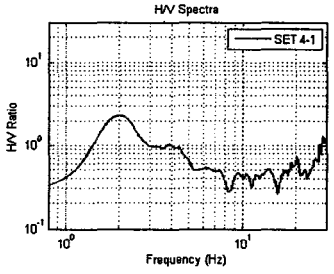

Point 479

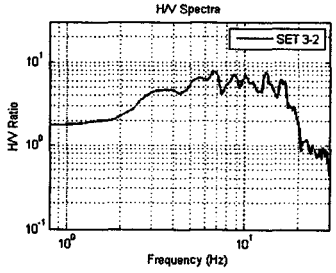

Point 484

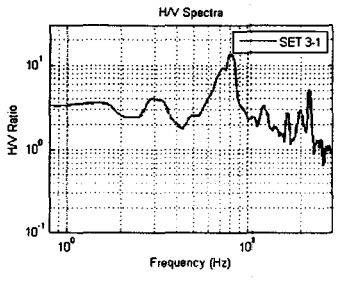

Point 487

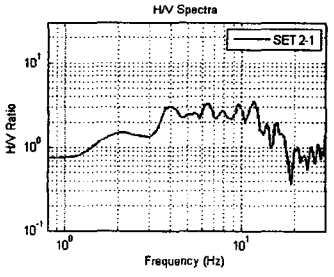

Point 476

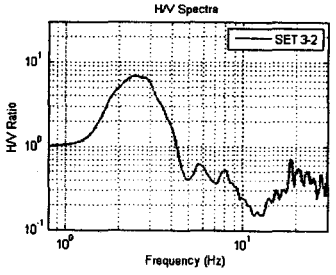

Figure 4.2: H/V spectra for each observation site (Cont'd.)

Point 485

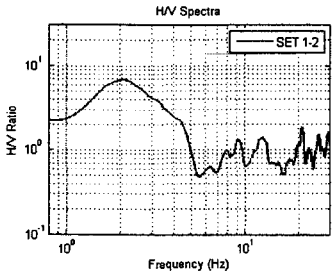

Point 486

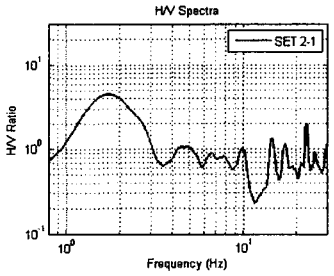

Point 478

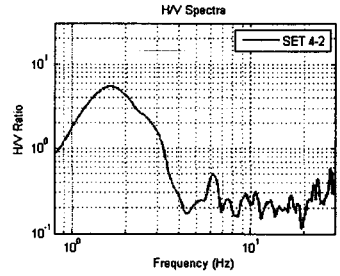

Point 483

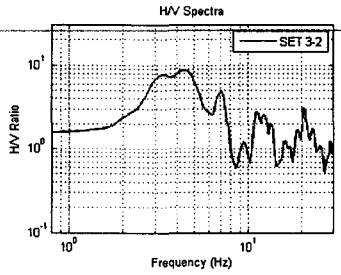

Point 470

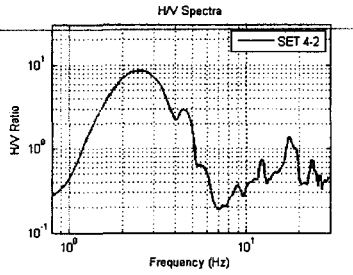

Point 454

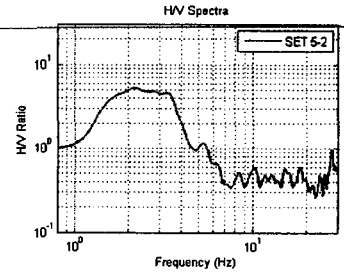

Point 461

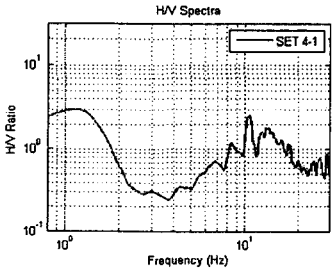

Point 455

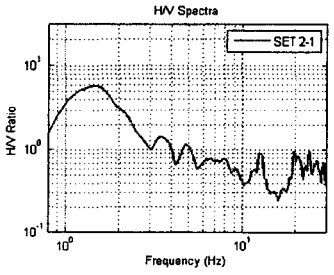

Point 443

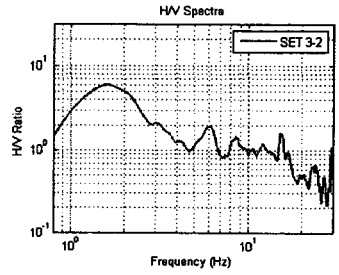

Point 449

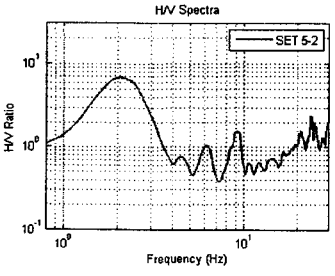

Point 432

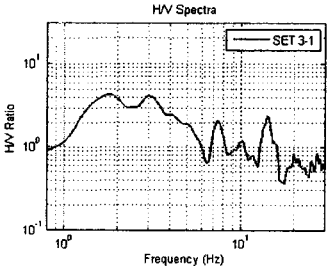

Point 413

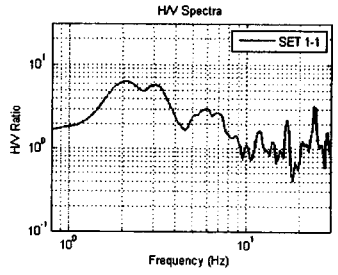

Figure 4.2: H/V spectra for each observation site (Cont'd.)

Point 403

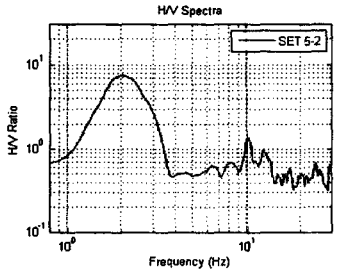

Point 374

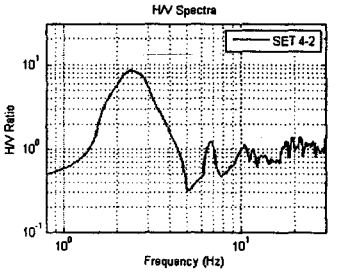

Point 391

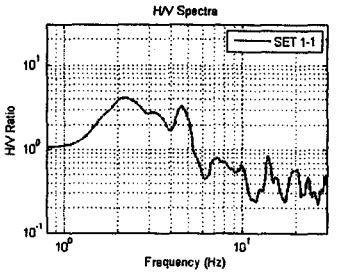

Point 396

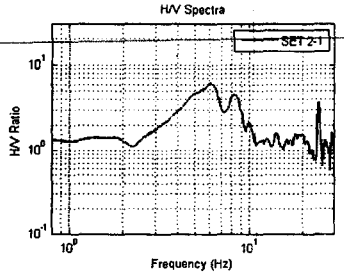

Point 398

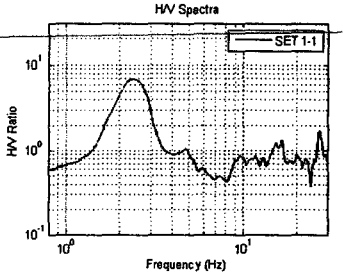

Point 400

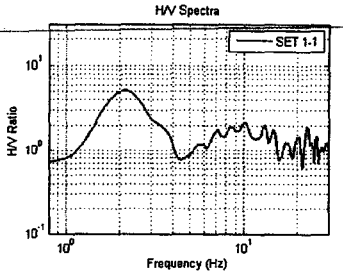

Point 410

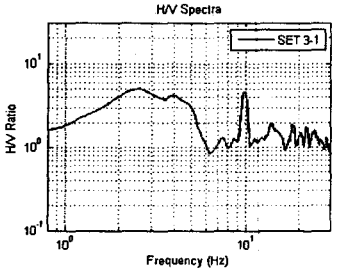

Point 416

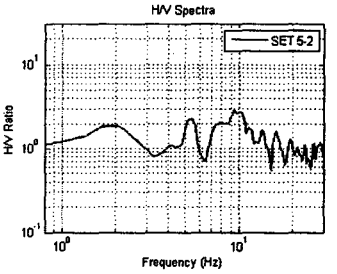

Point 418

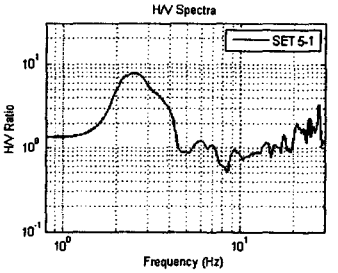

Point 430

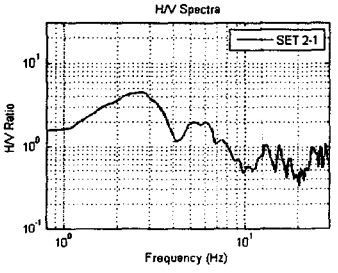

Point 433

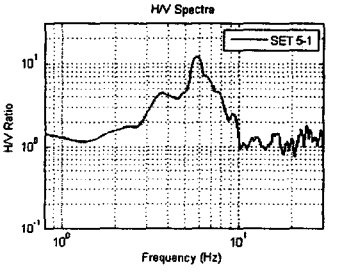

Point 439

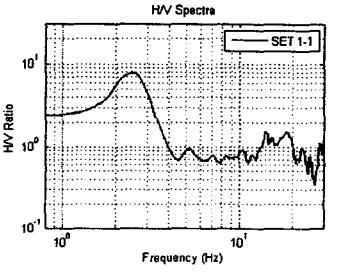

Figure 4.2: H/V spectra for each observation site (Cont'd.)

Point 441

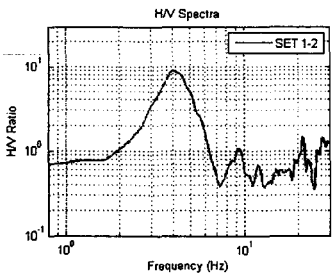

Point 444

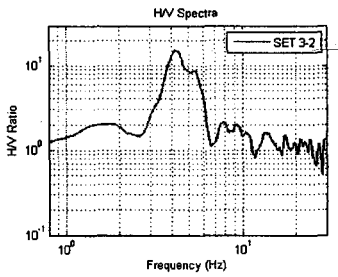

Point 445

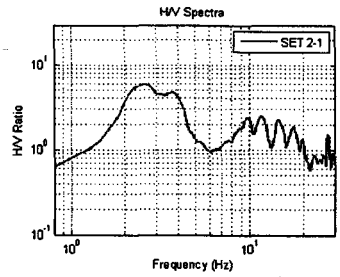

Point 447

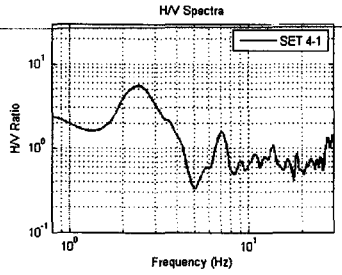

Point 458

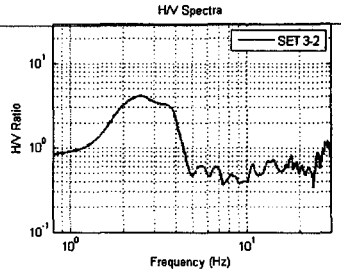

Point 459

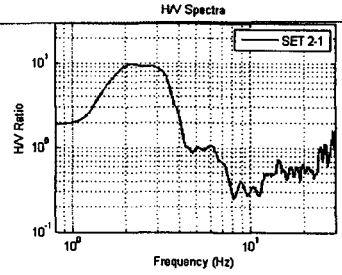

Point 466

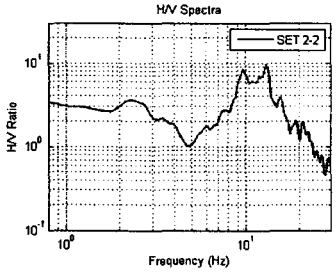

Point 466(2)

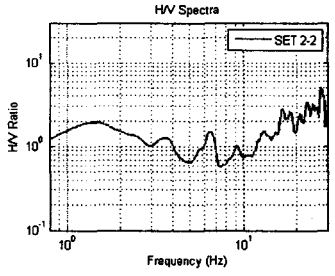

Point 468

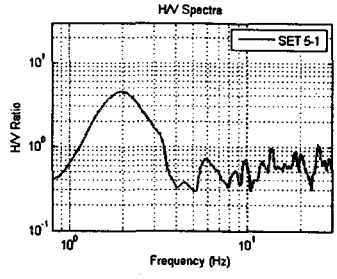

Point 365

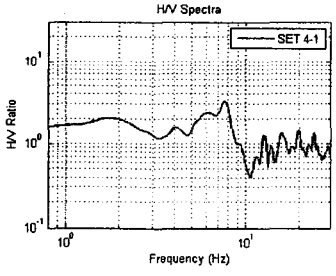

Point 352

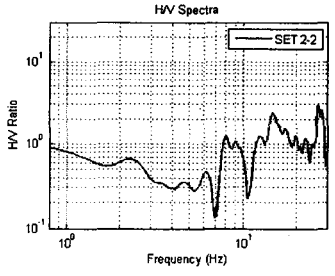

Point 366

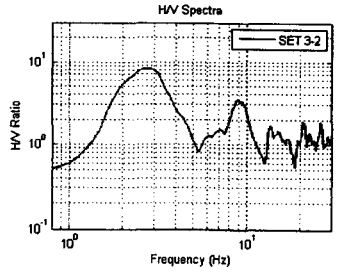

Figure 4.2: H/V spectra for each observation site (Cont'd.)

Point 377

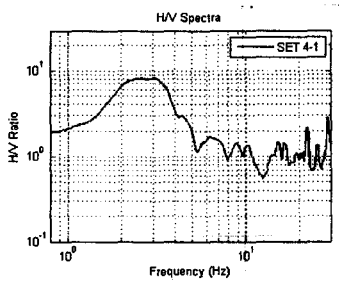

Point 367

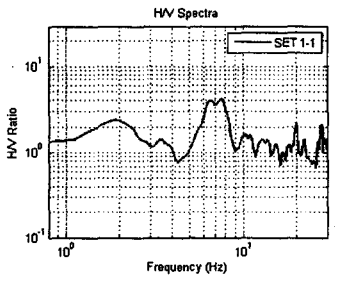

Point 359

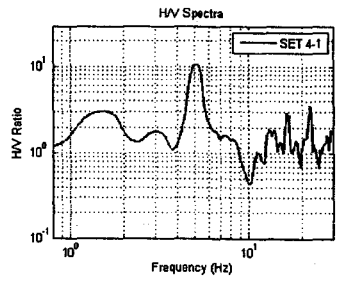

Point 338

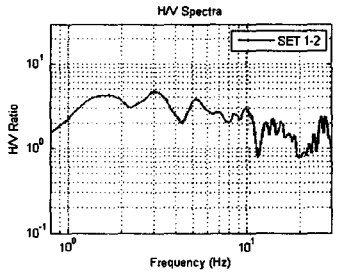

Point 339

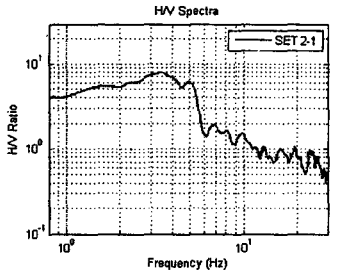

Point 333

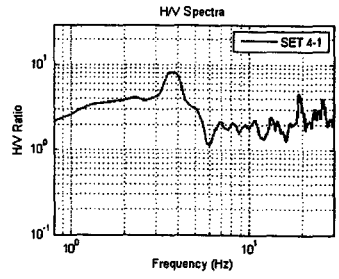

Point 335

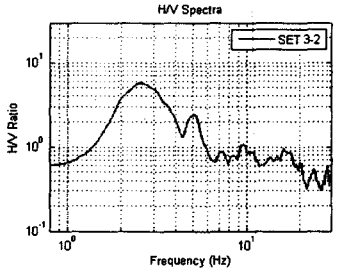

Point 354

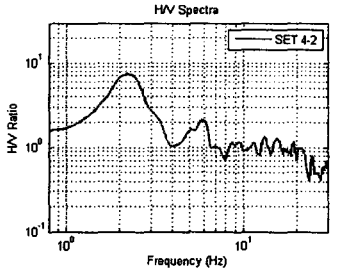

Point 353

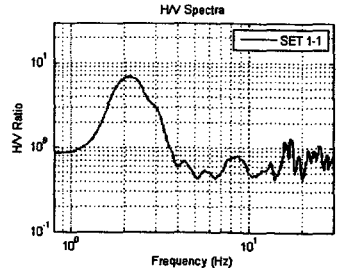

Figure 4.2: H/V spectra for each observation site (Cont'd.)

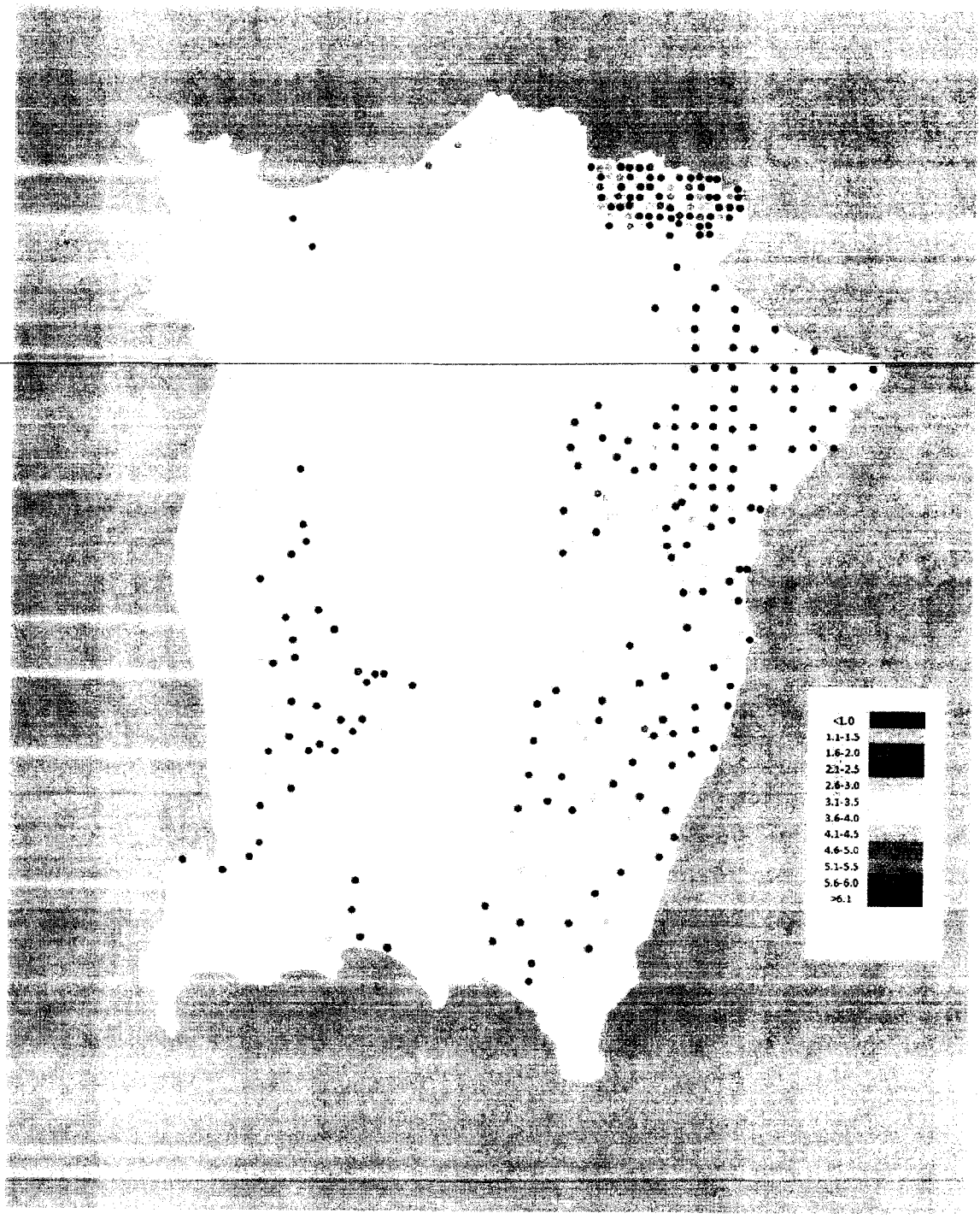

Figure 4.3: Map of predominant frequency for ground in Penang Island

Figure 4.4: Map of predominant period for ground in Penang Island

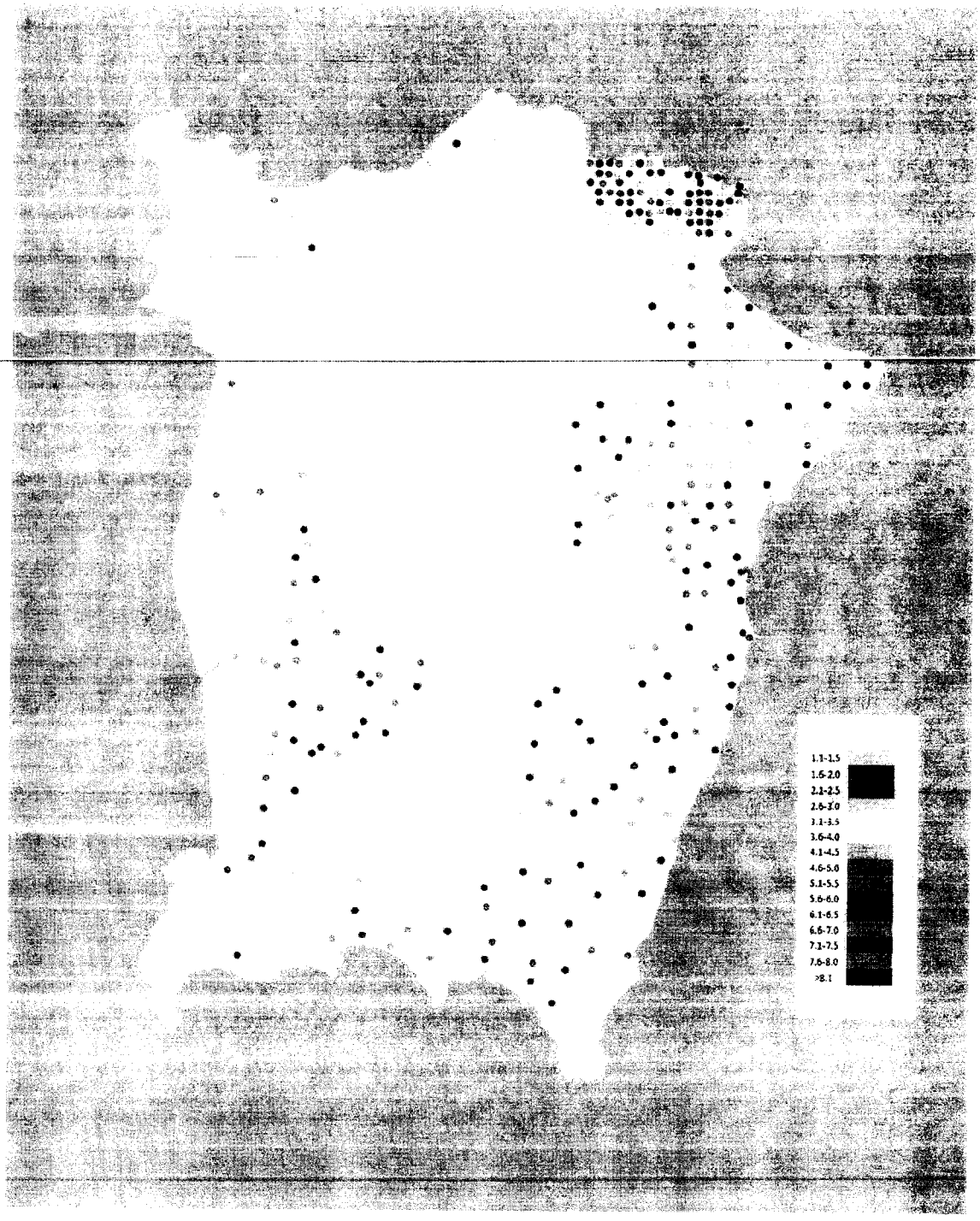

Figure 4.5: Map of maximum H/V ratio for ground in Penang Island

Nakamura (2008) have shown that the effect of Rayleigh wave can be determined by observing the shape of graph after the first peak of the H/V spectra. The effect of Rayleigh wave are observed in all sites and it is concluded that the influence of Rayleigh are different in all the data collection points. Even though the influence of Rayleigh wave are different in each point, the peak of the H/V spectra will not be affected as the main peak of the H/V spectra consist mostly of SH wave and only a small amount of Rayleigh wave.

From the results obtained. Some of the H/V spectra have shown more than one peak. The first peak of the graph usually will be having the highest amplitude while the amplitude of peaks following it will have diminished amplitude, Usually, the subsequent peak has lower amplitude than the first peak. There is a possibility that the subsequent peaks are affected by noise in vertical component, resulting in several peaks that are actually from a single peak. Having multiple peaks in a graph means that there are more than one resonance frequency. This characteristic of soil is also seen in other research done using microtremor. However, the first H/V spectra peak frequency is of the research priority as it represent higher period resonance which will most likely resonance with the natural frequency of buildings.

The study area consists of both soft and hard soil, the H/V spectra for soft soil and thick alluvium layer has the frequency of the soil is about 2 Hz. For harder soil or thinner alluvium layer, the amplification level are usually quite high and the natural frequency is also higher compared to softer soil. From the mineral resource map, it is shown that the data collection points are of granitic rocks, which is categorized as hard soil. Hence, the outcome of the analysis are in good terms representing the characteristic of these locations. The frequency of H/V spectra of more than 5 Hz are usually considered as stiffer soil. Most of the granitic are within the range of 5 to 10 Hz. However, frequencies of more than 10 Hz is also recorded in several places located at the exposed granite rocks.

4.3 Array Observation

Array observation was conducted to estimate the subsurface structure of the ground using microtremor. This was done to complement the findings of single point observation which is the main focus of this research. The array observation was completed successfully with

the technical support from Professor Hitoshi Morikawa and his students from 1 – 11 August 2012. A total of 34 arrays in 16 sites in the eastern part of Penang Island as shown in Figure 4.6 were investigated. Two or three types of triangular array networks with the radii vary from 3 m to 70 m (Table 4.2) are formed based on the condition of the site.

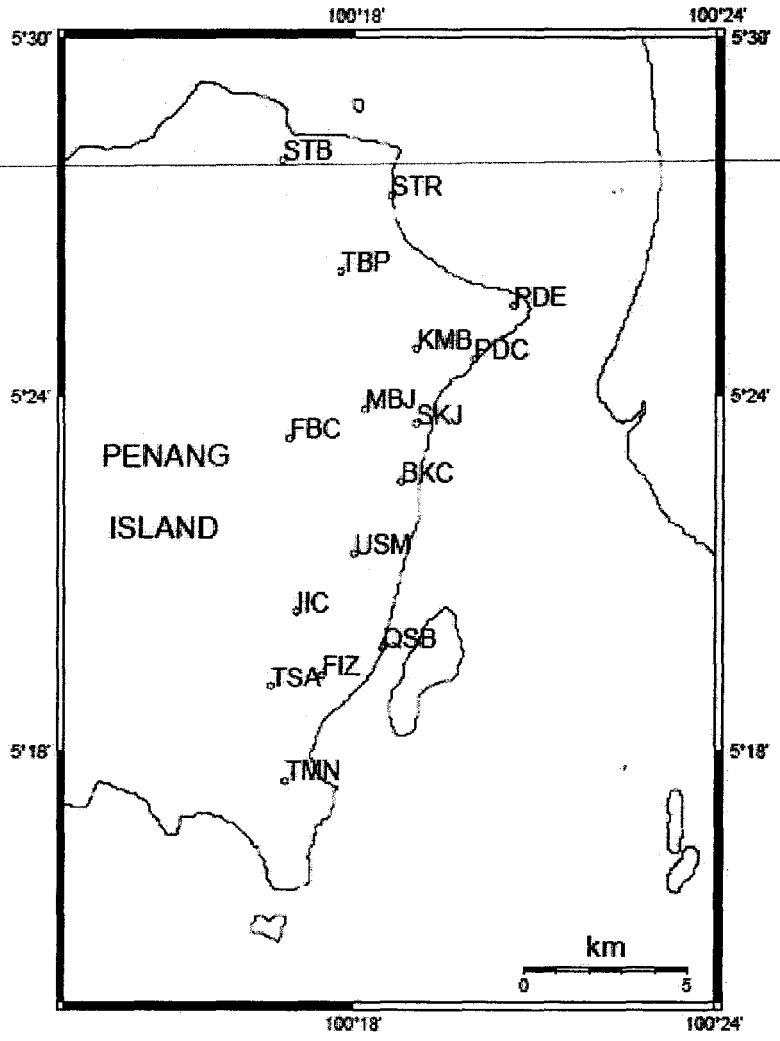

Figure 4.6: Array observation sites (Hamasaki et al., 2012)

Table 4.2: Summary of array observation (Hamasaki et al., 2012)

Site ID	Array Size	Array Radius (m)	Observation Time (min)
PDE	L	73	45
	M	11.4	30
	S	6	33
STR	L	8	32
	M	2	38
PDC	L	4	33
	M	1	35
QSB	L	40	40
	M	15	32
	S	5	30
TMN	L	4	30
	M	1	30
TSA	L	8	33
	M	2	33
IIC	L	10	30
	M	3	30
MBC	L	10	31
	M	3	33
FBC	L	30	34
	M	4.62	27
KMB	L	7.32	34
	M	2	30
BKC	L	18	43
TBC	L	12	34
	M	3	30
USM	L	40	30
	M	10	31
	S	3	30
STB	L	10	30
	M	3	31
SLJ	L	4	30
	M	1	30
FIZ	L	6	31
	M	2	31

Figure 4.7 shows the observation activities during the fieldwork. Four velocity sensors are used in each array observation. The recorded data are being analyzing in Tokyo Institute of Technology using the program developed in Morikawa Laboratory. Two research assistants of this study were sent to Morikawa Laboratory from 13 to 21 November 2012 for short term training on the data analysis using Spatial Autocorrelation (SPAC) Method.

Figure 4.7: Microtremor array observation in Penang Island

Figure 4.8 presents the result for one of the sites, PDE, using SPAC method by exploiting the S-wave velocity. The recorded data was analyzed by estimating dispersion of the recorded surface wave. The subsurface structure of the site was then estimated by means of inversion.

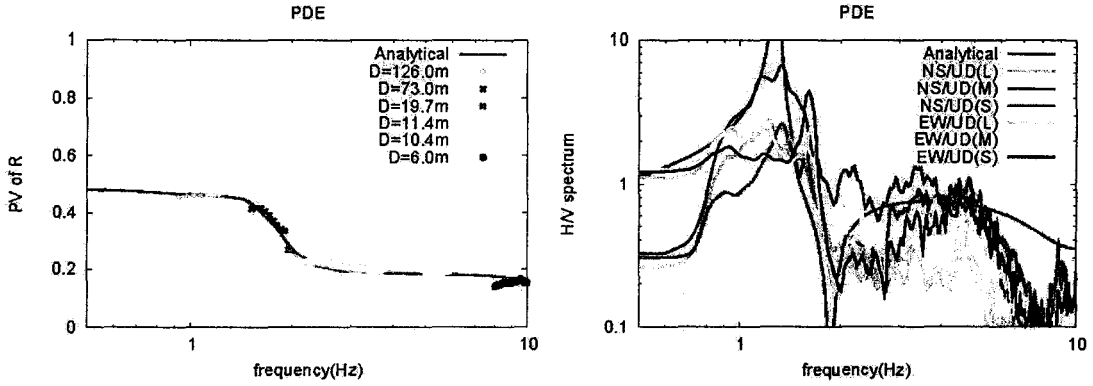

(a) Phase Velocity (b) H/V Spectrum

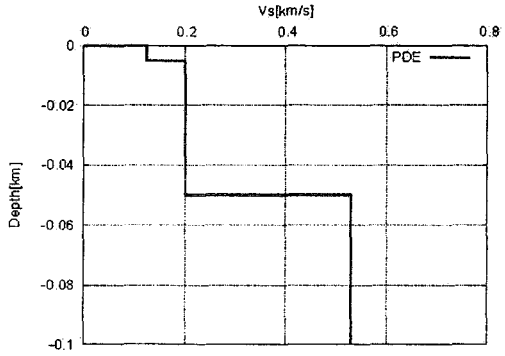

(c) Subsurface Structure

Figure 4.8: Result of array observation by SPAC method (Hamasaki et al., 2012)

CHAPTER 5
CONCLUSIONS

5.1 Summary of Research Findings

Microtremor single point observations were conducted in 339 sites covering the whole Penang Island in approximately six months time. The recorded data were analyzed based on Nakamura Method. The predominant period / frequency and amplification level (H/V ratio) were obtained and mapped. The findings have provided useful information for the design of structures considering ground motion.

The predominant periods / frequencies of sites determined from microtremor observation are coherent with the geological and geotechnical features of the area. However, the amplification level does not show clear correlation with the predominant period or frequency. The understanding of H/V ratio needs further enhanced in future. This can be improved through the investigation on other method such as microtremor array observation, reflection or refraction survey or soil boring.

This research has introduced and promoted the application of the new method or technique for seismic survey to estimate the dynamic characteristics of ground motion in Malaysia. The obtained fundamental period and amplification level of a site are two important parameters in seismic design of structures. This has definitely enhanced the understanding of the site effect on structures and further improved the design of structures to withstand earthquake loading.

5.2 Outcomes and Benefits of SRA Project

Apart from the direct findings as stated above, this research also gives many other benefits to Universiti Sains Malaysia and the country at large as follows:

(a) Human capital development: Three master students and eight undergraduate students from Universiti Sains Malaysia have involved in this research (Figure 5.1). They are Mr. Teoh Chun Li, Mr. Tan Teik Ning, Mr. Chow Tze Liang, Mr. Kuon Kok Huat, Mr. Lim Teik Tzuan, Mr. Tan Kang Chin, Mr. Lim Tse Yang, Mr. Leow Chee Sin, Mr. Tan Kwang Yew, Mr. Moon Wei Chek and Mr. Chong Fui Lip. The students have acquired new skills and knowledge on microtremor survey through practical fieldwork experience and data analysis. This has help in enriching the knowledge of seismic survey and earthquake engineering for students in Malaysia.

(b) Research collaboration: This research provides an excellent platform for Universiti Sains Malaysia and Tokyo Institute of Technology to work together on microtremor observation. This has enhanced the capability and competency to carry out this technique in Malaysia in future. Faculty staff and students from Tokyo Institute of Technology and Universiti Sains Malaysia have good opportunity to work together during the execution of this research. This will definitely foster more research collaboration in future.

(c) Technology Transfer: Through this joint research activity with Tokyo Institute of Technology, the field measurement and analysis technique of this new seismic survey method has been transferred to Universiti Sains Malaysia. Two graduate students from Universiti Sains Malaysia underwent short term training on data analysis for array observation in Morikawa Laboratory under this research (Figure 5.2).

(d) International networking: This research indirectly has strengthened the interaction and networking among faculty staffs and students from both institutions.

(e) New knowledge development and dissemination: The findings of this study are/will be published in international refereed journal and conference proceedings. An article on microtremor survey activity and a proceeding paper on array observation were published and a journal paper is being drafted. The generated new knowledge from this study would also be the supporting information for the establishment of Malaysian Annex for Eurocode 8, the seismic design code for Malaysia, in near future.

Figure 5.1: Microtremor observation team from both institutions

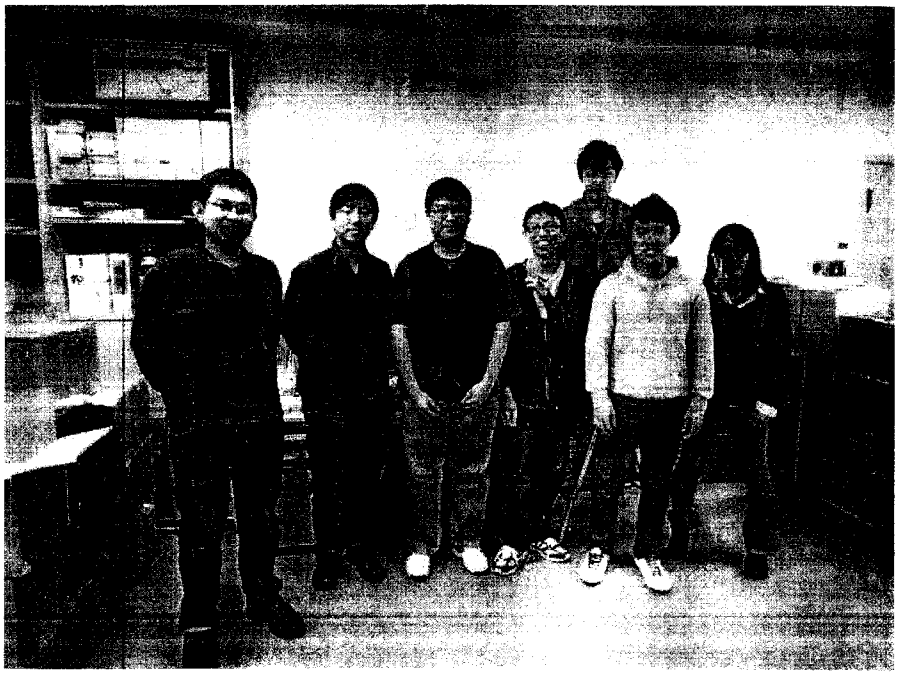

Figure 5.2: Short-term training in Morikawa Laboratory, Tokyo Institute of Technology

REFERENCES

1. Bour, M., Fouissac, D., Dominique, P. and Martin, C. (1998). On the use of microtremor recordings in seismic microzontaion. Soil Dynamics and Earthquake Engineering, 17, pp. 465-474.
2. Bonnefoy-Claudet, S., Cornou, C., Bard, P.-Y., Cotton, F., Moczo, P., Kristek, J. and Fäh, D. (2006). H/V ratio: a tool for site effects evaluation. Results from 1-D noise simulations. Geophysical Journal International, 167, pp. 827–837.
3. Field, E.H., Hough, S.E. and Jacob, K.H. (1990). Using microtremors to assess potential earthquake site response: A case study in Flushing Meadows, New York City. Bulletin of the Society of America, 80(6), pp. 1456-1480.
4. Field, E.H., Clement, A.C., Jacob, K.H., Aharinian, V., Hough, S.E., Friberg, P.A., Babaian, T.O., Karapetian, S.S., Hovanessian, S.M. and Abramian, H.A. (1995). Earthquake site-response study in Giumri (formerly Leninakan), Armenia, using ambient noise observation, 85(1), pp. 349-353.
5. Fnais, M.S., Abdelrahman, K., and Al-Amri, A.M. (2010). Microtremor measurements in Yanbu city of Western Saudi Arabia: A tool for seismic microzonation. Journal of King Saud University, 22(2), pp. 97-110.
6. Gosar, A. (2007). Microtremor HVSR study for assessing site effects in the Bovec Basin (NW Slovenia) related to 1998 Mw5.6 and 2004 Mw5.2 Earthquakes. Engineering Geology, 91(2-4), pp. 178-193.
7. JUPEM. (1983). Mineral resources map of Kedah, Perlis & Pulau Pinang, National Mapping, Malaysia No. 163/83.
8. Hamasaki, S., Lau, T.L., Morikawa, H. and Ogura, Y. (2012). Estimation of Ground Structure Using Microtremor Observation in Penang Island, Malaysia. Proceedings of the 32 Conference on Earthquake Engineering, 25-27 October, Tokyo, Japan (in Japanese).
9. Ivanovic, S.S., Trifunac, M.D., Todorovska, M.I. (2000). Ambient Vibration Tests of Structures—A Review. ISET Journal of Earthquake Technology, Bulletin of Indian Society of Earthquake Technology: Special Issue on Experimental Methods, 407(4), 165-197.
10. Kanai, K. (1957). The requisite condition for predominant vibration of ground. Bulletin of Earthquake Research Institute, Tokyo University, 31, pp. 457.

11. Kanai, K. and Tanaka, T. (1961). On microtremors VIII, Bulletin of Earthquake Research Institute, Tokyo University, 39, pp. 97-114.
12. Konno, K. (1996). Amplification factor estimated from spectral ratio between horizontal and vertical component of microtremor. Eleventh World Conference on Earthquake Engineering, Acapulco, Mexico. Paper No. 1247.
13. Konno, K. and Ohmachi, T. (1998). Ground-motion characteristics estimated from spectral ratio between horizontal and vertical components of microtremor. Bulletin of the Seismological Society of America. 88(1), pp. 228-241.
14. Lermo, J. and Chavez-Garcia, F.J. (1994). Are microtremors useful in site response evaluation? Bulletin of the Seismological Society of America. 84(5), pp. 1350-1364.
15. Mukhopadhyaya, S. and Bormann, P. (2004). Low cost seismic microzonation using microtremor data: an example from Delhi, India. Asian Earth Sciences, 24(3), pp. 271-280.
16. Nakamura, Y. (1989). A method for dynamic characteristics estimation of subsurface using microtremor on the ground surface. QR of RTRI, 30(1), 25-33.
17. Nakamura, Y. (2000). Clear identification of fundamental idea of Nakamura's technique and its application. Twelve World Conference on Earthquake Engineering. Auckland, New Zealand, Paper No. 2656.
18. Nakamura, Y. (2008). On the H/V spectrum. 14 Word Conference on Earthquake Engineering. Beijing, China.
19. Ojedaa, A. and Escallon, J. (2000). Comparison between different techniques for evaluation of predominant periods using strong ground motion records and microtremors in Pereira Colombia. Soil Dynamics and Earthquake Engineering, 20(1-4), 137-143.
20. Okada, H. (2003). The microtremor survey method. Geophysical Monograph Series number 12, Society of Exploration Geophysicists, 150 pp.
21. Panou, A.A., Theodulidis, N., Hatzidimitriou, P., Stylianidis, K. and Papazachos, C.B. (2005). Ambient noise horizontal-to-vertical spectral ratio in the site effects estimation and correlation with seismic damage distribution in urban environment: the case study of city of Thessaloniki (Northern Greece). Soil Dynamics and Earthquake Engineering, 25, pp. 261-274.
22. Parolai, S., Richwalski, S.M., Milkereit, C. and Bormann, P. (2004). Assessment of the stability of H/V spectral ratios from ambient noise and comparison with earthquake data in the Cologne area (Germany). Tectonophysics, 390, pp. 57-73.

23. Stubbs, I.R. and McLamore, V.R. (1973). The ambient vibration survey. In Proc. of Fifth World Conference on Earthquake Engineering, Rome, Italy, 286-289.
24. Teves-Costa, P., Matias, L. and Bard, P.Y. (1996). Seismic behaviour estimation of thin alluvium layers using microtremor recordings. Soil Dynamics and Earthquake Engineering, 15, pp. 201-209.
25. Tuladhar, R., Yamazaki, F., Warnitchai, P. and Saita, J. (2004). Seismic microzonation of the greater Bangkok area using microtremor observations. Earthquake Engineering and Structural Dynamics, 33, pp. 211-225.
26. Tuladhar, R., Cuong, N.H. and Yamazaki, F. (2004). Seismic microzonation of Hanoi, Vietnam using microtremor observations. In Proc. of 13th World Conference on Earthquake Engineering, Vancouver, B.C., Canada, August 1-6, Paper No. 2539.
27. Theodufidis, N.P. (1995). Horizontal to vertical spectral ratio and geological conditions: an analysis of strong motion data from Greece and Taiwan (SMART-l). Soil Dynamics and Earthquake Engineering, 14(3), 177-197.
28. Walling, M.Y., Mohanty, W.K., Nath, S.K., Mitra, S. and John, A. (2009). Microtremor survey in Talchir, India to ascertain its basin characteristics in terms of predominant frequency by Nakamura's ratio technique. Engineering Geology, 106(3-4), pp. 123-132.

APPENDIX A

SUMMARY OF RESULT

Site ID	Location	Longitude	Latitude	Predominant Period (s)	Predominant Frequency (Hz)	Amplification Level		
						At 2 Hz	At 4 Hz	Maximum
1	Pasir Panjang	100.1845	5.300806	0.27	3.8	1.4	2.1	2.8
2	Pasir Panjang	100.1869	5.307194	0.5	2.3	2.5	2.1	3.6
3	Jalan Pulau Betong	100.1965	5.304214	0.48	2.1	5.7	0.8	6
4	Jalan Sekolah Agama	100.2021	5.307056	0.41	2.5	3.5	1.1	5
5	Jalan Bahru	100.2045	5.319139	0.53	2	5.3	1.4	6.4
6	Pintasan Pondok Upeh 2	100.2179	5.333417	0.49	2	7.1	1.2	7.1
7	Jalan Pulau Betong	100.2215	5.331722	0.15	6.7	1.7	1.7	6.7
8	Lorong Pondok Upih 3	100.2256	5.336167	0.49	2.1	7.3	5.5	7.5
9	Lintang Pondok Upeh	100.2275	5.33925	0.44	2.3	5.2	2.7	5.7
10	Jalan Pulau Betong	100.2321	5.336694	0.38	2.6	3.6	2.2	5.9
11	Jalan Pulau Betong	100.2342	5.343861	0.3	3.4	2.6	4.2	5.1
12	Lintang Bukit Penara 4	100.2397	5.352389	0.36	2.8	3	3	5.3
13	Lorong Chong Teik	100.2389	5.347222	0.54	1.9	7.1	0.4	7.5
14	Jalan Quah Sin Keng	100.2324	5.349833	0.48	2.1	3	1	3.1
15	Jalan Paya Kongsi	100.2286	5.347861	0.49	2	5.5	1.6	5.7
16	-	100.2173	5.342222	0.42	2.5	3.6	2.1	5
17	Lebuh Seri Genting 1	100.2224	5.339167	0.44	2.3	2.8	1.7	3.3
18	Jalan Kampung Terang	100.2156	5.331917	0.41	2.4	4.3	1.8	6.5
19	Jalan Kampung Terang	100.2115	5.323111	0.46	2.3	5.7	2.6	6.3
20	Jalan Kampung Genting	100.2118	5.3155	0.66	1.5	2.3	1.6	3.9
21	Jalan Bahru	100.2044	5.3105	0.56	1.8	5.8	0.9	6.4
22	Jalan Bahru	100.2054	5.326389	0.74	1.4	4	1.2	5
23	Jalan Bahru	100.2063	5.331528	0.57	1.8	3.7	1.1	4.4
24	Jalan Sungai Nipah	100.2115	5.334972	0.47	2.2	4.9	2.4	5.6
25	Jalan Bahru	100.2073	5.336194	0.37	2.9	2.7	2.5	5.2
26	Jalan Bahru	100.2074	5.34175	0.66	1.5	2.2	1.9	3.4
27	-	100.2114	5.343167	0.48	2.2	6.7	2.9	8.7
28	P232	100.1981	5.353806	0.67	1.5	4.1	0.6	6.7
29	P232	100.2046	5.352806	0.39	2.6	3.1	2	4.2
30	Jalan Titi Teras	100.212	5.35325	0.45	2.2	4.9	3.2	5.3
31	Jalan Bahru	100.2116	5.357389	0.51	2	6	0.7	6
32	Jalan Bahru	100.2101	5.362222	0.58	1.7	6.4	1.2	8
33	Jalan Impian 3	100.2306	5.349583	0.46	2.2	5	1.2	5.5
34	Jalan Kongsi	100.2267	5.350111	0.54	1.9	8.5	1.5	10
35	Paya Kongsi	100.2075	5.351806	0.54	1.9	5	2.8	5.4
36	Solok Titi Teras 2	100.2307	5.35575	0.33	3	3.5	3.7	6.1
37	Jalan Titi Teras	100.221	5.359861	0.46	2.2	4.5	2.4	5.1
38	Jalan Bahru	100.2174	5.36425	0.58	1.7	2.1	0.5	2.7
39	Jalan Sungai Air Putih	100.2163	5.371861	0.23	4.4	3	7.9	10.1
40	Jalan Permatan Pasir	100.2042	5.371139	0.57	1.8	3	0.7	3.4
41	Jalan Tok Wan Don	100.2111	5.371028	0.36	3	4.4	4.1	5.3
42	-	100.2117	5.376861	0.46	2.2	5.4	2.8	6
43	-	100.2145	5.379861	0.46	2.2	4.1	3.3	4.5
44	Jln Kuala Sungai Pinang	100.2034	5.392278	0.68	1.5	3.2	0.5	4.9
45	Jln Kuala Sungai Pinang	100.1954	5.3875	0.85	1.2	1.9	0.6	4.2
46	Jln Kuala Sungai Pinang	100.1939	5.391194	0.93	1.1	1	0.6	5.3

Site ID	Location	Longitude	Latitude	Predominant Period (s)	Predominant Frequency (Hz)	Amplification Level		
						At 2 Hz	At 4 Hz	Maximum
47	Jalan Pantai Acheh	100.1969	5.409194	0.7	1.4	1.8	0.5	2.9
48	Jalan Pantai Acheh	100.1971	5.416722	0.35	2.8	2.3	2.7	5
49	-	100.2129	5.396111	0.46	2.2	6.3	2.4	6.8
50	P236 Teluk Bahang	100.2109	5.393306	0.27	3.8	0.4	3.5	3.8
51	-	100.2136	5.383631	0.46	2.2	2.1	0.6	2.4
S1	Jalan Sg. Batu	100.2423	5.283583	0.4	2.5	5.3	2.2	7.9
S2	Lintang Teluk Kumbar 3	100.2337	5.286333	0.4	2.5	5.1	2.1	6.7
S3	Jln Kampung Masjid	100.2256	5.295083	0.5	2	6.7	1.4	7.1
S4	-	100.2333	5.298	0.19	5.4	1.6	2.3	3.2
S5	Jln Haji Sulaiman Jusoh	100.2267	5.301944	0.42	2.4	3.2	1.1	4.3
S6	Lengkok Kampung Masjid	100.2278	5.289	0.55	1.8	5.2	1.9	6
S7	Tingkat Pasir Belanda	100.2205	5.288417	0.25	4.4	2.7	4.3	6.6
S8	-	100.1991	5.284211	0.51	2	6.2	0.7	6.3
S9	-	100.2376	5.290367	0.15	6.7	3.4	3.1	6.8
n1	Jalan Sungai Emas	100.2562	5.471139	0.28	3.6	1.1	3.2	3.9
n2	Persiaran Sungai Emas	100.2483	5.470028	0.2	5.2	3.5	5.6	10.3
n3	Batu Ferringhi Waterfall	100.2419	5.465333	0.21	4.8	2	2.7	3.9
n4	Teluk Bahang Dam	100.2156	5.446611	0.14	7.2	3.2	2.4	6.5
n5	Lengkok Teluk Bahang	100.2112	5.453472	0.45	2.2	6	0.9	6.6
n6	Lengkok Teluk Bahang	100.207	5.457139	0.3	3.3	2.5	3.5	4.9
260	Jalan Thean Tek Lama	100.28958	5.39622	0.42	2.4	2	1.1	2.6
270	Jalan Angsara & Lengkok Angsara	100.28463	5.39070	0.29	3.4	2.3	5.7	7.1
E275	Nudar Angsara 3 & 4	100.28333	5.38992	0.39	2.6	3.2	2.8	4.7
E285	Jalan Sarawak Api/ Lorong Sarawak Api 1	100.28402	5.38587	0.38	3	1.7	2.7	2.7
290	Lorong Sarawak Api 3	100.28095	5.38238	0.43	2.3	2.6	2.2	3.2
E286	Lebuh Rambai 9	100.27662	5.38408	0.32	3.1	1.8	3	6.7
296	Lebuh Rambai 1	100.27620	5.37988	0.26	3.8	1.7	7.5	8.2
309	Tingkat Paya Terubong 3	100.27623	5.37085					
295	Jalan Oriental 6	100.27312	5.37740	0.43	6.1	2.6	1.9	3.4
269	Jalan Ru 2	100.28122	5.39082	0.41	4.7	1.9	0.9	2.5
229	Lorong Kampung Melayu	100.28790	5.40302	0.43	2.3	4.4	0.8	5.6
E214	Jalan Padang Tembak	100.28913	5.41133	0.34	3	2.1	4.3	4.1
279	Solok Paya Terubong 7	100.27357	5.38700	0.56	1.8	2.5	2	2.9
257	Jalan Paya Terubong	100.27640	5.39695	0.54	1.9	1.9	1.3	2.1
245	Jalan Pisang Raja	100.28568	5.39927	0.45	2.2	3.4	0.6	5.7
242	Jalan Balik Pulau Air Itam	100.27498	5.40133	0.47	2.3	2.4	1.9	3.2
211	Jalan Taman Lintang	100.27567	5.40668	0.55	1.9	1.7	1.4	1.9
212	Jalan Taman Cantik 4	100.28117	5.41112	0.56	1.8	1.9	1.1	2.3
227	Jalan Matang Kucing	100.28200	5.40347	0.44	2.3	4.9	1.2	5.4
321	Persiaran Sungai Gelugor 2	100.31373	5.36685	0.46	2.3	4.9	2.3	6.6
308	Persiaran Tunku Kudin Gelugor	100.31288	5.37675	0.29	3.5	3.2	4.4	5.2
314	Jalan Akuarium Gelugor	100.31405	5.37352	0.4	2.5	3.3	1.1	4.4
313	Tingkat Sungai Gelugor 10	100.31160	5.37115	5.48	2.1	5.5	1.5	8

Site ID	Location	Longitude	Latitude	Predominant Period (s)	Predominant Frequency (Hz)	Amplification Level		
						At 2 Hz	At 4 Hz	Maximum
288(1)	Kintang Hajjah Rehmah Jelutong	100.30078	5.38913	0.46	2.2	5.8	2.2	6.4
288(2)	Metro Ave	100.31858	5.38737	10.38	25	7.1	1.4	11.2
308B	Lebuh Tunku Kudin 1	100.31530	5.37343	0.4	2.5	4.2	1.8	7.4
344A	Under Penang Bridge	100.31632	5.35810	0.42	7.6	2.4	2	4.5
351	Jalan Batu Uban 4	100.31160	5.35398	0.36	2.8	4	2.7	6.9
358	Persiaran Bayan Indah	100.31190	5.34738	0.37	11.7	8.3	1.6	10.8
364A	Jerejak Jetty	100.31150	5.34277	0.41	7.7	7.7	0.8	8.5
395	Queensbay Carpark	100.30823	5.33283	0.3	26.3	7.6	1.2	9.8
350	Jalan Batu Uban 2	100.30818	5.35160	4.71	19	2.3	1.9	5.1
363	Jalan Pantai Jerejak 9	100.30373	5.34213	0.13	34.3	3.2	0.5	6.3
383	Persiaran Pantai Jerejak 10	100.30375	5.33713	0.53	2.2	6.2	1.5	7.1
393	Lebuh Bukit Kecil 5	100.30328	5.33150	5.21	26.8	2	0.5	2.9
382	Jalan Bukit Kecil 1	100.29892	5.33630	0.44	2.3	6.7	1.8	7.7
370	Medan Nipah	100.29645	5.33927	0.43	2.3	7.9	1.8	9.3
381	Lebuh Nipah 2	100.29465	5.33558	0.44	2.4	7.8	2.7	9.8
380	Lebuh Nipah 5	100.29238	5.33710	0.2	5	1.4	3.4	6.2
294	Solok Dumber	100.31188	5.38498	0.12	11.1	1.6	1.9	6.1
292	Jalan Taman Gelugor	100.30722	5.38357	0.31	15.2	3.7	1	4.8
297	Cangkat Delima 3	100.29732	5.37880	5.93	20.1	1.5	2.2	4.8
298	Lorong Delima 13	100.30175	5.37903	0.33	7.8	4.9	0.9	6.3
291A	Cangkat Delima 6	100.29698	5.38325	5.21	16.5	2.3	2.3	4.7
291	Lintang Delima 5	100.30303	5.38510	0.3	4.4	3.6	3.4	6.8
319	Pemancar Hilir	100.30557	5.36870	0.49	2.4	2.7	2.6	7.1
311	Pemancar Hilir	100.30110	5.37365	0.3	3.3	3.6	3.8	7.5
304	Cangkat Bukit Gambir	100.29812	5.37613	0.05	27.4	1.7	1.1	3.9
318	Tingkat Permai	100.30130	5.36828	0.45	9.7	1.9	2.1	5
415	Kampung Jawa Highway	100.29958	5.31228	0.51	2	2.5	0.8	2.7
479	Jalan Batu Maung,Restoran Ocean Bay Seafood	100.28867	5.28531	0.3	3.5	2.4	3.5	4.2
484	Taman Jeliti	100.27411	5.27994	0.29	4	2.1	1.9	3.7
487	Lorong Kekabu 1	100.27139	5.27428	0.51	2	2	2.2	2.3
476	Jalan Permatang Damar Laut	100.25617	5.28436	0.41	2.4	4.8	1.6	6.6
485	Jalan Damar	100.26631	5.27928	0.47	2.1	5.2	2.3	5.6
486	LintangBeringin 9	100.26681	5.28336	0.54	1.9	3.5	0.9	4.3
478	Lorong Batu Maung 4	100.28006	5.28650	0.58	1.7	3.9	0.4	4.9
483	Medan Batu Maung 4	100.27425	5.28192	0.3	3.3	2.7	7.7	8
470	Airport-Jalan Batu Maung	100.27533	5.29244	0.41	2.5	7.5	2.2	9.4
454	Pintasan Batu Maung 6	100.28167	5.29919	0.46	2.2	4.7	2.2	5.3
461	Lintang Bayan Lepas	100.28433	5.29267	0.87	1.2	0.9	1.1	2.9
455	Medan Bayan Lepas-near HW Factory	100.29178	5.29953	0.68	1.5	3.9	0.9	6
443	Jalan Sungai Keluang	100.29606	5.30728	0.55	1.9	5.1	0.9	6
449	Sg Keluang 5 Hilir	100.28753	5.30417	0.49	2.1	6.9	0.9	7
432	Gerbang Kampung Jawa	100.29733	5.31828	0.57	1.8	3.7	2.7	4

Site ID	Location	Longitude	Latitude	Predominant Period (s)	Predominant Frequency (Hz)	Amplification Level		
						At 2 Hz	At 4 Hz	Maximum
413	Lengkok Kampung Jawa 1	100.29139	5.32156	0.5	2	6.8	1.6	7
403	Lebuh Kampung Jawa	100.29842	5.32872	0.51	2	7.7	0.5	8
374	Cangkat Sungai Ara 10	100.26714	5.33417	0.42	2.4	6.2	1.6	8.3
391	Pintasan Mashuri	100.28989	5.32939	0.44	2.3	3.8	1.9	4.2
396	Jalan Sungai Ara 7	100.26603	5.32661	0.64	1.7	1.2	2.7	1.5
398	Persiaran Bayan	100.27344	5.32603	0.43	2.3	5.7	1	7.2
400	Lintang Mayang Pasir 4	100.28539	5.32450	0.47	2.1	5.4	1.4	5.7
410	Medan Mashuri 1	100.28072	5.32122	0.38	2.6	3.7	4.2	5.3
~~416~~	~~Changkat Kerani~~	~~100.26358~~	~~5.31861~~	~~0.57~~	~~1.9~~	~~1.1~~	~~1~~	~~2.4~~
418	Lorong Kenari	100.27033	5.32050	0.4	2.5	4.7	1.8	7.2
430	Jalan Sungai Keluang	100.28903	5.31603	0.37	2.7	2.2	1.5	4.1
433	Kenari Ptn	100.26225	5.31297	0.36	3	2	4.1	3.7
439	Solok Sungai Pasir	100.27597	5.31844	0.4	2.5	4.9	1.5	7.9
441	Lorong Sungai Tiram	100.27783	5.30622	0.25	4	1	7.9	8.4
444	Lengkuk Kericap	100.25583	5.30083	0.24	4.2	1.9	13	14.5
445	Lorong Merbah 1	100.26461	5.30464	0.38	2.6	4.3	2.8	5.8
447	Lorong Sungai Tiram 1	100.27022	5.30247	0.39	2.6	3.1	1.7	4.7
458	-	100.25608	5.29642	0.41	2.5	3	1.8	4.3
459	Jalan Garuda	100.26422	5.29261	0.45	2.2	8.3	2.2	9.2
466	Tingkat Kampung Bukit	100.24669	5.28889	0.46	2.3	2.7	1.4	3.1
466(2)	Tingkat Kampung Bukit (1)	100.24761	5.29044	0.62	1.6	1.8	1.2	2.1
468	Jalan Permatang Damar Laut	100.25792	5.28814	0.5	2	4.5	0.3	4.5
365	Lebuh Relau	100.26769	5.34300	0.56	1.8	2	1.5	2.1
352	Lebuh Relau 4	100.27172	5.34625	0.54	2.1	0.4	0.2	0.7
366	Persiaran Paya Terubong 1	100.27703	5.33914	0.39	2.7	5.4	3	8.2
377	Persiaran Bukit Jambul 9	100.27967	5.33508	0.38	2.7	5.5	3.9	8.3
367	Persiaran Bukit Jambul	100.28192	5.33897	0.56	2.1	1.5	0.9	2.4
359	Lintang Bukit Jambul 1	100.28258	5.34372	0.64	1.6	1.8	1.3	3
338	Halaman Bukit Gambir 9	100.28894	5.35644	0.54	1.9	3.5	2.3	4
339	Filter Lane	100.29428	5.35608	0.29	3.4	3.6	6.7	7.2
333	Jalan Tadika	100.30206	5.36072	0.44	2.4	4.5	5.8	5.5
335	Jalan Universiti (E)	100.31442	5.35950	0.37	2.7	3.6	2.1	5.6
354	Lorong Merak 2	100.29706	5.34947	0.45	2.2	7	1	7.6
353	Jalan Bukit Gambier	100.29133	5.34772	0.45	2.2	6.4	0.6	6.8
306	Jalan Bunga Raya (Solok)	100.30606	5.37486	0.27	3.7	2	7.5	7.6